ADDIS ABABA SCIENCE AND TECHNOLOGY UNIVERSITY

FLOODPLAIN INUNDATION MODELING AND MAPPING

FOR GILGEL ABAY RIVER: NILE BASIN, ETHIOPIA

By

EYUOEL FRANCO

A Thesis submitted as a Partial Fulfillment to the Requirements for the Award of the

Degree of Masters of Civil and Architectural Engineering

(Hydraulic Engineering)

to

DEPARTMENT OF HYDRAULIC ENGINEERING

COLLEGE OF CIVIL AND ARCHITECTURAL ENGINEERING

OCTOBER 2020

Declaration

I hereby declare that this thesis entitled **"Floodplain Inundation Modeling and Mapping for Gilgel Abay River: Nile Basin, Ethiopia"** was prepared by me, with the guidance of my advisor. The work contained herein is my own except where explicitly stated otherwise in the text, and that this work has not been submitted, in whole or in part, for any other degree or professional qualification.

Author: Signature, Date:

EYUDEL FRANCO EA. 04/12/2020

Witnessed By:

Student Advisor: Signature, Date:

Dr. FITSUM TESFAYE 04/12/2020

Certificate

This is to certify that the MSc. thesis prepared by **Mr** EYUOEL FRANCO entitled **"Floodplain Inundation Modeling and Mapping for Gilgel Abay River: Nile Basin, Ethiopia"** and submitted as a partial fulfilment for the award of the degree of Master of Science in Civil and Architectural Engineering (Hydraulic Engineering) complies with the regulations of the university and meets the accepted standards with respect to originality, content and quality.

Principal Advisor:

1. Dr. Fitsum Tesfaye _______ 04/12/2020
   (Advisor) Signature Date

Members of the Examining Board:

1. Dr. Tilahun Derib _______ 30-11-2020
   (External Examiner) Signature Date
2. Dr. Habtamu ~~Kebede~~ Hailu _______ 04/12/2020
   (Internal Examiner) Signature Date
3. Dr. Melaku Sisay _______ 04/12/20
   (ERA PG, Program Coordinator) Signature Date
4. Mr. Alemayehu Feyisa _______ 04-12-2020
   (Head, Civil Engineering Department) Signature Date
5. Dr. Sisay Demeku _______ 08/12-2020
   (Dean, College of Architectural & Civil Engineering) Signature Date

College of Architecture & Civil Engineering
Addis Ababa Science & Technology University

I dedicate this paper to my Mother BEZUAYEHU DEGEFU, My Aunt KOKEB DEGEFU and My Sister BETHELHEM TAYE!

Abstract

Flood is an overflowing of water over land surface when the volume of water raises higher than the banks of the water body. Ethiopia is one of the east African countries that is severely affected by it due to the countries rainfall characteristics in which, more than 80% of its annual precipitation falls in four wet month. The objective of this research was to model the flow characteristics of Gilgel-Abay River and to develop flood map for the area. Integration of HEC-HMS and HEC-RAS with ARC-GIS was used to create a regional model for floodplain determination, modeling analysis representation. HEC-HMS was used for hydrologic model calibration with the use of daily time series data for return periods of 2, 10, 25, 50 and 100 years and the model was compared with different frequency analysis methods. HEC-RAS with HEC-GEORAS interface in coordination with ARC-GIS was used to carry out the two dimensional hydraulic modeling and generation of flood maps. Daily discharge and rainfall data were used for HEC-HMS Calibration and Validation with both results showing good match between measured and simulated precipitation data, with acceptable range of coefficient of determination R^2 *(between 0.7 and 1, Calibration value being 0.72 and Validation 0.73) and Nash-Sutcliffe (NSE) (between 0.5 and 0.75, Calibration value being 0.51 and Validation 0.54). The result of hydrologic model demonstrated peak discharges of 223.9* m^3/s*, 367.5* m^3/s*, 438.4* m^3/s*, 440.5* m^3/s *and 501.6*m^3/s *for return periods of 2, 10, 25, 50 and 100 years respectively. According to the flood map generated, flooded area for the return periods 2, 10, 25, 50 and 100 years were 6.2* km^2*, 7.3* km^2*, 7.8* km^2*, 7.9*km^2 *and 8.3* km^2 *respectively. Flood damage of the area was assessed using depth damage function method and the estimated damage to the agricultural land use with water depth greater than 1m was 32.18* km^2*. Therefore, non-structural measures like afforestation as well as structural flood protection measures like dikes and levees were recommended to be constructed around the agricultural area.*

Key words: HEC-HMS, HEC-RAS, Floodplain map, Gilgel Abay and 2D Modeling

Acknowledgement

First of all, I thank and glorify God Almighty through His Son Jesus Christ for opening this door of education and for helping me from the start till the finish of my paper.

Secondly, I am very thankful for my beloved family, My Mother Bezuayehu Degefu, My Aunts Kokeb and Yeshihareg Degefu, My Sister Bethelhem Taye and My Uncle Hailu Tegegnework for their love, support prayer and belief in me.

Thirdly, I thank my advisor Dr. Fitsum Tesfaye for guiding, supporting and correcting me throughout the research.

Last but not list I appreciate my friends Bezuneh Melese and Abenezer Girma for their prayer and encouragement and Yosef Mekonen for his cooperation.

Finally, I thank every person who prayed and wished me well. Thank you and God bless!

Table of Contents

Abbreviations & Acronyms

HEC	Hydraulic Engineering Center
SNNPR	Southern Nations and Nationalities and Peoples region
MODIS	Moderate Resolution Imaging Spectroriadiometer
NASA	National Aeronautics and Space Administration
HMS	Hydraulic Modeling System
GIS	Geographic Information System
TIN	Triangular Irregular Network
GEORAS	Geospatial River Analysis System
DEM	Digital Elevation Model
A.M.S.L	Above Mean Sea Level
ASTER	Advanced Space Bourne Thermal Emission and Reflection Radiometer Images
GEOHMS	Geospatial Hydraulic Modeling System
DTM	Digital Terrain Model
2D	Two Dimensional
3D	Three Dimensional
CN	Curve Number
DMC	Double Mass Curve
ERA	Ethiopian Road Authority
XS	Cross Section
SCS	Soil Conservation Service
IDF	Intensity Duration Curve
ASF	Alaska Satellite Facility
NDRM	National Disaster Risk Management Commission

List of Figures

List of Tables

1. Introduction

1.1 Background

A natural or a manmade phenomenon that is caused due to an overflowing of water over a land surface or river banks, when the volume of water is more than the carrying capacity of the drainage system is called flooding. It is caused naturally when there is high or long lasting precipitation or other natural hazards such as earthquake and tsunamis. Whereas when hydraulic structures such as dams, levees and spillways are damaged or breached floods are caused and this is known as man induced flooding (Ohimain, 2014).

Floods are further classified into two. Flash floods which occur suddenly or unexpectedly are generated from high precipitation that creates excess runoff. It is mostly caused naturally but it may also occur when a reservoir is breached. The other is river flood which occurs naturally when the volume of water in water bodies like rivers is increased due to heavy rainfall (Aris, 2003).

Serious environmental and economic losses are caused by floods. One third of all natural disasters that result in different kinds of losses are due to floods. This hazardous phenomena is among the world's costliest natural disasters which annually bring global damages that are worth $6-$8 billion affecting more people than any other form of natural disaster. Loss of human life, damage to property, destruction of crops, loss of health conditions owning to water borne diseases are major impacts of the phenomena. Due to damage of different infrastructures like roads, bridges, and power plants economic activities will be forced to seize and people will also be displaced from their homes leading to disruption of life. Psychological impacts are also the results of flood causing trauma on people who lost their loved ones (especially children) due to the phenomena (Lampros, 2009).

Ethiopia is one of the east African countries which is severely affected by flooding due to its rainfall characteristics where more than 80% of its annual precipitation falls in four wet month. There are three distinct seasons of the country called Bega, Belg and keremt. Bega starts from October and extends to January. This season is mostly dry. Belg starts from the month February and extends to May. This season is the main rainy season for pastoral areas and short rainy season for crop growing areas. The third season, Keremt, which the amount of rainfall becomes high and flooding mostly occur starts from the month of June and extends to mid September (NDRM, 2020).

Flood has affected many parts of the country mainly Dire dawa, SNNPR, Amhara, Oromiya, Gambella, Tigray, Somali and Afar regions. The results of flooding in Ethiopia are due to flash floods, river floods and heavy rains causing overflow. According to the 2020 year data of NMA, Average of 336,810 people in Somali regions, 539,761 people in Oromia region, 398,491 people in SNNPR, 44,340 people in Gambela, 63,410 people in Afar, 14,550 people in Tigray, 15,000 people in Dire-Dawa, 2000 people in Harari, 10,000 people in Addis Ababa and 586,342 people in Amhara regions were affected by flood. Flooding in the Country at times results in displacement, loss of property, depletion of natural resources, disruption of social services and damage to infrastructure. Therefore from this information it is seen that flood modeling is necessary (NDRM, 2020).

The aim of this study is to develop a reliable flood model and to simulate flood events of Gilgel Abay River. On August 19, 2006 NASA's tera satellite (MODIS) captured the top image of the area and the image showed that the river was flooded. The satellite image does not normally show the river. But on the beginning of July where heavy rain began to occur, the river was visible and it observed to be larger than the Blue Nile. Since the catchment is a densely populated part of the Amhara region, it was found necessary to develop a flood map for the area in case any hazardous phenomena occurs in the future (Nasa, 2006).

In the past only mitigation of effects of flooding was adopted but its cause and effect was not considered. This day's flood effects can be modeled and simulated using different soft wares. Developing flood maps for different areas is advantageous because it allows people to see whether a flood will occur or not and help them to use different mitigation measures which will allow them to avoid different kinds of disasters that could happen to them and their properties (Ohimain, 2014).

1.2 Statement of the Problem

Gilgel Abay is the largest contributors to Lake Tana which is located south of the lake. Other main tributaries to the lake are Megech, Gumera and Rib rivers. In 2006 there was an overflow of Rib and Gumera rivers causing floods and displacing people from their residential places, forcing them to stay under temporary shelters. In that same year the NASA tera satellite (MODIS) captured the top image of Gilgel Abay River and reported the river was flooded. The satellite image before the incident showed only the slightest of hint that the river ever exists. But on August 19, the river was larger than the Blue Nile to its east. Due to the flood, the land adjacent to the river was degraded causing destruction of habitat and biodiversity, erosion and damage on agricultural areas. Since 62% of the catchment area is agricultural and many small scale agricultural systems are being adopted around the river, it was found necessary that the flood potential of the river is assessed and reliable flood map is prepared for the catchment in case any significant damage in this areas happen in the future due to flooding of the river.

1.3 Objective of the study

1.3.1 General objective

The general objective of this study is to model the flow characteristics of Gilgel Abay River and to develop flood map for the area.

1.3.2 Specific Objectives

- To determine probability distributions that best fit the flow data.
- To estimate peak flood discharge for different design precipitations.
- To develop 2D flood modeling and create a flood map for the river.

1.3.3 Research Questions

- ➢ Which type of fitting distribution is the best fit probability distribution for Gilgel Abay catchment?
- ➢ How much is the peak flood discharge for different design precipitations?
- ➢ What does the flood map indicate?
- ➢ What is the area of coverage and extent of the likely damage?

1.4 Significance of the Study

Flood models are mainly used to simulate flood inundation extent and depth at different sections of the studied flood rivers. Hydraulic and hydrologic engineers use them to better study and analyze the hydrologic system of floods. Models that are physically based have the capability of defining spatial and temporal variables in terms of discharge, water level, velocity flow duration, and inundation extent on the processive flood events.

These models are now a days basic solutions to flood hazards which is defined as floods that cause sudden threats to the lives and properties of human beings at flood prone areas. The aim of these studies is to decrease the susceptibility and vulnerability of both economic and human lives aspects. They are also a major help in supporting the hydro-system operation, flood warning, risk quantification and decision making for the design and planning of flood mitigation measures. Governments and Insurance companies can use these studies to separate areas of land at high risk and guide the investment and emergency response strategies (Ukessays.com, 2018).

The study is significant for developing a reliable flood map for Gilgel Abay watershed ensuring safety for the farmers of the Gojam living around the area of the river. It will also be useful to flood management bodies for any decision making for flood management strategies. In general the research would be significant for the society as well as for different authorities related to flood management.

2. Literature Review

2.1 Flood Inundation Mapping and Modeling

2.1.1 Rainfall-Runoff modeling

Different tasks like modeling of flood events, monitoring of water levels during different water conditions or prediction of floods are done by rainfall-runoff models (Jia Y. et al , 2009). Hydrologic models are further classified into two: stochastic and deterministic. Models that produce outputs with partial randomness are called stochastic whereas models that don't have randomness are called deterministic. Deterministic models are further classified in to three (Cunderlik, 2003).

Firstly, the lumped model, which assesses the catchment response simply at the outlet without obviously counting for an individual sub-basins response. Secondly, the semi-distributed model, which is partly permitted to change in space with a division of the catchment into a number of sub-basins. The third type of model is the distributed model, which permits its parameters to change in place at a resolution normally chosen by the client (Cunderlik, 2003).

Distributed hydrological models such as the European Hydrological System Model (MIKE-SHE) and Modular Modeling System (MMS), and semi-distributed models like the Hydrological Engineering Center Hydrological Modelling System, Soil and Water Assessment Tool (SWAT),Topography Based Hydrological Model (TOPMODEL), Hydrologiska Byråns Vattenbalansavdelning (HBV) and Hydrological Simulation Program-Fortran (HSPF) are developed for a runoff estimation based on the data availability and complexity of the hydrological systems.

2.1.1.1 Hydrologic Modeling Software (HEC-HMS)

Flash flood occurrence and relationship between rainfall and runoff data's is resolved using hydrological modeling. Hydrological modeling takes the hydrological process to calculate stream flow over river basin and helps forecasters in making a comparison between simulated stream flow and observed flooding to predict and understand the hydrologic process (Derdour, 2018).

The Hydrologic Engineering Center's Hydrologic Modeling System (HEC-HMS) is designed to simulate the precipitation-runoff processes of dendritic watershed systems. It is designed to be applicable in a wide range of geographic areas for solving the widest possible range of problems. Hydrographs produced by the program are used directly or in conjunction with other software for studies of water availability, urban drainage, flow forecasting, future urbanization impact, reservoir spillway design, flood damage reduction, floodplain regulation, and system operation (SCHAFFENBERG, 2016).

The model is physically based and conceptually semi-distributed model designed to simulate rainfall-runoff processes in a wide range of geographic areas, from large river basin water supplies and flood hydrology to small urban and natural watershed runoffs. It easily operates huge tasks in relation to hydrological studies, including losses, runoff transform, open channel routing, analysis of meteorological data, rainfall-runoff simulation and parameter estimation (Feldman, 2000).

HEC-HMS model setup consists of four main model components: basin model, meteorological model, control specifications, and input data (time series, paired data, and gridded data). An assortment of different methods is available to simulate infiltration losses (deficit and constant, exponential, Green and Ampt, initial and constant, SCS curve number, Smith Parlange and Soil Moisture Accounting – SMA). Seven methods are included for transforming excess precipitation into surface runoff (Clark unit hydrograph, kinematic wave, ModClark, SCS unit hydrograph, Snyder unit hydrograph, user specified graph and user specified unit hydrograph). Six methods are included for routing model (kinematic wave routing, lag routing, modified puls routing, Muskingum routing, Muskingum–Cunge routing and Straddle Stagger routing). For the meteorological model eight methods are included (frequency storm, gage weights, gridded precipitation, inverse distance, HMR52, SCS storm, specified hyetograph, standard project storm) (Derdour, 2018).

Reshma showed that the software has a good performance by applying HEC-HMS for well monitored experimental watershed having a good database of hydrological parameters. The model has been used to calibrate and validate seven rainfall events. The simulation results of the calibration events showed that volume of runoff and time to peak has simulated more variation when compared to the observed hydrographs and the peak runoff showed less variation (Reshma, 2013).

Derdour studied rainfall runoff modeling using HEC-HMS program integrated with DEM data as an input for basin model in semi-arid environment to simulate peak discharges for four different return periods. Data's used were time series data, stream flow data and spatial data. There was a selected historical event for the control and the simulated results for this events showed that the peak discharge is lower than the observed. But after calibration the difference between the simulated and observed hydrographs were found to be very close (Derdour, 2018).

Sok applied the model for simulating stream flow and assessed water availability. The model performance was evaluated for daily and monthly time steps using different performance measures and the results obtained were satisfactory (Sok, 2016).

Bosamiya simulated the rainfall runoff characteristics of Khari catchment of Sabarmati basin using HEC-HMS model. Data's needed were Shuttle Radar Topography (SRTM), digital elevation model (DEM), rainfall data, discharge data and land use land cover map of the region. The digital elevation model was processed and different watershed characteristics were estimated using the ARC-HYDRO tool in ARC-Map. Soil characteristics of the watershed were also defined to estimate the runoff curve number. Then the catchment's physical characteristic data was exported to HEC-HMS to run the simulation and compare the simulation flow with observed flow (Bosamiya, 2018).

The catchment was subdivided into eight sub basins. Methods used to determine infiltration loss, transform method and metrological model were SCS-CN loss method, SCS unit hydrograph and Inverse distance method respectively. Finally the simulated result of the calibrated event gave 13.45% deviation in volume of runoff and 10.65 % deviation in peak runoff. The simulation result of the validation event gave 15.04% of deviation in volume of runoff and 8.64% deviation in peak runoff. Therefore, it was concluded, the volume of runoff and peak runoff were simulated with more variations (Bosamiya, 2018).

Darji modeled the rainfall runoff relationship of Machhu river basin. Data's needed were metrological data, thematic maps such as land use, geology, topography and soil, land sat images and digital elevation model (DEM). River basin was created from the DEM and metrological model of rain gauges were created from rainfall data using HEC-GEOHMS. Then, data was exported to HEC-HMS (Darji, 2019).

Time series data was inputted in the model and simulation was done by integrating basin model, metrological model and control model. The loss rate was estimated using initial and constant rate method and gauge weight method was used to estimate the metrological model. Using regression analysis, the coefficient of determination value was equal to 0.89 and result of evaluation of rainfall runoff relation was equal to 0.85 which indicates the model performance and rainfall runoff relationship are both good (Darji, 2019).

Wang and Zhang used HEC-HMS to simulate runoff in a semi-arid region of north western China. Their objective was to evaluate the use of the model's capability to investigate the rainfall runoff interactions. Data's required were rainfall data, runoff data and digital elevation model. ARC-GIS with its extension tools ARC HYDRO and HEC-GEOHMS was used for DEM processing, defining streams and watershed characteristics, terrain and basin processing. Finally, the processed data was imported to HEC-HMS for simulation (Wang, 2016).

The result of the simulation demonstrated that the model unsatisfactorily simulated runoff volume and peak runoff including the peak volume and time of peak. This was due to the model's poor base flow simulation, presence of hydraulic engineering works and inability of the continuous model to capture sub basin specific features due to its semi-distributed structure (Wang, 2016).

From the studies, it is noticed that HEC-HMS model significantly simulates the relationship between rainfall and runoff processes in different geographic areas. Stream flow data, rainfall data and digital elevation model (DEM) are the necessary data's needed for the model to give good results. ARC-GIS tools ARC HYDRO and HEC-GEOHMS are useful for processing, interfacing purpose and overall preparation of data's compatible with the model.

2.1.1.2 Model Calibration and Validation

Model calibration is a systematic process of adjusting model parameter values until model results match acceptably the observed data. The purpose of calibration is to identify the parameters whose variation causes significant changes in the outputs of the model. The calibration procedure involves a combination of both manual and automated calibrations. The manual calibration proceeds the automate optimization to ensure a physically meaningful set of initial parameters generated from HEC-GeoHMS and Arc Hydro for the catchment. Historic hydrologic data of the catchment is used for calibration.

Model Validation is the process of testing the model ability to simulate observed data, Other than those used for the calibration, within acceptable accuracy. During this process, calibrated model parameter values are kept constant. The quantitative measure of the match is the degree of variation between computed and observed hydrographs.

2.1.2 River Analyzing Software (HEC-RAS)

Different research had been undertaken dealing with Hec-Ras software in flood hazard and risk assessment. Awal integrated the hydraulic model with GIS and presented a systematic approach of this application with a case study of Lakhhandei River in Nepal. The objectives of the study were to analyze the flood plain by using one dimensional steady and unsteady flow model and to make a flood risk map of the study area. The data collected were documents from previous studies, stream flow and precipitation data, population data, topographical map and survey data of previous studies, GIS/Remote sensing data (Awal R. et al, 2007).

Preparation of TIN in ARC-view GIS, pre-processing by HEC-GEORAS to generate import file for HEC-RAS, Calculation of water surface profiles by HEC-RAS, post processing of HEC-RAS results and finally flood plain mapping and risk assessment of flood plain were the procedures used to complete the study. GPS was used to collect information about the extent and depth of flood in certain location of the study area and to identify some points of river course shifting. Probable maximum flood was estimated using different empirical methods for different return periods at various sites. The flood risk was then assessed by separating hazard and vulnerability components (Awal R. et al, 2007).

The assessment of vulnerability to flooding indicated that about 75% of the vulnerable area consisted of cultivated land. And the assessment of flood hazard indicated that most of the flooded areas had water depth of less than two meters. Combining this two results the risk assessment indicated that agricultural areas were greatly impacted by flooding, having a flood water depth of more than one meter. Finally the number of people that would be affected by two year and hundred year flood were estimated (Awal R. et al, 2007).

Amia integrated GIS with HEC-RAS software in flood modeling of Martil River (Northern Morocco). The river has a unidirectional flow with low slopes varying between 10^{-4} and 10^{-6}, depth not exceeding 4 meters. Data needed were DEM and hydro-metrological data. Three steps were taken for this investigation. First, geometrical data of the river with minor, major river beds and cross-section were created using the ARC-GIS tool, the HEC-GEORAS extension (Amia, 2018).

Then application of flow modelling with HEC-RAS model was executed. Finally the results of the water stain: flood surfaces and depth grids were generated. The modeling executed was of one dimensional type. Results obtained from HEC-RAS were then exported to the tool HEC-GEORAS to create three different flood zones for each profile that is applied to flow for each return period with velocities and heights of water in each zone being determined (Amia, 2018).

Kute studied the flood modeling of river Godevardi using HEC-RAS at the Rakund site, India. There is a dam located at 14km distance from the river. Input parameters that were used as data's for modeling include catchment area, cross section of the site, alignment details of river and dam, maximum flood intensity and contour details of river cross section. Then storage area data, inline structure data entering flow data and the boundary conditions, maximum flood intensity and geometric data were performed using HEC-RAS. And the results obtained were cross section out puts, flood levels for given discharge and rating curve (Kute S. et al, 2014).

Sahiriparsa integrated one dimensional steady model and two dimensional model using HEC-RAS and CCHE2D to simulate flood zoning in the Sungai Maka district in Kelantan State, Malysia. Data's required for HEC-RAS model were plan data, geometric data, flow data and hydraulic design data. Change in depth, velocity flow area and Froude's number were calculated for different return periods. The results showed that the difference in expanding flood retention zone was primarily stemmed from the route topographical features (Shahiriparsa et al., 2016).

Patel performed hydrodynamic flood modeling for Ambica River. The objective of the study was to implement one dimensional hydrodynamic model using HEC-RAS. The data's used were geometric data, cross sectional data and steady flow data. Geometric and cross sectional data were geo-referenced using HEC-GEORAS tool in ARC-GIS. Geometric cross sections defined were then exported to HEC-RAS. Steady flow data for different peak discharge was entered in the model and boundary conditions were defined. Finally, simulation was carried out and water surface profiles were extracted (Patel S.B et al, 2018).

Ahmed applied the model for flood studies in the river Jhelum Kashmir valley. Data's required were geometric and flow data. The model was run for one dimensional steady flow water surface profile computations. By getting satisfactory results, it was concluded that HEC-RAS model is appropriate in simulating water surface profiles (Ahmad H.F et al, 2016).

Vozianaki compared one dimensional and combine one dimensional two dimensional hydraulic simulations using high resolution topographic data in Koilioris basin, Greece. The research focused on the effect of high resolution DEMs on hydraulic modeling. The floodplain and channel friction were used as main calibration parameters. The study indicated that combined one dimensional two dimensional model performed better than the one dimensional HEC-RAS model when using a high spatial resolution topographical data (Vozinaki et al, 2017).

The flood plains of the above studies were all analyzed using one dimensional flow model. The data's collected were mostly similar except Kute et al (2014). This is because the flood being modeled is released from a reservoir upstream of the river. Therefore, the characteristics of the reservoir were also considered. The flood modeling software used in all the studies was also the same. With the advantage of being compatible with soft wares such as ARC-GIS and Google earth, HEC-RAS offers a wide variety of options for modeling hydraulic systems.

It has also been used in comparable areas of medium mountains and has been subject of several international publications and thesis work. The HEC-RAS model is a simplified way to model a river flow. It evaluates the velocity and heights of water on all parts of a river under different regimes (permanent and non-permanent, subcritical and supercritical). It also includes hydraulic structures such as dams, bridges, pumping systems etc. (Gary W. , 2014).

2.2 Types of flood modeling

2.3.1 One dimensional Steady and Unsteady Modeling

Older versions of HEC-RAS were limited to computing water surface profiles for steady state gradually varied flow in channels. Conservation of Energy from one cross- section to the next cross-section along the length of the channel is applied to determine the water surface profiles in 1D steady state modeling.

But in reality, it is uncommon for natural channel flows to be steady. Instead, natural channel flows are unsteady meaning that the flow rates in the channels actually differ with time. In an unsteady flow routing, velocity, discharge and depth are functions of location and time. Depth and discharges are determined at different locations and points in time.

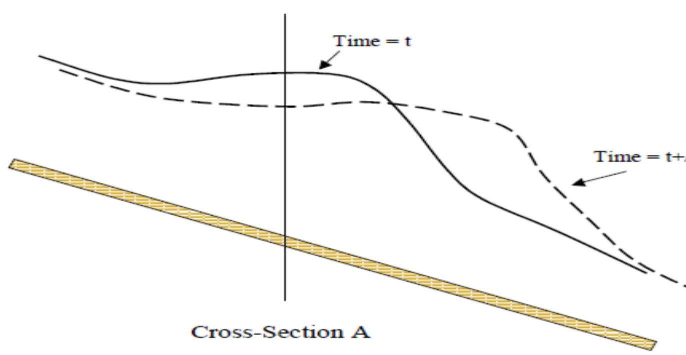

Figure 2- 1 An Unsteady Flow Routing Concept (Chase, Donald V., 2016)

Saint-Venant Equation

1D unsteady flow routing solves the Saint-Venant equations. These equations were developed from Conservation of Mass (equation 1) and Conservation of Momentum (equation 2) applied to a small control volume of fluid (Gary, 2016).

$$\frac{dA_t}{d_t} + \frac{dQ}{dx} - q = 0 \quad \text{……………………………...................................2.1}$$

$$\frac{dQ}{dt} + \frac{dQ_v}{dx} + gA\left(\frac{dz}{dx} + S_f\right) = 0 \quad \text{……………………………………….2.2}$$

Where A is the area of cross-section, t is a time, Q is the flow, X is the distance along channel, q is a source or sink term, V is a velocity of flow, g is the gravity acceleration, S_f is the friction slope and dz/dx is the water surface slope.

2.3 Two-Dimensional Unsteady Modeling

2D modeling discretizes the river and adjacent flood plain areas into a collection of individual cells called grid cells. Each grid cell is composed of multiple GIS cells that make up the terrain model, which describes the continuous ground geometry that is so important in analyzing the two-dimensional behavior of floodplains. A water surface elevation is computed at each grid cell for each point in time. The size of the grid cells defines the resolution of the model and model results.

HEC-RAS will combine continuity and the Diffusion-Wave form of the momentum equation to compute the water surface elevation at a point in time (Gary, 2016).

The unsteady differential form of the Mass Conservation (Continuity) equation is:

$$\frac{\partial H}{\partial t} + \frac{\partial (Uh)}{\partial X} + \frac{\partial (vh)}{\partial Y} + q = 0 \quad \text{………………………………………..2.3}$$

Where t is time, H is a water surface elevation, h is the water depth, q is a source or sink term, and u and v are the velocity components in the X and Y direction. In vector form, the Continuity equation takes the form:

$$\frac{\partial H}{\partial t} + \nabla \cdot hv + q = 0 \quad \text{……………………………………………….2.4}$$

Where V= (u,v) is the velocity and (∇) is the vector of the partial derivative given by $\nabla=(\partial/\partial x, \partial/\partial y)$.

The Diffusion-Wave form of the Momentum Equation can jest regarded the barotropic pressure gradient and bottom friction.

$$-g\nabla H = CfV \text{...} 2.5$$

Where g is gravity acceleration and C_f is the bottom friction. HEC-RAS use Manning's formula, the Diffusion-Wave Equation results:

$$-g\nabla H = \left(\frac{n^2 gv}{R^{\frac{4}{3}}}\right) V \text{...} 2.6$$

Where n is the Manning's Roughness Coefficient and R is Hydraulic Radius.

The velocity will be determined by a balance between barotropic pressure gradient and bottom friction.

$$V = \frac{-(R(H))^{2/3}}{n} \frac{(\nabla H)}{(\nabla H)^{1/2}} \text{...} 2.7$$

Now, the Diffusion Wave can be directly substituted in the Mass Conservation.

$$\frac{\partial H}{\partial t} + \nabla \cdot \frac{-(R(H))^{2/3}}{n(\nabla H)^{1/2}} \nabla H + q = 0 \text{..} 2.8$$

Generally both types of modeling can be used to simulate flood flows in HEC-RAS. But each has its own advantages and limitations. The 1D model only computes the depth of the water in the channel and flood plain. Whereas, 2D modeling additionally determines in which direction the water is going to go (Brunner, 2016).

Finite volume Equation

Is a widely used method in computational fluid dynamics (MouKalled, , 2016). There are two methods in finite volume: cell vertex and cell centered.

Cell Vertex

This method uses a secondary mesh made up of a cell for every vertex. It has an advantage of simplifying the application of boundary condition because the cell centroids lie on the boundaries.

Finite volume equation is given as:

$$A\frac{\partial m\prime}{t} + \sum_{faces}\left(f_{n,x} + g_{n,y}\right)\Delta L = S'A \ldots\ldots\ldots\ldots\ldots\ldots\ldots\ldots\ldots\ldots\ldots\ldots\ldots .2.9$$

Where A is the area of a cell, m' and S' are averaged scalars or vectors, n,x ans n,y are unit normal components of x and y.

Alzahrani applied two-dimensional hydraulic modeling in riverine systems using HEC-RAS. In the study, both one dimensional and two dimensional simulations were performed on a reach of the Great Miami river and Bear Creek in Montgomery county, Ohio and the results were compared. Topographic data that were in raster form, geometric and cross-sectional data, land use classifications in terms of Manning's n value and flow data were data's needed to execute the research (Alzahrani, 2017).

The final results showed that building 2D flow areas by using HEC-RAS provides accurate flood plain mapping and also reduces time and effort required by modelers for building a 1D hydrodynamic model (Alzahrani, 2017).

3. Materials and Methods

3.1 Description of the Study Area

3.1.1 Geographic Location

The Gilgel Abay basin is located in north western Ethiopia. Geographical coordinates of the area are $10^{0}56'$ to $11^{0}51'$N latitude and $36^{0}44'$ to $37^{0}23'$E longtudes. It is one of the main sub-basins of the Lake Tana basin. Runoff from the Gilgel Abay contributes about 60% of the flow to the Lake (Wale et al, 2009). The river originates from a small spring at Gish Abay Mountains near Sekela town at elevation of 2900m.

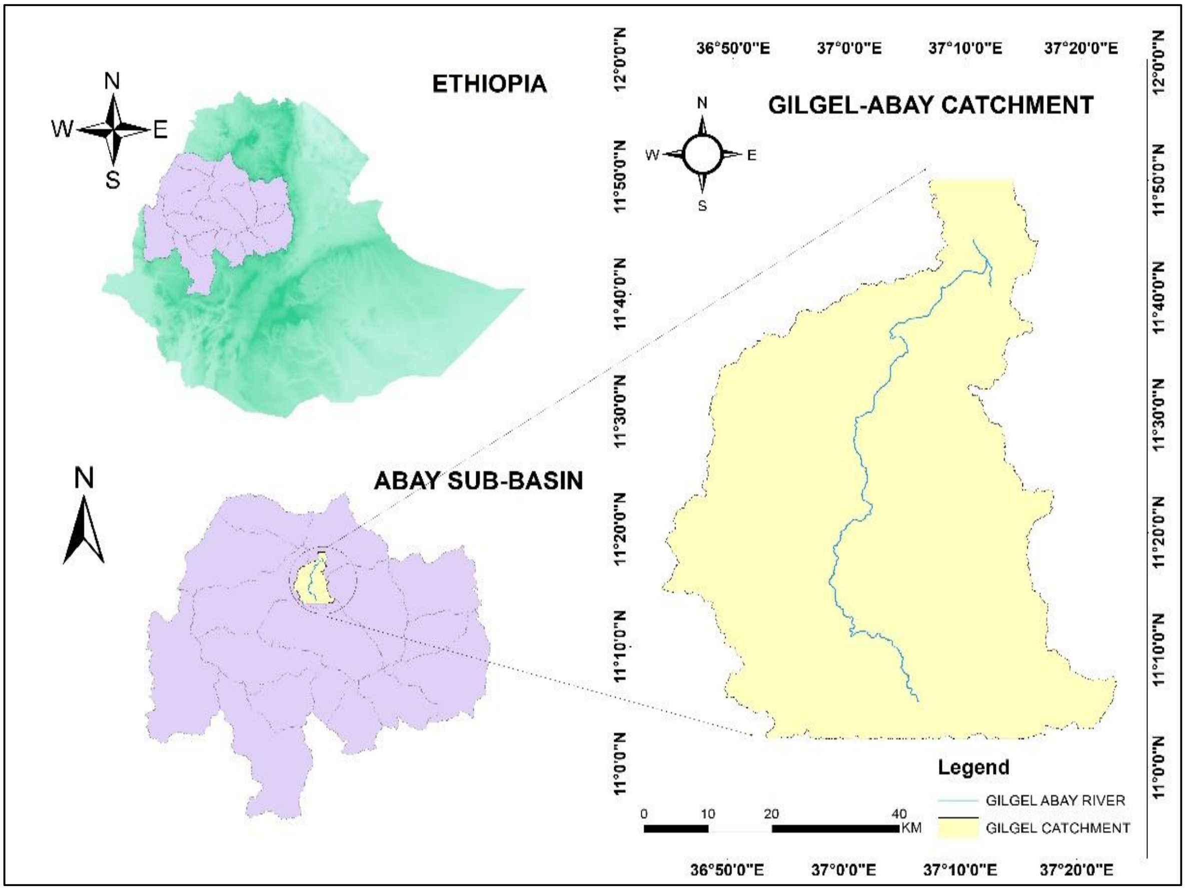

Figure 3- 1 Location map of the Gilgel Abay Catchmnet (ASF, 2020)

3.1.2 Topography

Rugged mountains topography characterizes most part of the catchment especially in the southern part but there is some low land within the basin as well. Elevation ranges from 1805m above the mean sea level (a.m.s.l) to 2900m amsl. Around 80% of the catchment area falls in the slope of (0-6%), 15% of the area falls in the slope range of (7-14%) and the remaining 5% is steeper than (14%) (Ashenafi, 2007).

3.1.3 Climate

Ethiopia's climate is generally affected by the inter-tropical convergence zone (ITCZ). The ITCZ passes over Ethiopia twice a year and this migration alternatively causes the onset and withdrawals of winds from north and south (SMEC, 2007). The Gilgel Abay basin falls within the cool semi-humid zone with mean annual temperature of 17-20^{0}C. The dry season occurs between October and May while the wet season occurs mostly between June and September when the ITCZ is to the north of the country. The climate is generally temperate at higher elevations and tropical at the lower elevation. The long term mean annual rainfall (1992-2003) at Bahir Dar station (1828m a.m.s.l.) south of Lake Tana is estimated to be 1416mm. According to Wale et al (2009) the mean annual humidity (1994-2004) at the station is estimated to be 58%.

3.1.4 Soil

There are five types of soils observed in this area: Lithosols, Luvisols, Nitisols, Vertisols and Cambisols (BCEOM, 1998) in combination with four diagnostic horizon modifiers: chromic, eutric, dystric and lithic. According to the work of BCEOM (1998), the whole Gilgel Abay catchment is mostly covered by Chromic Luvisols with an aerial coverage of around 2583 km^2. The cultivated areas mostly lie on this type of soil throughout the study area. In low lying areas particularly north on the Gilgel Abay basin, soils have been developed on alluvial sediments (SMEC, 2007).

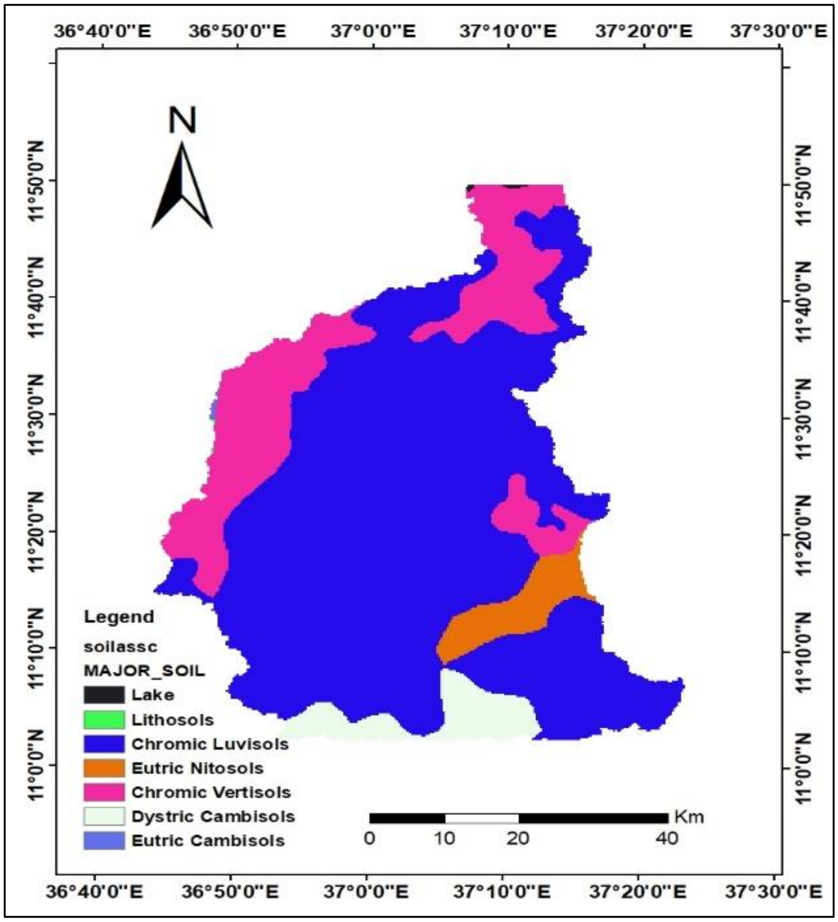

Figure 3- 2 Major Soil Types of Gilgel Abay Catchment

3.1.5 Land use and Land cover

Most of the catchment area is characterized by cropland with scarce woodlands and forested highlands. Besides the cultivated lands, the main land cover types are grassland, marshland and forest. The land cover classification include 62% agriculture, 17% forest, 11.6% shrub land, 9% grass land and 0.4% water and marshy lands. Land degradation is a major problem in the area (Tessema, 2006).

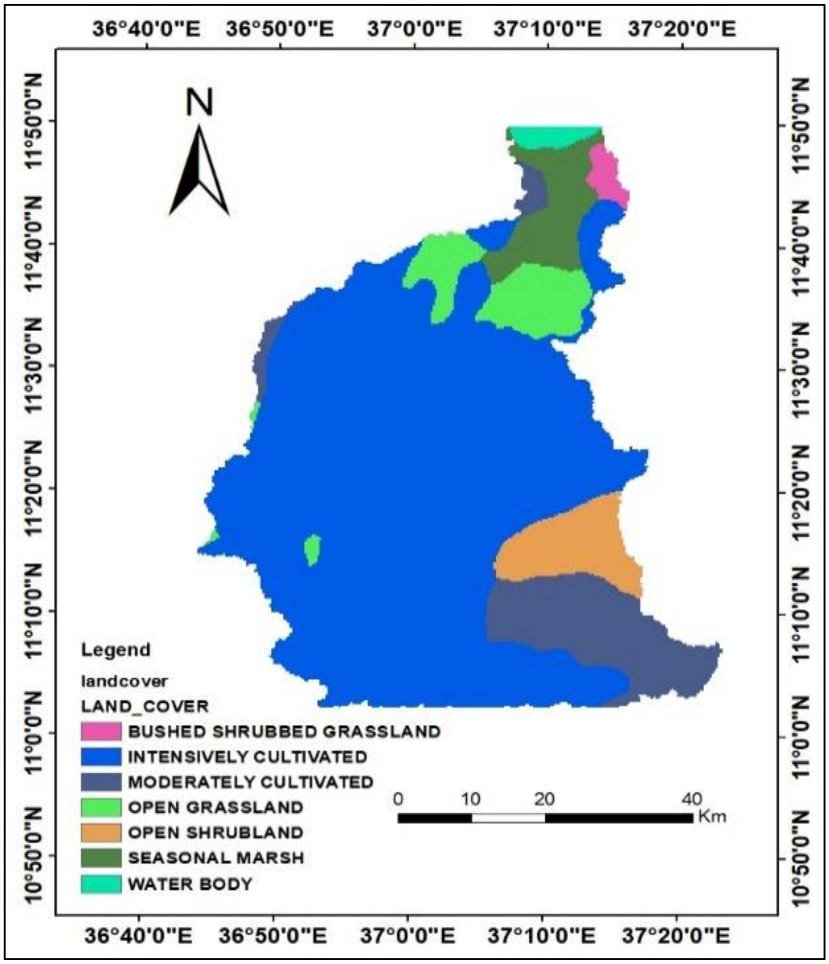

Figure 3- 3 Land Use, Land Cover of Gilgel Abay Catchment

3.2 Methodology

3.2.1 Data Collection

Metrological (rainfall and temperature) data, hydrological (stream flow) data and digital elevation model were collected from National metrological service agency (NMSA), Ministry of water irrigation and electricity and from Alaska Satellite Facility respectively.

Table 3- 1 Data's needed and their source

Data	Source
Metrological (rainfall and temperature) data	National metrological agency (NMSA) (1992-2018)
Hydrological (stream flow) data	Ministry of water irrigation and electricity (MOWIE) (2002-2017)

Digital elevation model (DEM)	Alaska Satellite Facility

3.2.2 Estimation of Missing data

This procedure is important because there may be discontinuity of rainfall records due to different reasons like damage of rain gauge or lack of recording. Methods used to estimate missing data are many (WMO, 2008). Common methods are station average, normal ratio, quadrant and regression methods. The station average method is the simplest method but may not be accurate when the total annual rainfall at any of the m region gauges differs from the annual rainfall at the point of interest by more than 10%. In this case, the normal ratio method is preferred. Due to its simplicity, the normal ratio method was adopted for this study.

$$P_x = \frac{1}{3}\left(\frac{N_x}{N_a}P_a + \frac{N_x}{N_b}P_b + \frac{N_x}{N_c}P_c\right) \qquad 3.1$$

Where: P_x is the current rainfall value for station X

P_a, P_b, and P_c are the current rainfall values for stations A, B, and C.

N_a, N_b, N_c, and N_x are the annual values for stations A, B, C, and X

Table 3- 2 List of selected gauging stations used for this study

No.	Station Name	Latitude	Longitude	Elevation	Database
1	Adet	37.49	11.27	2179	1986-2019(33)
2	Dangla	36.85	11.43	2116	1987-2019(32)
3	Meshenti	37.28	11.47	1958	1987-2019(32)
4	Merawi	37.16	11.41	2000	1991-2019(28)

3.2.3 Adjustment of Rainfall records

There may be lack of consistency of records therefore adjustments may be needed to be done. This may be due to unreported shifting of the rain gauge, significant construction work or change of observational procedure. The method used to check the inconsistency of records is double mass curve analysis.

3.2.4 Determination of Areal Rainfall

Rainfall point that is recorded at a single point must be converted to an aerial rainfall. Three methods are commonly used to determine the areal rainfall according to the characteristics of the rainfall. They are arithmetic average method, Thiesson polygon method and Isohytal method. In this paper, the Thiessen polygon method was used to determine the areal rainfall.

Thiessen polygon method- is used when rainfall varies from place to place in intensity and duration.

$$\bar{\bar{I}} = \frac{1}{A}\sum_{j=1}^{N} A_j \, I_j \quad \text{...3.2}$$

3.2.5 Fitting a flood probability distribution

A probability density function (PDF) is a continuous mathematical expression that determines the probability of a particular event. If a prediction is to be based on a set of hydrologic data, then the distribution that best fits the set of data may be expected to give the best estimates usually an extrapolation of the probability of an event occurring (Research, 2013).

Different probability distribution methods are considered to test the goodness of fit. These are General extreme value, Log- Pearson type three, Normal, Extreme value type 1, Log-normal, Gamma, Weibull, and Inverse Gaussian distribution methods.

3.2.5.1 Normal Probability distributions

The Normal distribution is the most familiar probability distribution (Alem M. , 2018), Its PDF is given by:

$$f(x) = \frac{1}{\sigma\sqrt{2\pi}} * exp(-\frac{\overline{(x-x)}^2}{2\sigma^2}) \quad \text{..3.5}$$

It is defined by two distribution parameters; the mean ($\bar{}$µ), and standard deviation (σ)evaluated by:

$$\frac{1}{N}\sum_{i=1}^{N} X_1 \quad \text{..3.6}$$

Where: xi is the magnitude of the ith event

N is the total number of events

The standard deviation (σ) which is a measure of the dispersion or spread of data set is given by:

$\sigma = \frac{1}{N} * \sum_{i=1}^{N}(X_i - \mu)^2$ 3.7

The normal distribution describes many random processes but it generally does not provide satisfactory fit for flood discharge and other hydrologic data (Ajumuka, 2013)

A particular event x can be related to the probability of excedence P by the following equation:

X $=\bar{x} + K * \sigma$..3.8

Where k is the frequency factor. Though, the normal distribution is not well suited to hydrologic data, the related distribution; the lognormal distribution works reasonably well (Research, 2013) The Log- normal distribution assumes that the logarithms of the discharge are themselves normally distributed. The equation describing normal distribution is modified for use in the case of log normal distribution if the following substitution is made with: -

$yi = \log xi$ 3.9

With x replaced by y, the mean of the logarithms and standard deviation becomes

$\bar{x} = \frac{1}{N}\sum_{i=1}^{N} \log X_i$..3.10

$\sigma = \frac{1}{N}\sum_{i=1}^{N}(\log X_i - \mu)$^2 ....3.11

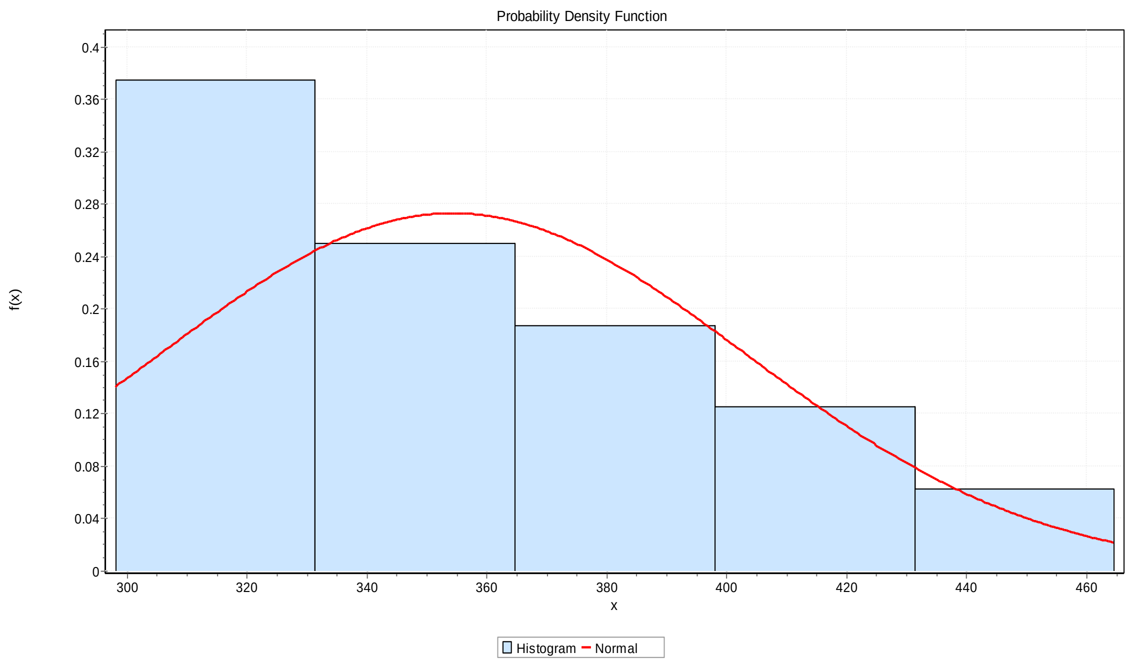

Figure 3- 4 Histogram of observed flow for Normal distribution

3.2.5.2 Lognormal Probability distributions

If the random variable $Y = \log X$ is normally distributed, then X is said to be lognormally distributed. Chow (1954) reasoned that this distribution is applicable to hydrologic variables formed as the products of other variables since if $X = X_{1,}X_2X_3 \cdots X_n$ then, $Y = log\ X = \sum_{i=1}^{n} X_i = \sum_{i=1}^{n} Y_i$, which tends to the normal distribution for large Z provided that the X; are independent and identically distributed (Freeze R. A., 1975).

$$\boldsymbol{f(x) = \frac{1}{x\sigma\sqrt{2\pi}}\left(-\frac{(y-\mu_y)^2}{2{\sigma_y}^2}\right)}\text{..................................}\ \boldsymbol{1}$$

Where, Y=log X, and the probability density function ranges between $x > 0$, and the equations for parameters in terms of the sample moments are, $\mu = \bar{y}, \sigma = s_y$.

The magnitude x_T of a hydrologic event for the lognormal distribution, the same procedure applies except that it is applied to the logarithms of the variables, and their mean and standard deviation are used in the normal distribution equation.

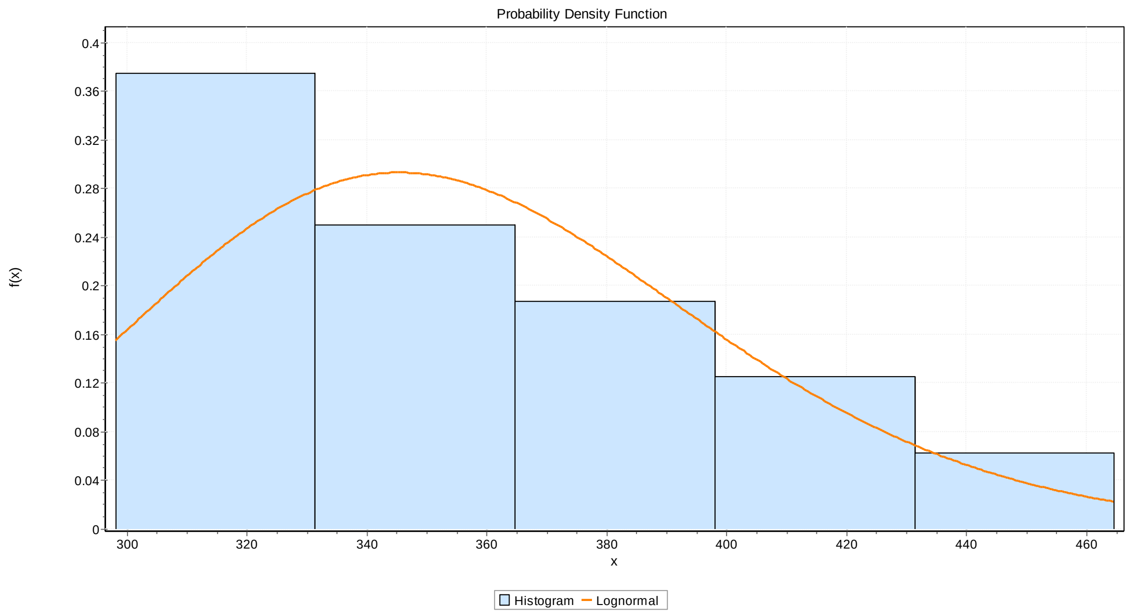

Figure 3- 5 Histogram of observed flow for Log-normal distribution

3.2.5.3 Log-Pearson type III

The problem with most hydrologic data was that an equal spread does not occur above and below the mean. The lower side is limited to the range from mean to zero while there is theoretically no limitation on the upper range thereby contributing to what is called a skewed distribution. The coefficient of skew (G) is defined mathematically by:

$$G = \frac{N * \sum (X - X)^3}{(N-1)(N-2) * S^3} \quad \text{.......3.12}$$

In wich: X=Logarithm of annual peak flow

N=number of items in data set

$\bar{x}$ = mean logarithm

S=Standard deviation of logarithms

G=Skew coefficient of Logarithms

It is to take account of the skew that may exist in data that the log Pearson type III distribution was developed to improve the fit (Ajumuka, 2013). The distribution uses three parameters namely: mean, standard deviation and skew coefficient which are obtained using equations (3.10), (3.11) and (3.12) respectively.

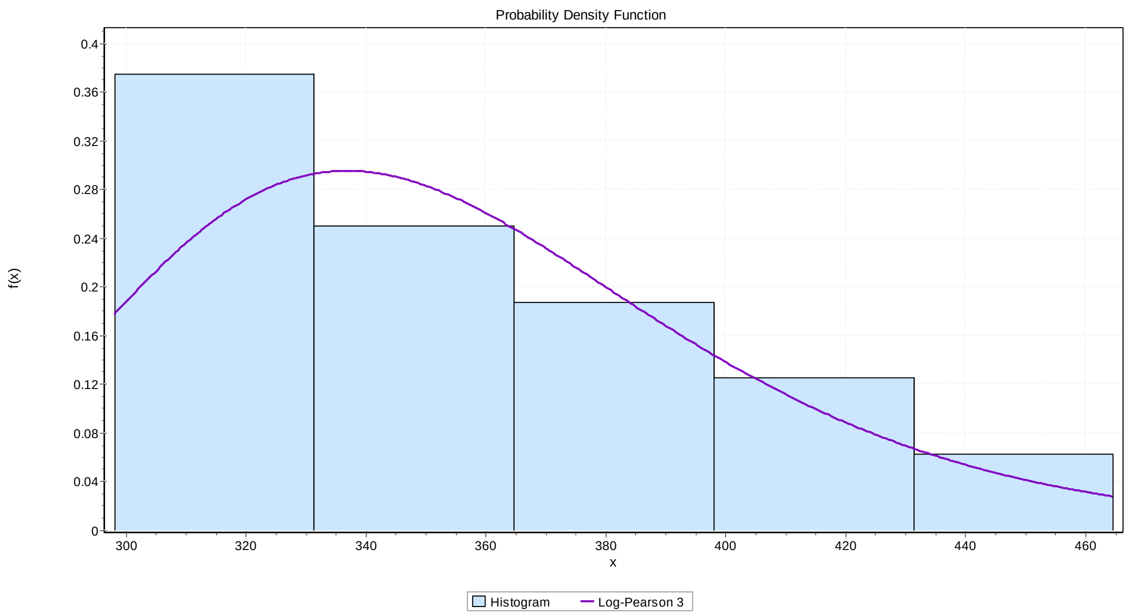

Figure 3- 6 Histogram of observed flow for Log-pearson 3 distribution

3.2.5.4 Easy fit Software

Sample data's are simulated and fit with statistical distributions by using this software. After the best model is chosen, the analyzed result will be used to make decisions. The software can be used as an add-on on Excel spread sheet or can function as standalone windows application.

Goodness of fit tests such as Kolmogorov-Smirnov, Anderson-Darling and Chi-square were conducted at significance level (α=0.05) for choosing the best probability distribution (Alem M. , 2018). The distribution with minimum statistics value will be the value that is best fit with the data.

Kolmogorov-Smirnov Test

This test was used to decide if a sample comes from a hypothesized continuous distribution. It is based on the empirical cumulative distribution function (ECDF). Assume that to have a random sample X1, ...,Xn from some distribution with CDF F(x). The empirical CDF is denoted by:

$F_n(x) = \frac{1}{n}$ *[Number of observations $\leq x$] ……………………..........................3.15

The Kolmogorov-Smirnov statistic (D) is based on the largest vertical difference between the theoretical and the empirical cumulative distribution function:

$D = \max(F(xi) - \frac{i-1}{n}, \frac{i}{n} - F(xi))$……………………………………………………3.16

Anderson-Darling Test

The Anderson-Darling procedure is a general test to compare the fit of an observed cumulative distribution function to an expected cumulative distribution function. This test gives more weight to the tails than the Kolmogorov-Smirnov test. The Anderson-Darling statistic (A2) is defined as

$A2 = -n - \frac{1}{n} \sum_{i=1}^{n} (2i - 1) * [\ln F(X_i) + \ln(1 - F(X_{n-i+1}))]$ ……………………….3.17

Chi-Squared Test

The Chi-square test assumes that the number of observations is large enough so that the chi-square distribution provides a good approximation as the distribution of test statistic. The Chi-squared statistic is defined as.

$X^2 = \sum_{i=1}^{k} \frac{(O_i - E_i)^2}{E_i}$……………………………………………………..3.18

Where: Oi =is the observed frequency

Ei =Expected frequency $Ei = F(X_2) - F(X_1)$

i= number of observations (1,2, 3……. k)

F = the CDF of the probability distribution being tested.

The observed number of observation (k) in interval 'i' is computed from equation given below

$K = 1 + \log_2 n$…………………………………………………………...3.19

n = sample size

This equation is for continuous sample data only and is used to determine if a sample comes from a population with a specific distribution (Olofintoye, 2009).

3.2.6 Terrain Pre-processing using ARC-GIS

Terrain processing is processing of DEM to delineate watersheds. Basic watershed properties such as area, slope, flow length and stream network density are extracted from delineating streams and watersheds. ARC-HYDRO tool was used for such work. The following procedures: DEM reconditioning, fill sink, flow direction, flow accumulation, stream definition, stream segmentation, catchment grid delineation etc. were done.

Then the other tool, HEC-GEOHMS uses DEM and undergoes sub-basin delineation and prepares a number of hydrologic units that are provided as an input for HEC-HMS.

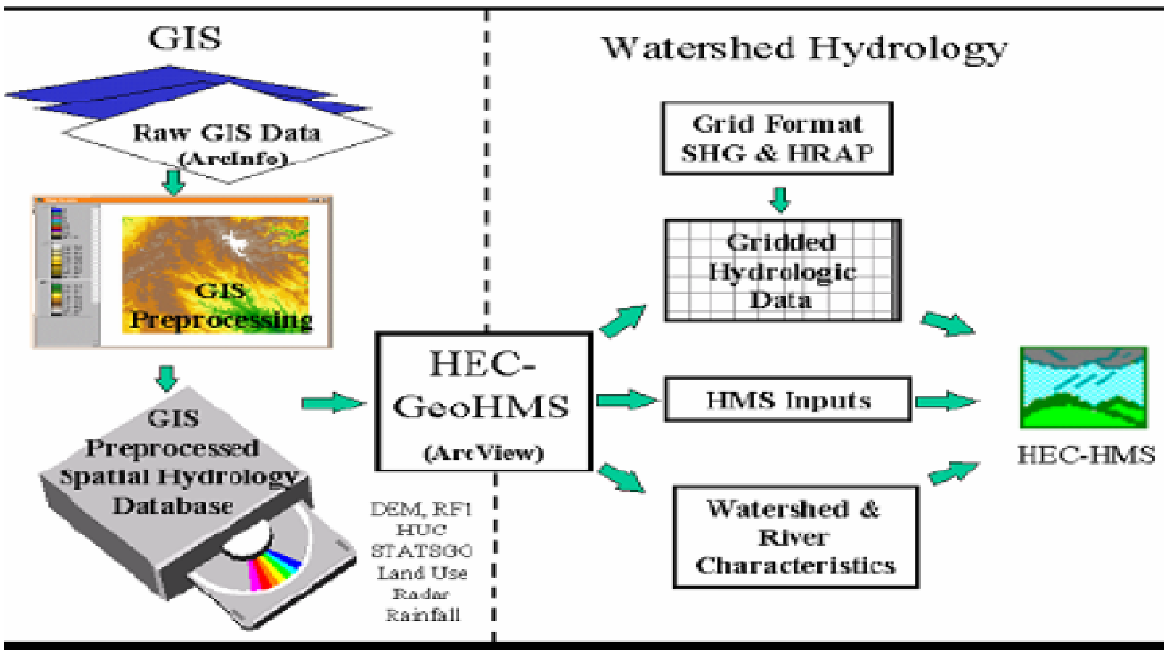

Figure 3- 7 Relation between GIS, HEC-GEOHMS, HEC-HMS (Davis, 2009)

3.2.7 HEC-HMS Modeling

After the hydrologic units were prepared by HEC-GEOHMS to be inputs for the software, infiltration loss, runoff transformation, flow routing and basin flow were determined. Infiltration loss was determined using SCS curve number method due to its simplicity and non- demanding of too much data. Runoff transformation was determined using, SCS-unit hydrograph method due to its good performance than the other methods. Base flow was computed using constant monthly values. Musk Ingham routing was used to route the channel for continuous hydrological modeling.

3.2.7.1 Basin Model

A basin model consisting of three sub basins was generated with Arc-GIS and was setup in HEC-HMS. Depending on the available time and data requirement, simulation was done with SCS curve number method, SCS unit hydrograph and Monthly Constant base flow condition.

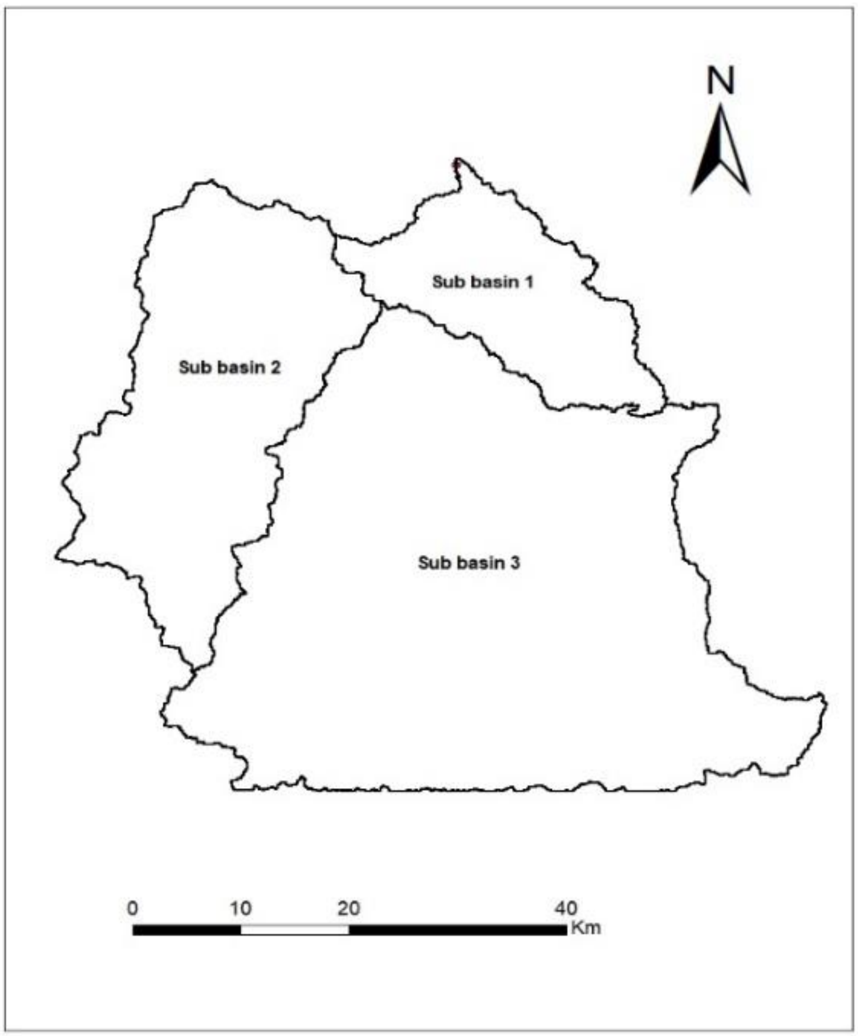

Figure 3- 8 Sub basins for Gilgel catchment

The components of basin model are classified into four. These are loss determination, transform method, base flow and routing method.

Loss determination which is defined as the amount of rainfall infiltrated into the soil, was estimated using SCS curve number method. This was due to the method's capability of calculating precipitation excess as a function of cumulative precipitation, soil cover, land use and antecedent moisture.

$$Q = \frac{(P+I_a)^2}{P-I_a+S} \ldots\ldots\ldots\ldots 3.20$$

Where Q is accumulated direct runoff, mm, P accumulated rainfall (potential maximum runoff), mm, Ia initial abstraction including surface storage, interception, and infiltration prior to runoff, mm and S potential maximum retention, mm.

The relationship between Ia and S was developed from experimental catchment area data. It removes the necessity for estimating Ia for common usage. The empirical relationship used in the SCS runoff equation is:

$$S = 25.4\left(\frac{1000}{CN} - 10\right) \ldots\ldots\ldots\ldots 3.21$$

$$I_a = 0.2 * S \ldots\ldots\ldots\ldots 3.22$$

By substituting the CN determined from HEC-GeoHMS in equation 3.21, the potential maximum retention was determined. Then the potential maximum retention was used to determine the initial abstraction using equation 3.22.

Transform method converts excess precipitation on a sub basin to direct runoff at the sub basin outlet. The SCS unit hydrograph model for direct runoff was chosen due to its simplicity, minimum data requirement, and good performance than the other methods.

Base flow which is an important parameter as it defines a minimum river depth over which additional runoff accumulates was estimated using the constant monthly flow method. This method was used for it is the simplest base flow model in the program and it represents the flow as a constant flow. The initial value before calibration was taken as the average of minimum flow.

The method that was used to route the channel for continuous hydrological modeling is the musk Ingham routing method. The objective function used for optimization was the peak weighted RMS error with uni-variate gradient search optimization algorism.

3.2.7.2 Metrological Model

The metrological modeling succeeded after completing the basin model and so, the specified hyetograph method was chosen for this paper. For evapotranspiration, specified evapotranspiration was used.

The value of each parameter found in HEC-HMS must be specified to use the model for estimating run-off volume and routing hydrographs. Some of the model parameters cannot be estimated by observation or measurement of the watershed characteristics. For example, the parameter X and K in the Muskingum routing model cannot be measured but can be estimated approximately.

Optimization begins from initial parameter estimates and adjusts them so that the simulated results match the observed stream flow as closely as possible.

3.2.7.3 Muskingum Model

The Muskingum method is often used in channel routing. The method is dependent primarily upon the following factors: the number of integer steps for the routing, Muskingum K coefficient in hours and Muskingum X coefficient. This model uses a simple finite difference approximation of the storage continuity equation. Storage is modeled as the sum of prism storage and wedge storage. The Muskingum defines the storage as:

$$S_t = KO_t + KX(I_t - O_t) = K(XI_t + (1 - X)O_t \qquad 3.20$$

Where K=travel time of the flood wave through routing reach; and X=dimensionless weight ($0 \leq X \leq 0.5$). The quantity K(XIt+(1-X)Ot is a weighted discharge.

Following the computation of basin model, metrological model and control specifications calibration and validation of the model was executed. Then sensitivity analysis was done to determine which parameters of the model have the greatest impact on the results. Finally model performance was evaluated using coefficients of determination (R^2) and Nash Sutcliff (ENS).

3.2.7.4 Modeling by frequency storm method

With the input from HEC-GeoHMS and some edition from the main HEC-HMS, the model is simulated for rainfall intensity of 2, 10, 50, and 100 year return periods. The frequency intensity values are found from the Ethiopian Roads Authority drainage manual (Ethiopian Roads Authority, 2013).

The study area's meteorological station is found in A_2 meteorological area, therefore, rainfall intensity is selected from the graph of A_2, ERA drainage manual shown in the figure below.

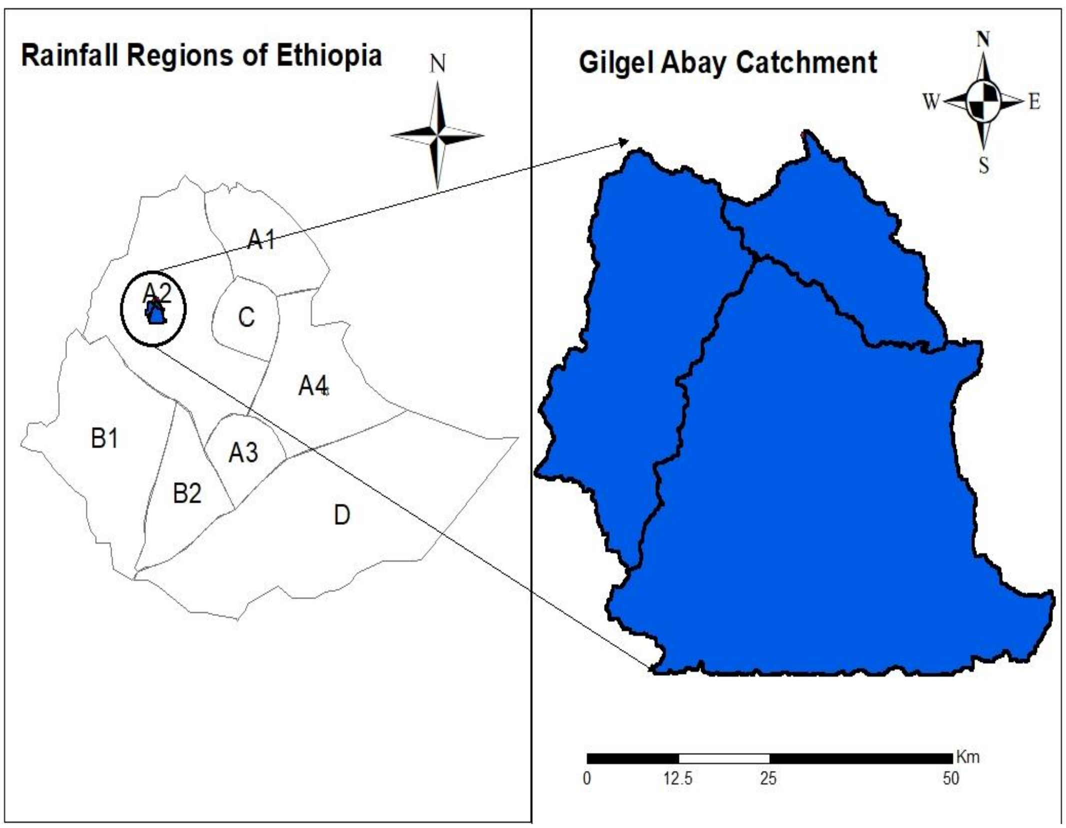

Figure 3- 9 Rainfall regions and Gilgel Abay Catchment

Table 3- 3 IDF table for the study area (Ethiopian Road authorities, 2001)

Duration (hr)	RF depth for various return period				
	2	**10**	**25**	**50**	**100**
1	22.51	32.28	37.19	40.79	44.42
2	28.53	40.91	47.14	51.69	56.29

3	32.05	45.96	53.13	58.07	63.24
6	38.22	54.81	63.42	69.25	75.42
12	44.76	64.18	73.7	81.1	88.32
24	52	74	85.7	94	102

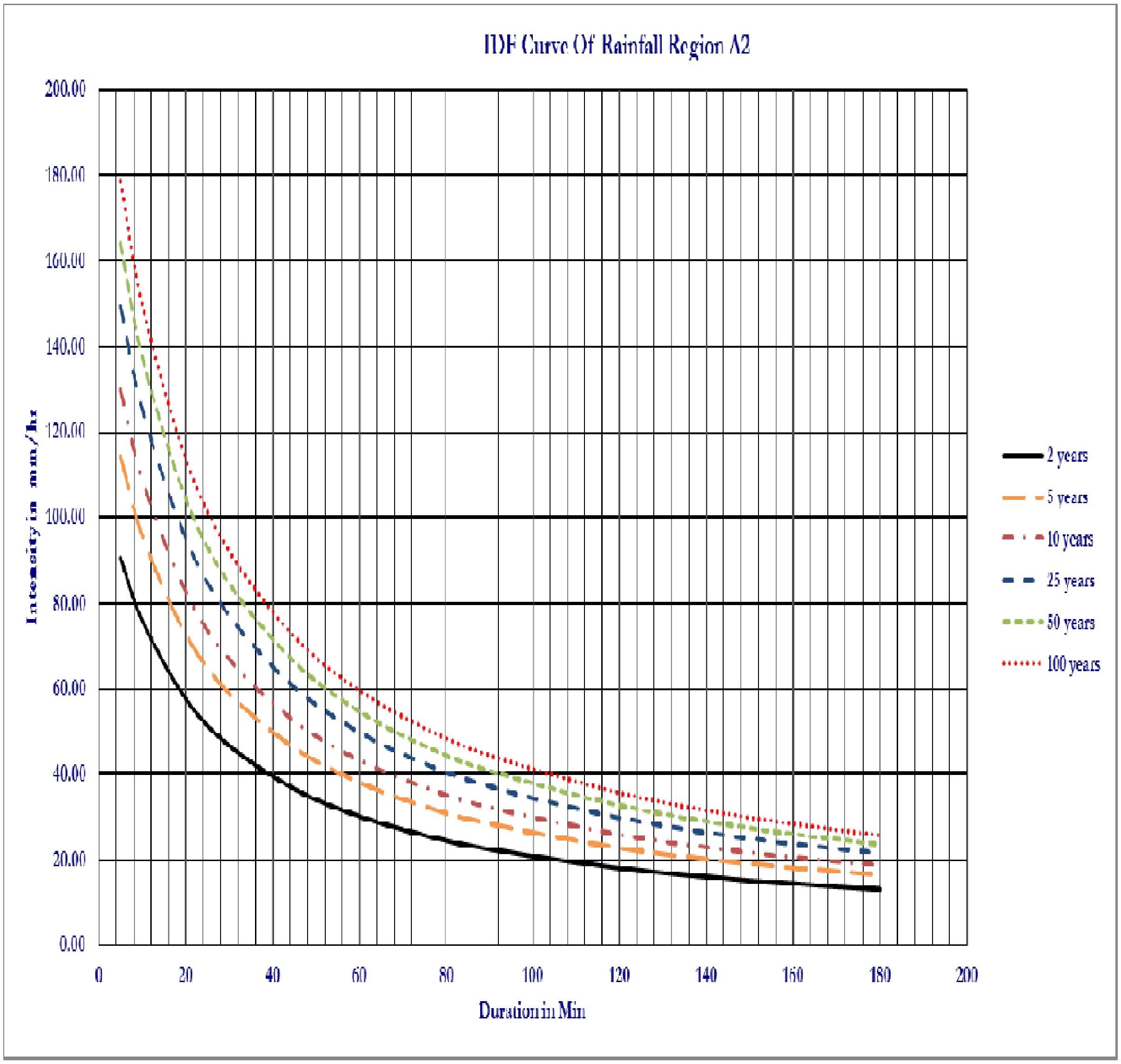

Figure 3- 10 IDF Curve for Rainfall Region A2 (Ethiopian Roads Authority, 2013)

3.2.8 Calibration and Validation

HEC-HMS modeling can be performed considering different time series values. A total of sixteen years historical data from 2002-2017 was used. Two years was used for startup and then calibration was performed for a period of nine years (2004-2012) and validation was executed for a period of five years (2013-2017) on the catchment area using daily flow basis. By using the observed flow, calibration was done both manually and automatically at the outlet of the catchment.

3.2.9 Sensitivity Analysis

Sensitivity analysis is a method to determine which parameters of the model have the greatest impact on the model results. There are three parameters (curve number, initial abstraction and lag-time) of the event model that were subject to the sensitivity analysis. The SCS curve number method, which is used to handle the infiltration loss in the sub-basins has three parameters such as curve number, initial abstraction and percent impervious area in the basin.

3.2.10 Model efficiency/performance

The performance of a model must be evaluated on the extent of its accuracy, consistency and adaptability (Abushandi, 2013). A forecast efficiency criterion was therefore necessary to judge the performance of the model. Assessing performance of a hydrologic model requires subjective and/or objective estimates of the closeness of the simulated behavior of the model to observations.

For the Gilgel Abay catchment study, model simulation has been evaluated using efficiency criteria such as coefficient of determination (R^2) and [Nash Sutcliff (ENS), 1970]. The R^2 coefficient and ENS simulation efficiency measure how well trends in the measured data are reproduced by the simulated results over a specified time period and for a specified time step.

The statistical index of modeling efficiency (ENS) values range from 1.0 (best) to negative infinity. The model simulation can be judged as satisfactory if NSE is greater than 50%, good if it is greater than 65% and very good if it is greater than 75% (Moriasi, D.N, 2007).

The range of values for R^2 is 1.0 (best) to 0.0. Zero indicates no linear relationship, 1 indicates a perfect positive linear relationship as one variable increases in its values and the other variable also increases in its values through an exact linear rule. Values between 0 and 0.3 indicate a weak linear relationship through a shaky linear rule. Values between 0.3 and 0.7 indicate a moderate linear relationship through a fuzzy firm linear rule. Values between 0.7 and 1 indicate a strong linear relationship through a firm linear rule (Ratner, 2009).

The Nash Sutcliffe (ENS) efficiency equation is given by:

$$E_{NS} = 1 \frac{\sum_{i=1}^{n}(q_{oi}-q_{si})^2}{\sum_{i=1}^{n}(q_{oi}-q_{o})^2} \ldots\ldots 3.21$$

And the standard R^2 is given by:

$$R^2 = \frac{[\sum_{i=1}^{n}(q_{si}-q_{s})(q_{oi}-q_{o})]^{\wedge}2}{\sum_{i=1}^{n}(q_{si}-q_{s})^2 \sum_{i=1}^{n}(q_{oi}-q_{o})^2} \ldots\ldots 3.22$$

Where: qo, i = observed value at the i th time interval

qs, i = simulated value at the i time interval

qo, av = average value of the observed discharge

qs, av =average value of the simulated discharge

3.2.11 Hydraulic Modeling

3.2.11.1 Input Data and Model Components

Hec-Ras computes water surface elevations at all locations using steady flow simulations or unsteady flow simulation (routing hydrographs through the system). The data needed to carry out these computations include geometric data, steady flow data or unsteady flow data. The program allows users to determine surface elevations at any point of interest. For this paper the data's used to carry out the computations are geometric data and unsteady flow data. The input data was imported from ARC-GIS (Gary, 2016).

Pre-Ras processing

The geo-spatial data used in Hec-Ras was processed using an Arc-GIS extension tool called Hec-GeoRAS, which is specifically designed for this purpose. An interface method is used by the tool to provide a direct link to transfer information between ARC-GIS and HEC-RAS. The model uses geometric attribute data from an existing digital terrain model (DEM) in TIN format and exports results to HEC-RAS model (Akerman, 2009).

The overall aim of this sub-section is to develop the spatial data required to create the geometry file that is going to be imported in Hec-Ras. The digital terrain model was first generated, then 2D spatial features were defined. After that, the 3D spatial data was generated and finally the output was imported to Hec-Ras.

2D Spatial features Definition

After the digital terrain representation was generated, the geometric information that was required by Hec-Ras was extracted. The geometric data extracted included the stream center lines, left and right bank lines, flow paths and cross-sections along the streams.

The bank and flow path lines were drawn dependently. Cross-sectional lines drawn crossed stream centerlines exactly once, bank lines exactly twice (left and right) and flow paths exactly three times (left, right and center).

Cross-Section Geometry

Ground surface profiles (cross sections) and the measured distances between them are important to analyze flow in natural streams. The cross-section of a river is defined by setting the station and elevation data (X-Y data) from left to right along the downstream direction (Gary, 2016).

Cross section that extends about 30 km was extracted from Google earth and the DEM data. The TIN was also made from the points that were extracted from Google earth and DEM. The channel geometry was best represented by the Google earth data than the DEM.

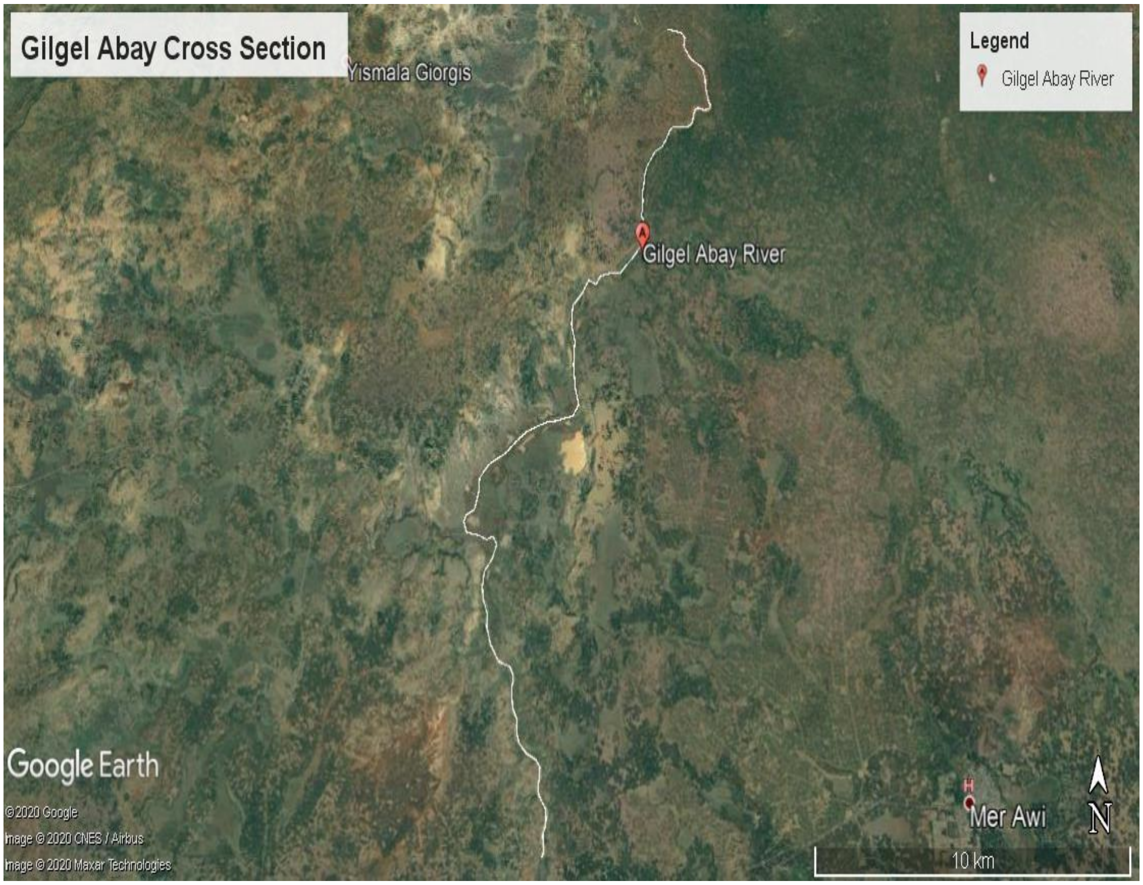

Figure 3- 11 Gilgel Abay River Cross-Section taken from Google Earth

A tool that accesses aerial, satellite imaginary and other geographic data over the internet and ocean bathymetry to represent the earth as a three dimensional globe is known as Google Earth. It uses a digital elevation model (DEM) data that is collected by NASA's Shutter Radar Topography Mission (STRM) (Pandya, 2017).

Using this software, geometric data that extends up to 30 km was extracted. A total number of 111 cross sections with varying width as well as distance of left and right bank and river center line were drawn along the river.

Figure 3- 12 Gilgel Abay River Cross Section in Google Earth

Then the layers stream center line, flow path centerline, flow path lines (left and right), bank lines (left and right) and cross-sections were defined on the TIN layer, according to the data extracted from Google Earth.

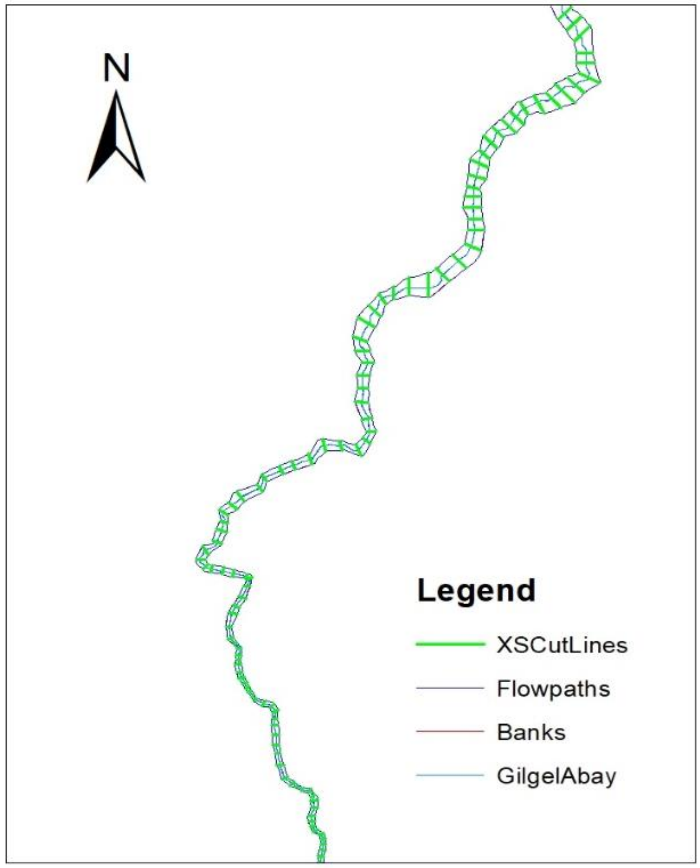

Figure 3- 13 Digitized Gilgel Abay River Scheme with Ras Layers

Finally, 3D spatial data, which identifies the stream network and the HEC-RAS model layout was generated. Then the generated geometric data was exported to HEC-RAS.

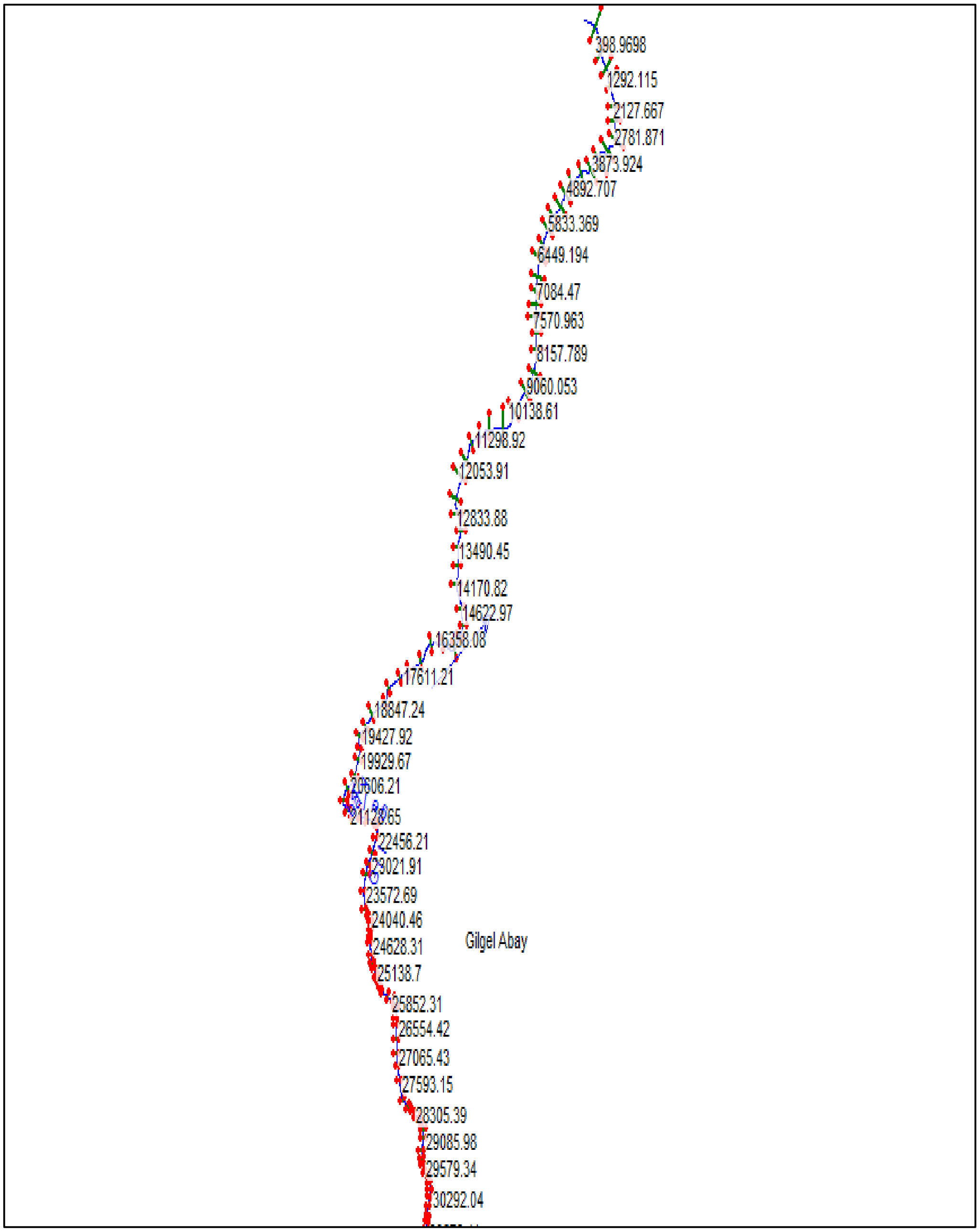

Figure 3- 14 Cross Section Exported to HEC-RAS

3.2.11.2 Two-Dimensional Modeling

After the geometric data was exported to HEC-RAS, it was opened in RAS-Mapper. The spatial co-ordinate projection of the data was defined and the DEM of the study area was imported to create the terrain model.

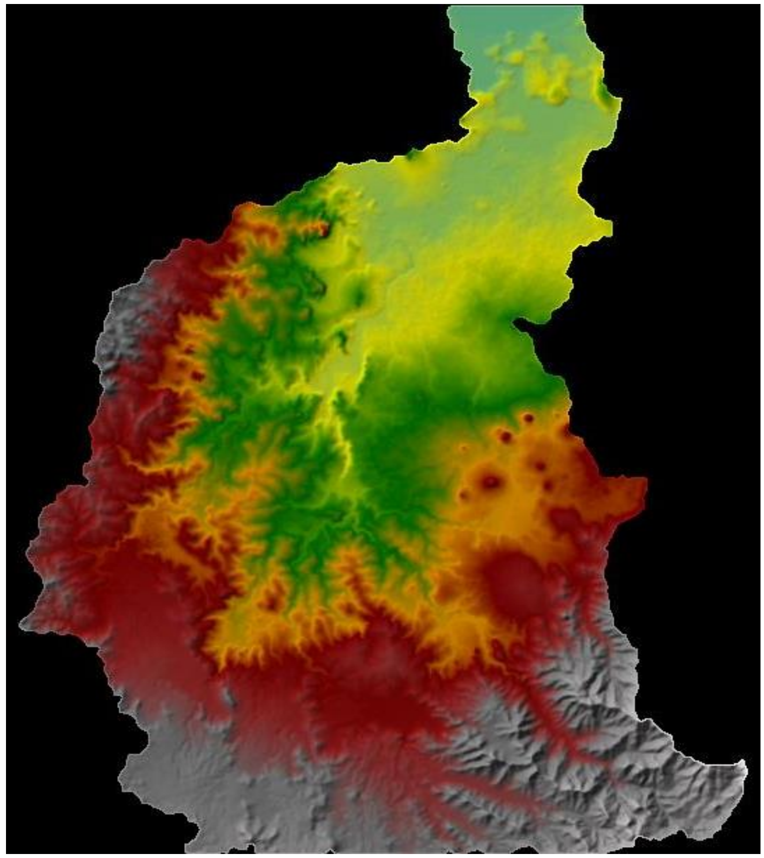

Figure 3- 15 Terrain Data Layer

In hydraulic modeling the terrain data does not often include the actual terrain underneath the water surface in the channel region. This can be improved by creating a terrain model of the channel region and combining it to the general surface terrain model. Terrain model of the channel was created using geometric data's: stream centerline, bank line, cross sections and cross sections interpolation surface (Gary W. Brunner, 2016).

Then the base terrain model was combined with the newly created channel only terrain model and a new combined terrain model was created.

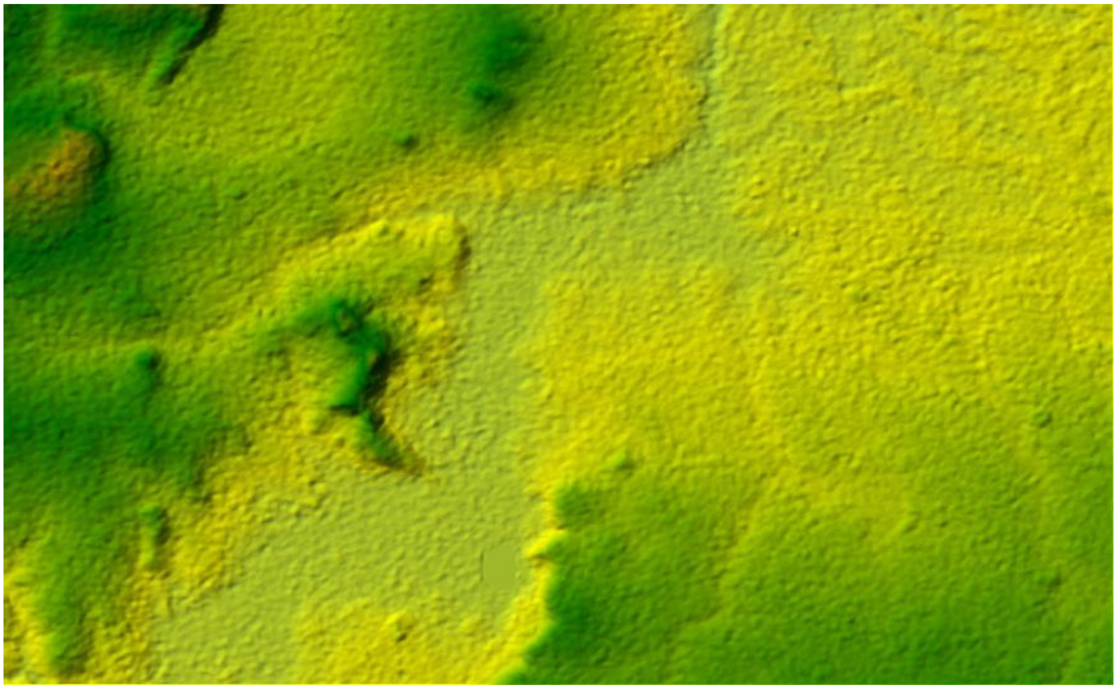

(a)

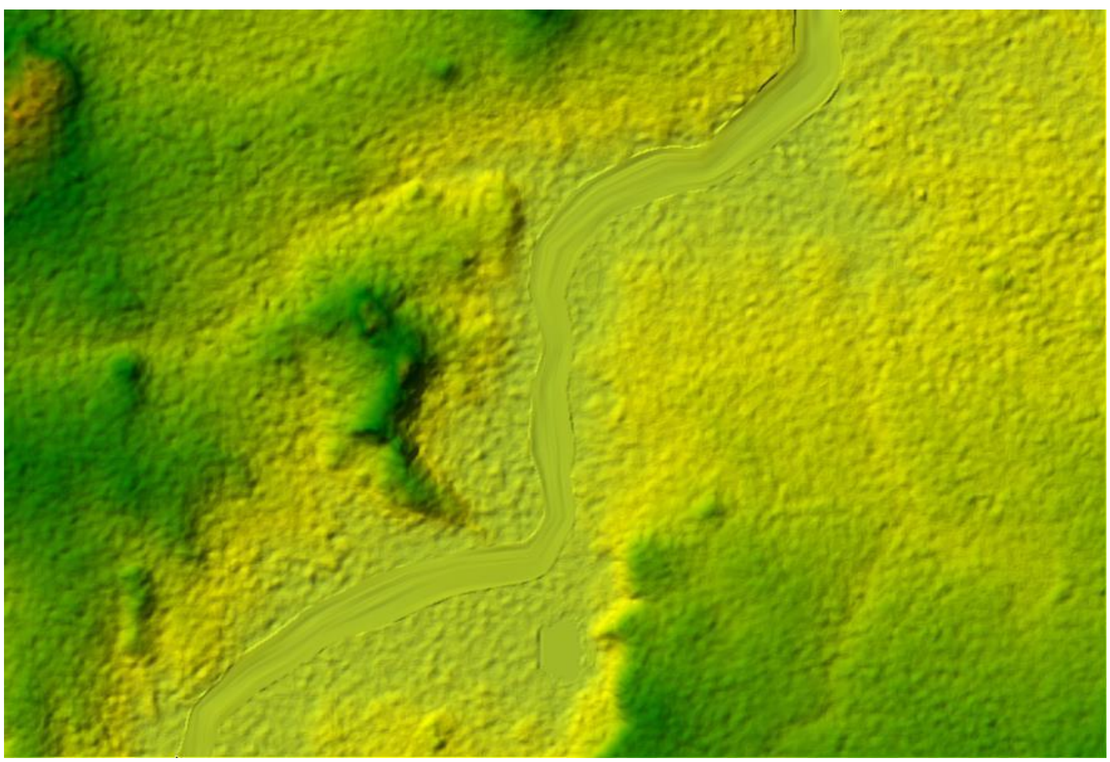

(b)

Figure 3- 16 a) Original Terrain Model   b) New Terrain model with channel data

2D Flow Area Mesh

The main concept of two dimensional modeling is the use of computational mesh. Water elevation at every computational grid cell generated is estimated for a given computational time step. The computational mesh generated depends on the slope of the water surface. If the slope of water surface is flat, larger grid cell sizes are appropriate and if it is steep, smaller grid, cells are used. A 2D flow area polygon, which defines the boundary for computation was drawn. After that, 100*100 size computational mesh was generated (Gary W. Brunner, 2016).

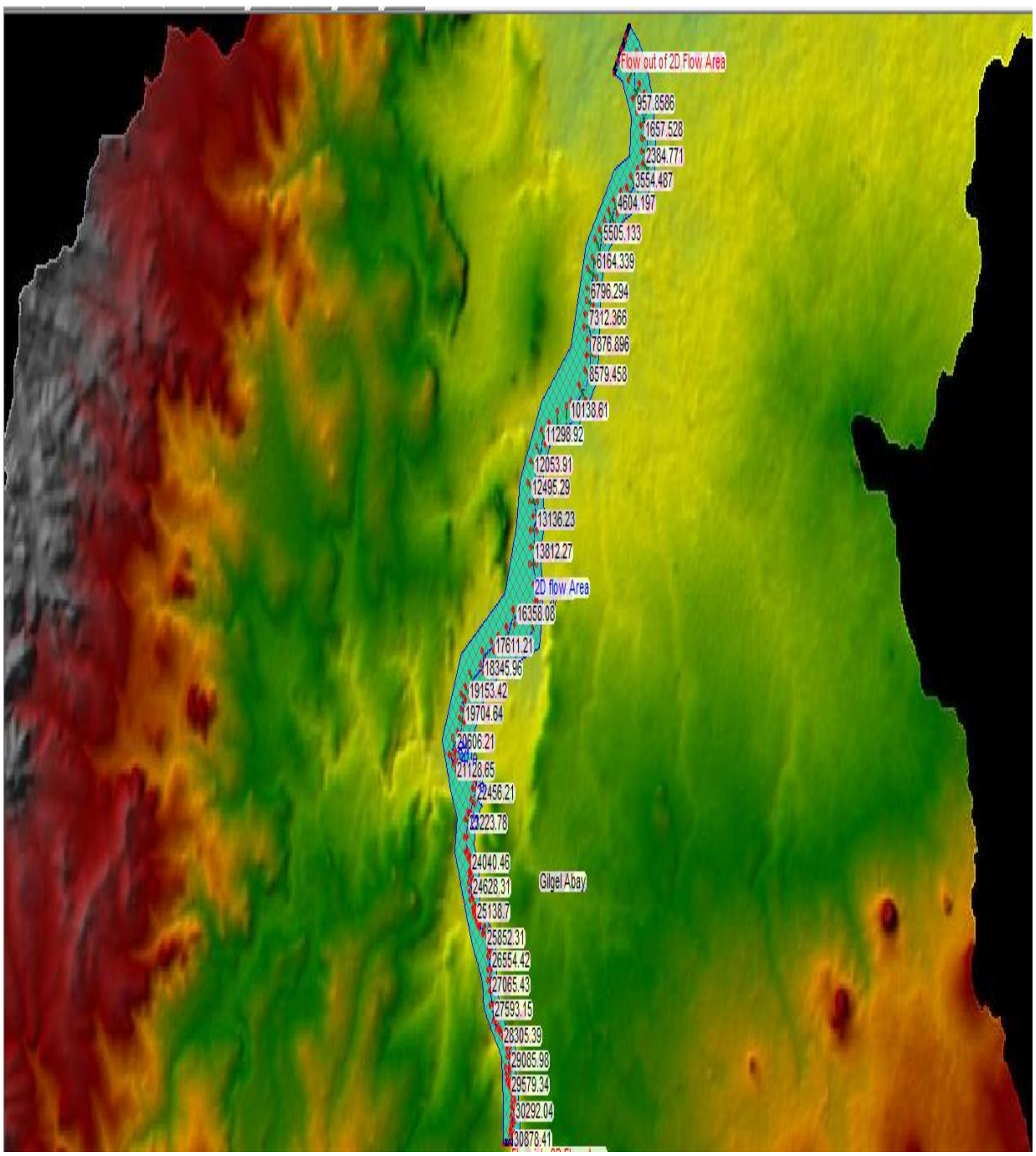

Figure 3- 17 Created 2D Flow Area Mesh

Land Use classification

HEC-RAS uses manning's formula to compute friction losses along the ground surface. Friction losses are used in the solution methodology employed by the conservation of momentum equation. A land cover data set was associated with the geometry file to specify manning's n values that were used for every type of land cover in the terrain.

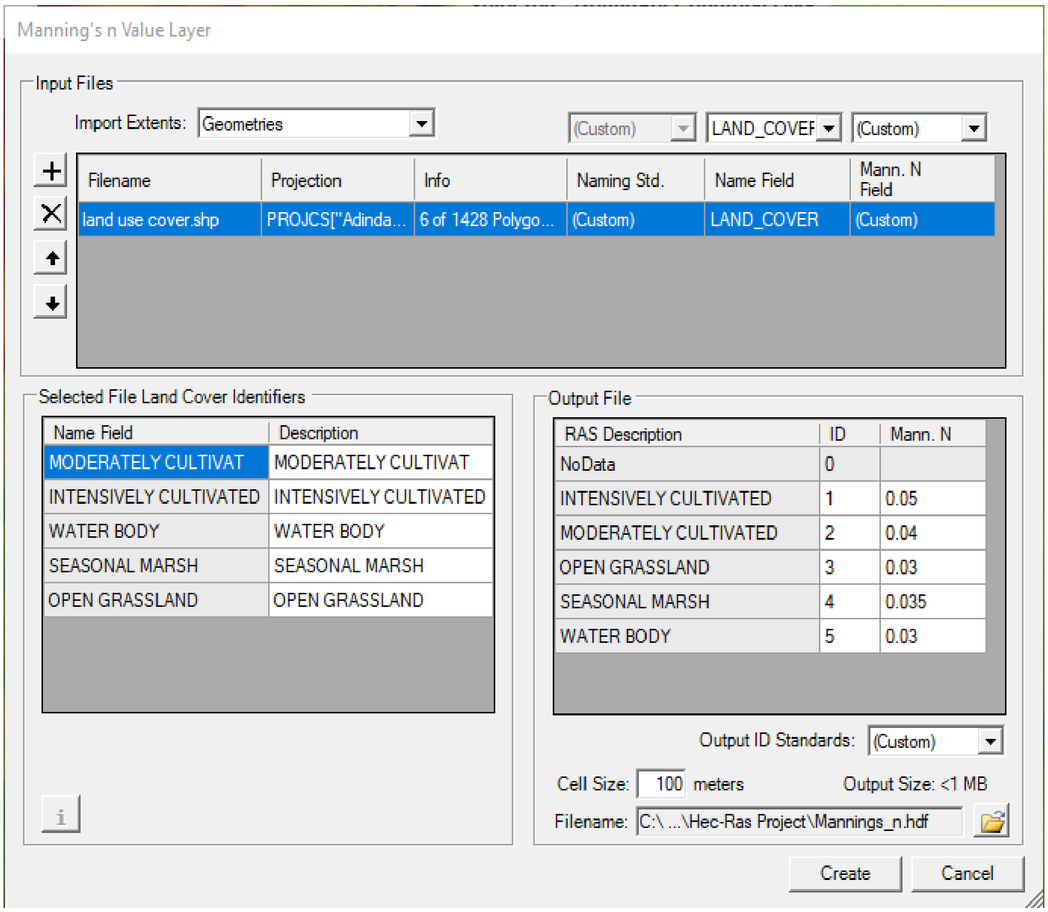

Figure 3- 18 Figure Land Classification Layer Editor

The land use classification of the area was taken from MOWIE and manning's n values for each type of land use characteristic was provided based on published values for similar conditions (Ethiopian Roads Authority, 2013) and on engineering judgment.

Finally, land cover versus manning's n value table was developed in order to define roughness values for 2D flow area.

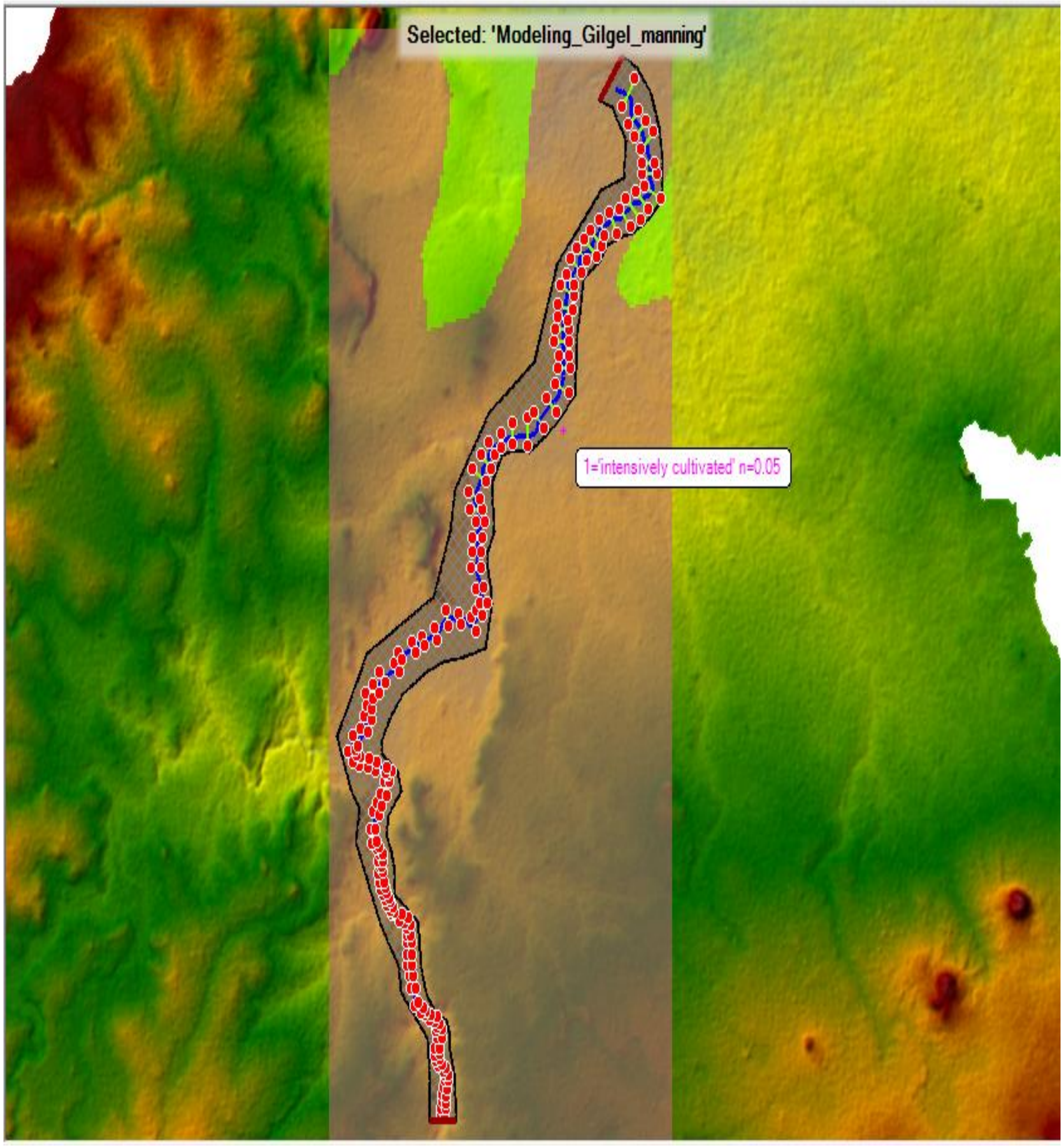

Figure 3- 19 Polygon Shape File Containing Land Classification Values

The main channel, left and right overbank were selected based on their description of land use and it was observed that it was under intensively cultivated areas therefore the roughness values were taken as 0.05 and 0.055 respectively.

3.2.11.3 Calibration of HEC-RAS for Manning's Roughness Coefficient 'n'

Sensitivity and uncertainty analysis of the roughness coefficient were performed using the software AHYDRA. The software is a freeware application that automates features from hydraulic software such as HEC-RAS. It allows updating boundary conditions, executing the simulations and viewing the results from a single screen and a single instruction (button click) (Vladyman, 2011).

River and reach names, overbank and channel roughness, upstream and downstream cross sections are the data's needed to simulate the river with the boundary conditions and the results can be shown in either 2D plot, 3D plot or in tables.

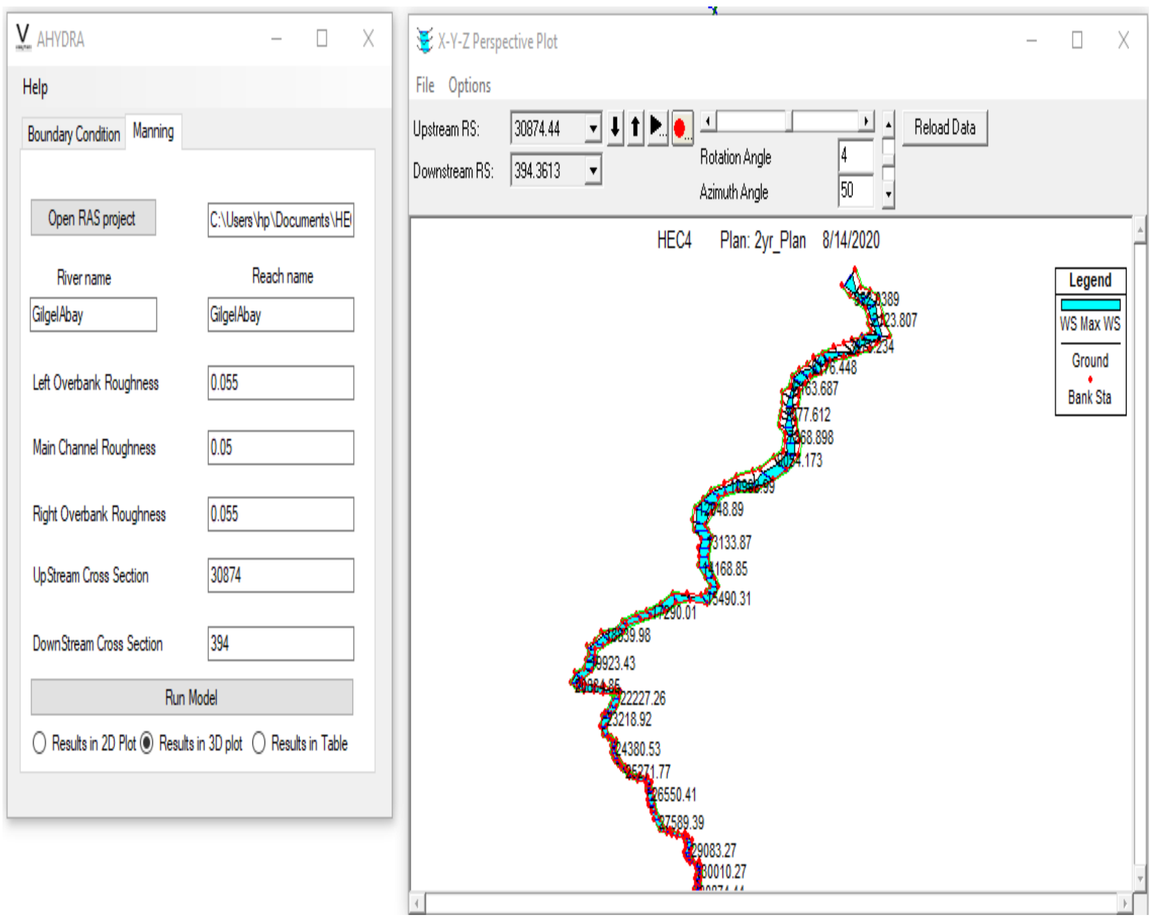

Figure 3- 20 AHYDRA Results in 3D Plot

Hydraulic Property Tables

The computational mesh was pre- processed in order to develop an elevation versus storage volume curve for each cell and a series of hydraulic property curves (elevation vs. wetted perimeter, area and roughness) for each cell face. These property tables were derived from the details of the underlying terrain as well as the manning's n value (Alzahrani, 2017).

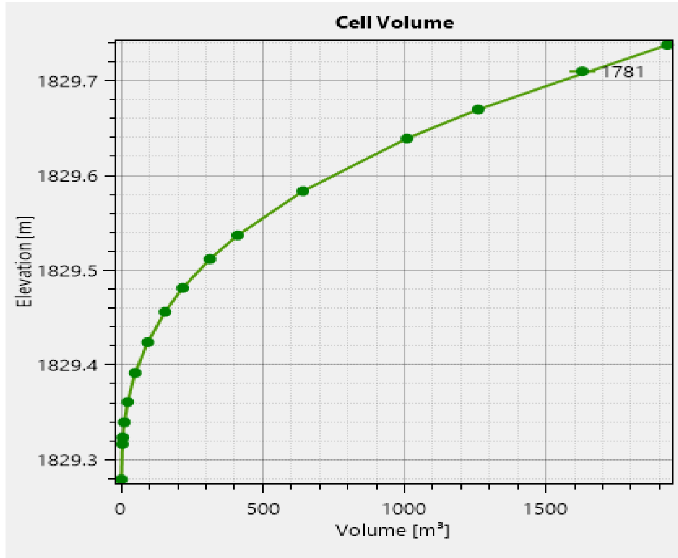

Figure 3- 21 Elevation-Volume relationship for a 2D cell

Flow of water into, through and out of the cells is controlled by the details of these face properties and cell elevation-volume relationships. The advantage of HEC-RAS over other models is that it produces more detailed results for a given cell size while other models use a single elevation for every cell and cell face.

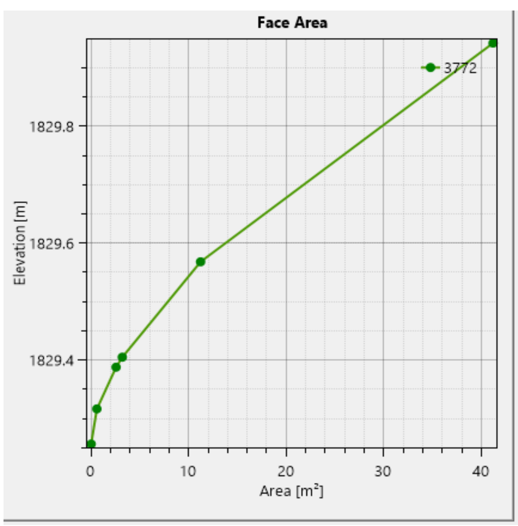

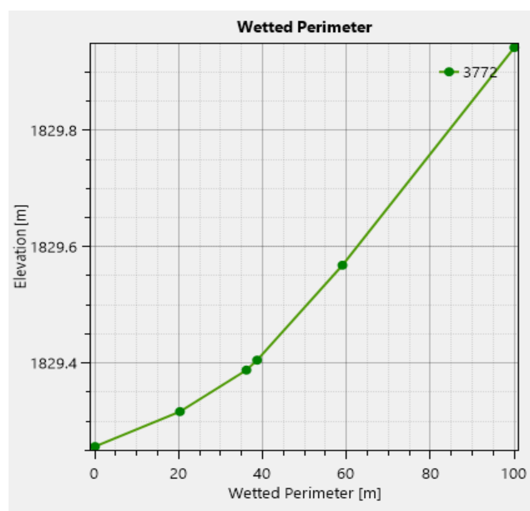

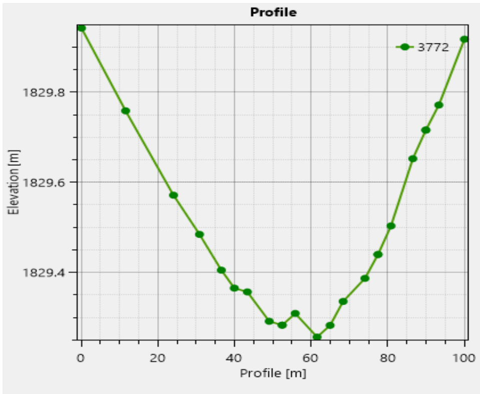

Figure 3- 22 Detailed hydraulic Tables for a Specific Cell Face

3.2.11.4 Boundary Conditions

An unsteady state simulation was conducted with the 2D mesh created and 1D geometry data. The most commonly used boundary condition flow hydrograph, was assigned at the upstream end and the normal depth boundary condition was assigned at the downstream end. A flow hydrograph is the variation of discharge with respect to time. HEC-RAS allows flow hydrograph to be assigned at either upstream or downstream end of the 2D flow area. However, for most applications, the hydrograph reflects the upstream boundary (Alzahrani, 2017).

Discharge data obtained from HEC-HMS was manually added in the flow hydrograph with data's starting time reference. The manning's equation is used by the program to compute the stage based on the flows obtained from the unsteady flow analysis.

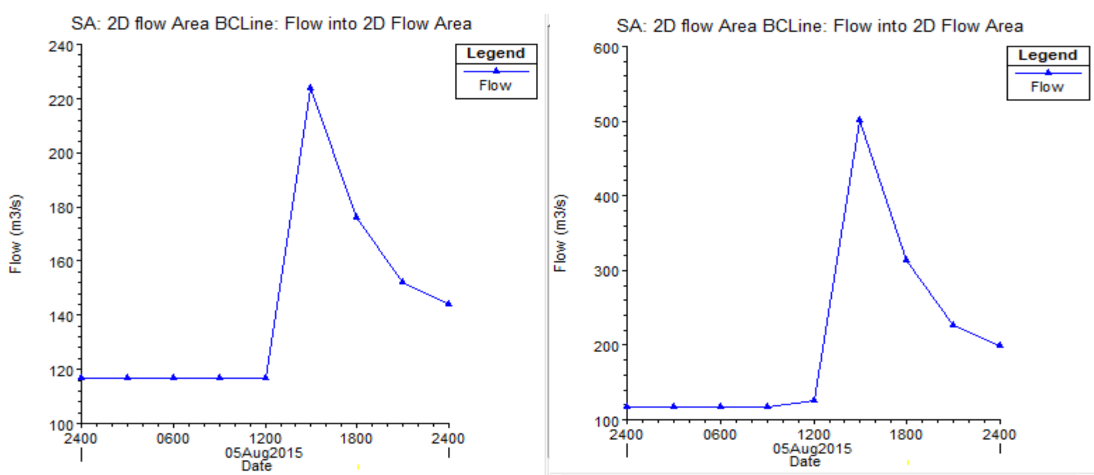

(a) 2 year (b) 100 year

Figure 3- 23 Flow hydrograph

3.2.12 Flood Inundation Map

Finally, the model was executed by selecting the unsteady flow analysis from the run menu item on the main HEC-RAS window. A plan was created by selecting the geometry that contains the 2D geometric data and unsteady flow data file to examine the flood event. Depth, velocity and water surface elevation were the significant results obtained from the model.

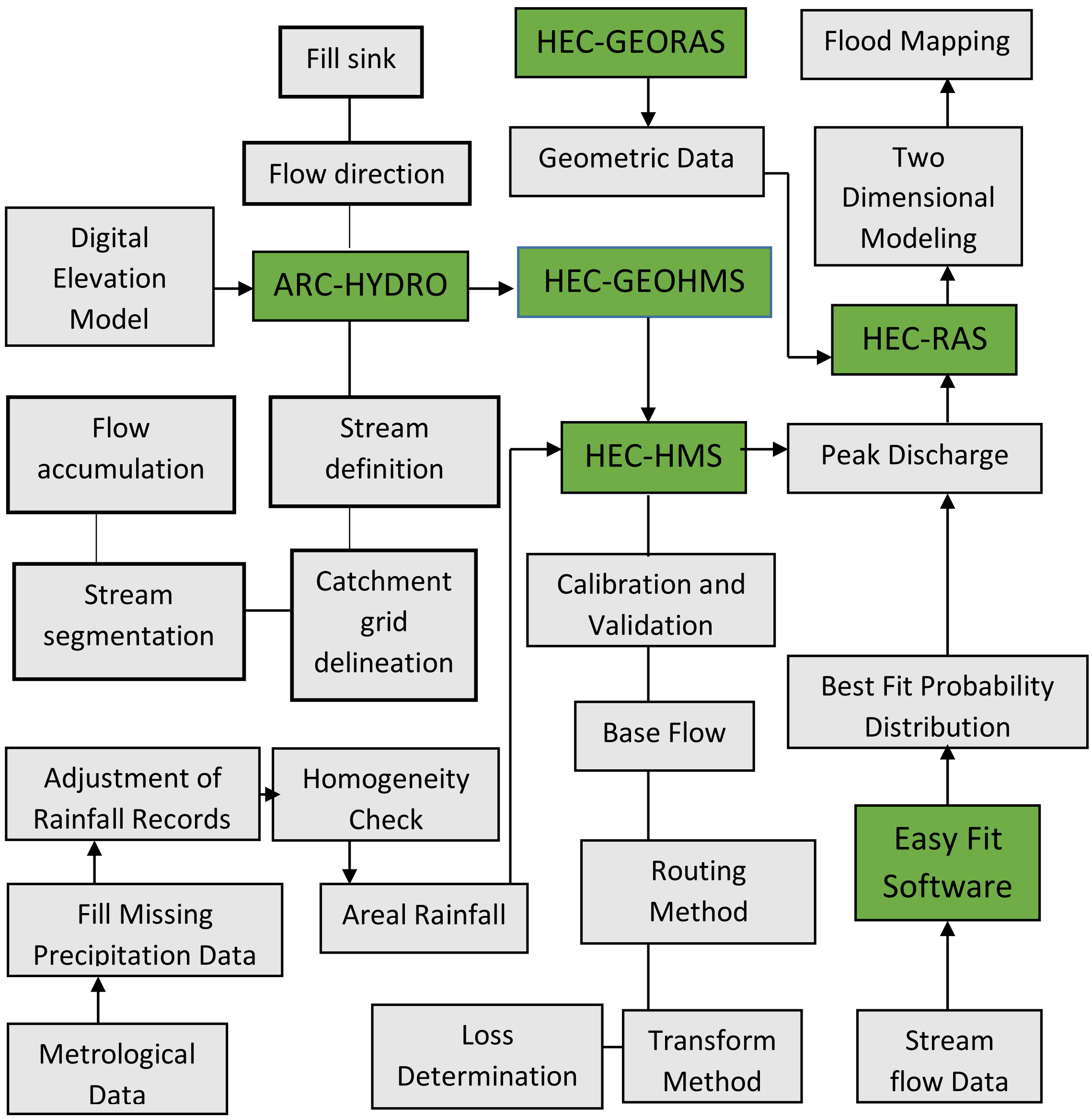

Figure 3- 24 Flow Chart

4. Results and Discussion

4.1 Consistency and Homogeneity Results of Rainfall Data

Consistency of Recorded data's was done by double mass curve analysis technique. Accumulated annual values at the station in question are plotted against those that are near and reliable group of stations. If an abrupt deviation in the slope of the curve were observed they should be corrected. However, all the selected stations in this study were consistent therefore there was no need of correction.

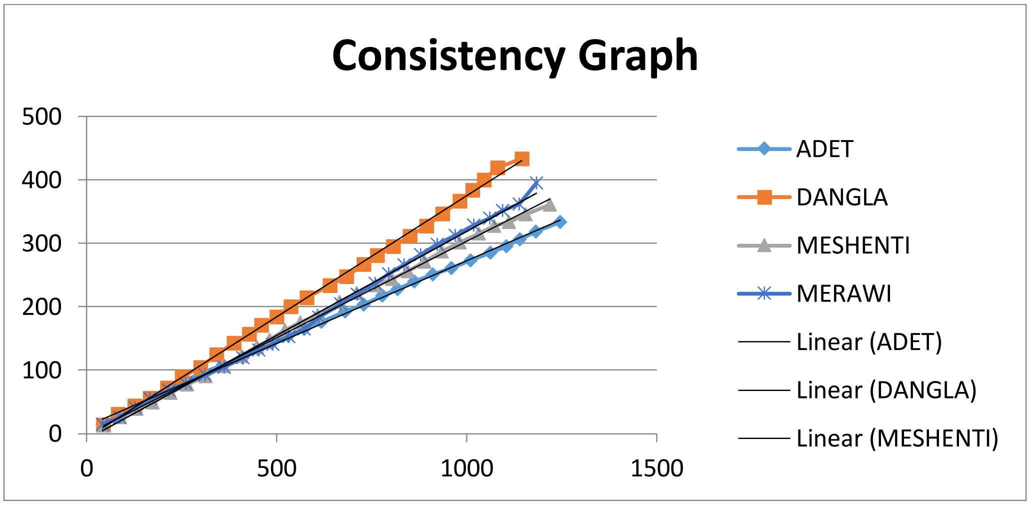

Figure 4- 1 Consistency of Selected Stations

The homogeneity of precipitation data was checked for the analysis of areal precipitation.

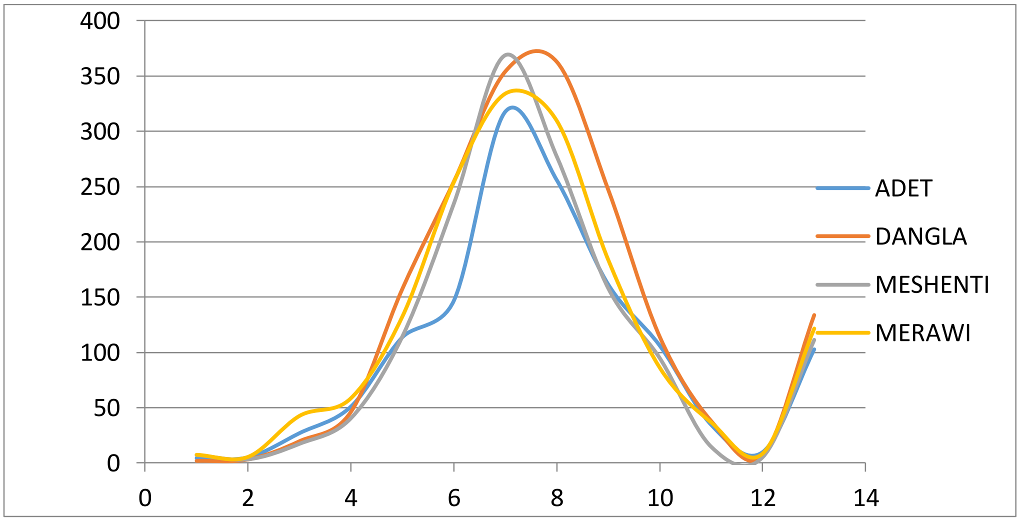

Figure 4- 2 Homogeneity Test for Rainfall Stations

The figure above shows the metrological stations of Dangla, Meshenti, Merawi and Adet have the same pattern.

4.2 Areal Precipitation

Rainfall varies in intensity and duration from place to place. Hence the rainfall recorded by each rain gauge station should be weighted according to the area it is assumed to represent.

In order to determine the areal precipitation of the catchment, the theisen polygon method was used. The method is a good choice for catchments that have rainfall gauges more than one.

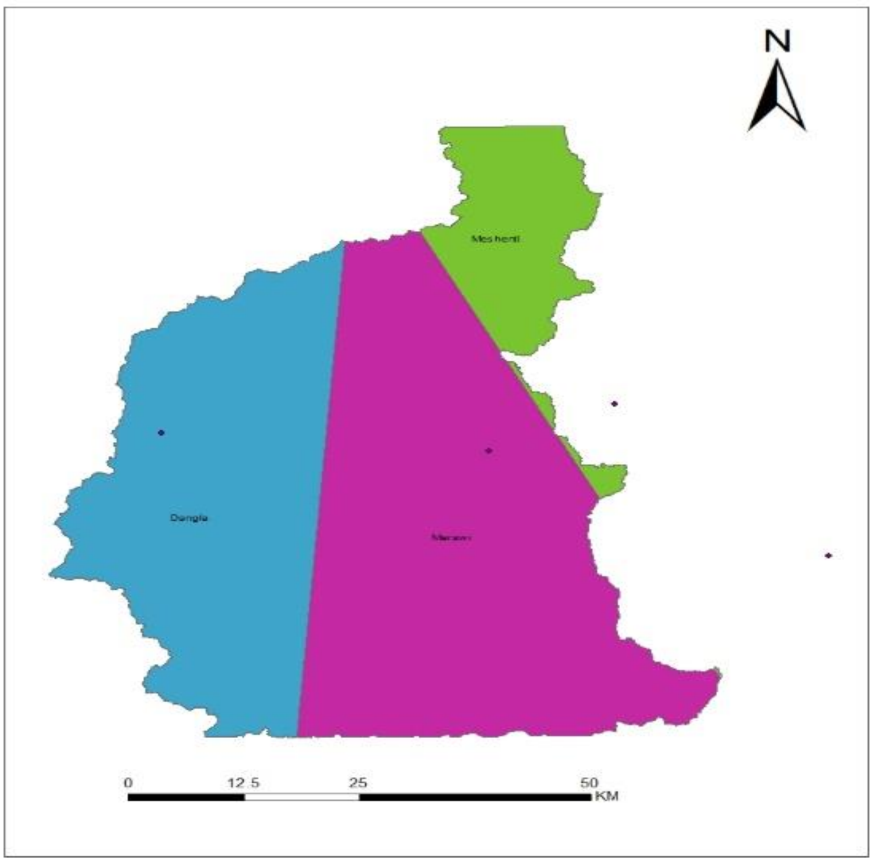

Figure 4- 3 Theisen Polygon of the Catchment

4.3 Best Fit Probability Distribution

Using easy fit software, the test statistics for Kolmogrov-Smirnov (D), Anderson Darling (A^2) and Chi-square test (X^2) were estimated for five probability distributions. Probability distribution having the first rank along with their test statistic is presented by the software.

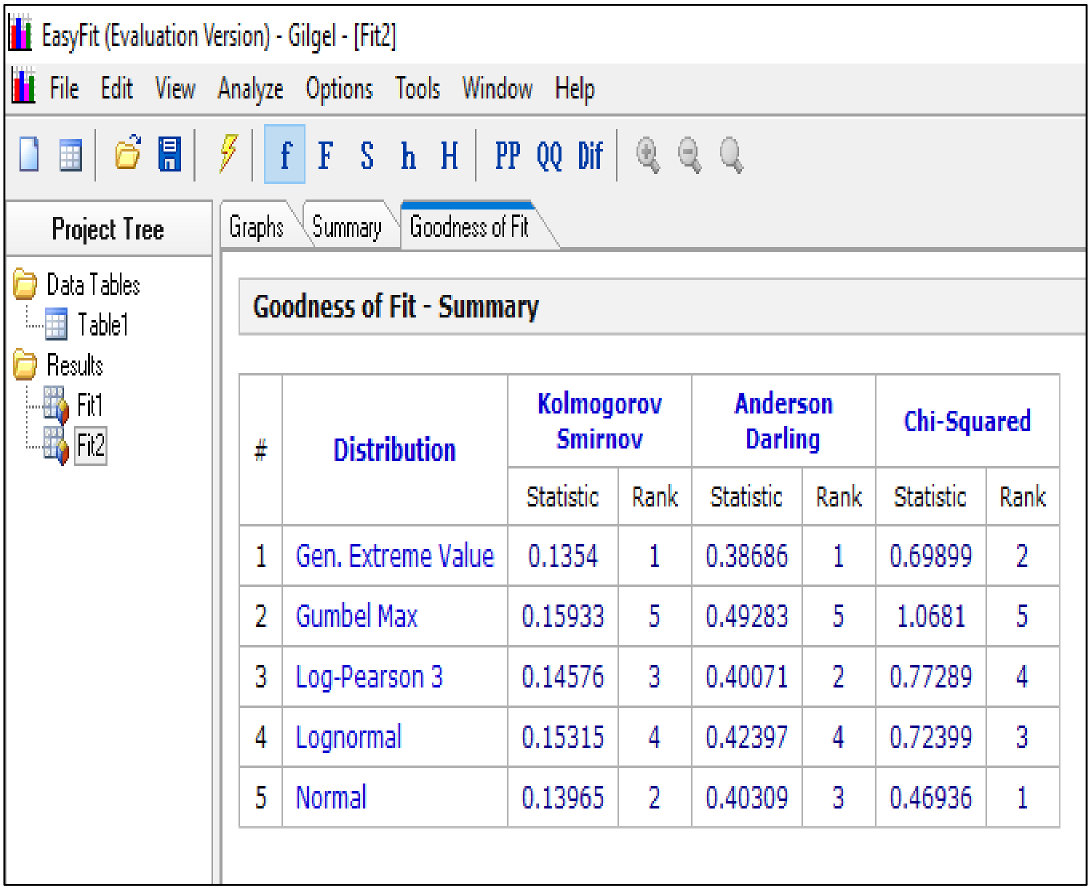

#	Distribution	Kolmogorov Smirnov		Anderson Darling		Chi-Squared	
		Statistic	Rank	Statistic	Rank	Statistic	Rank
1	Gen. Extreme Value	0.1354	1	0.38686	1	0.69899	2
2	Gumbel Max	0.15933	5	0.49283	5	1.0681	5
3	Log-Pearson 3	0.14576	3	0.40071	2	0.77289	4
4	Lognormal	0.15315	4	0.42397	4	0.72399	3
5	Normal	0.13965	2	0.40309	3	0.46936	1

Figure 4- 4 Goodness of Fit (GOF) Statistics Comparison

As shown in the figure, five types of fitting distributions were compared and the statistic with minimum distribution value has been best fitted with the data.

Using Kolmogrov-Smirnov test (D) and Anderson Darling test (A^2) test it was observed that the General Extreme value distribution provides good fit to the yearly discharge data at the outlet. Using Chi-squared test (X^2), the result showed that normal distribution provides good fit at the outlet. Comparing the three goodness of fit tests, the Kolmogrov-Smirnov test (D) has been found to provide a good fit for selected discharge at the outlet.

4.4 Terrain Processing

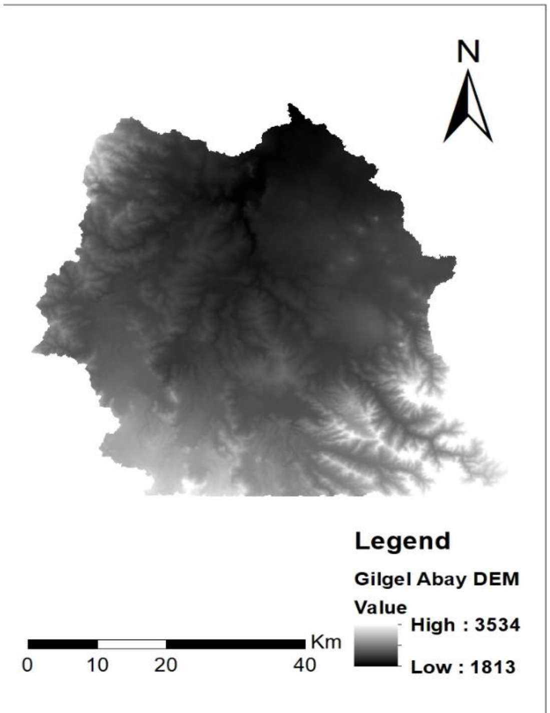

(a)

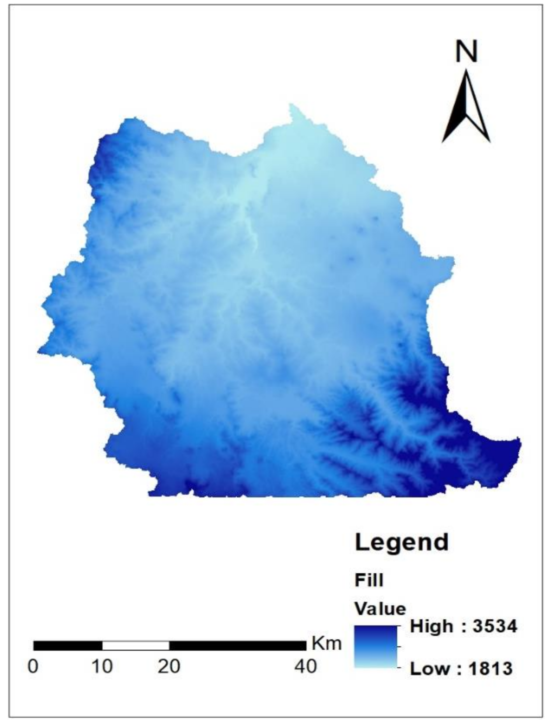

(b)

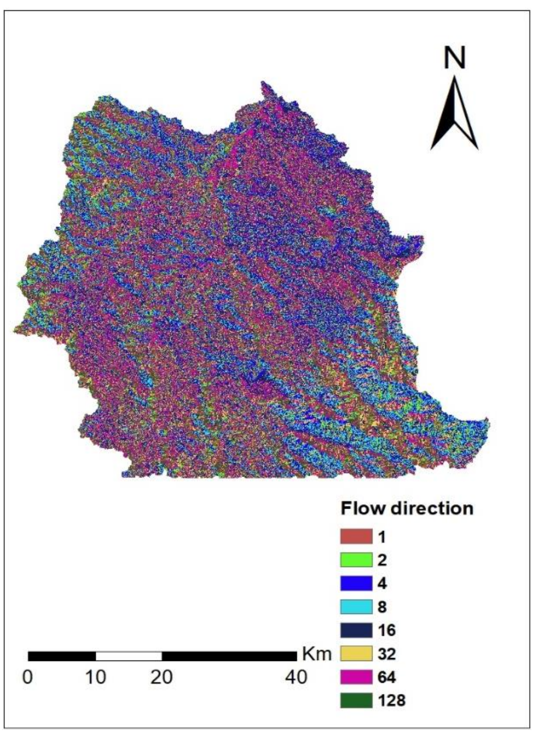

(c)

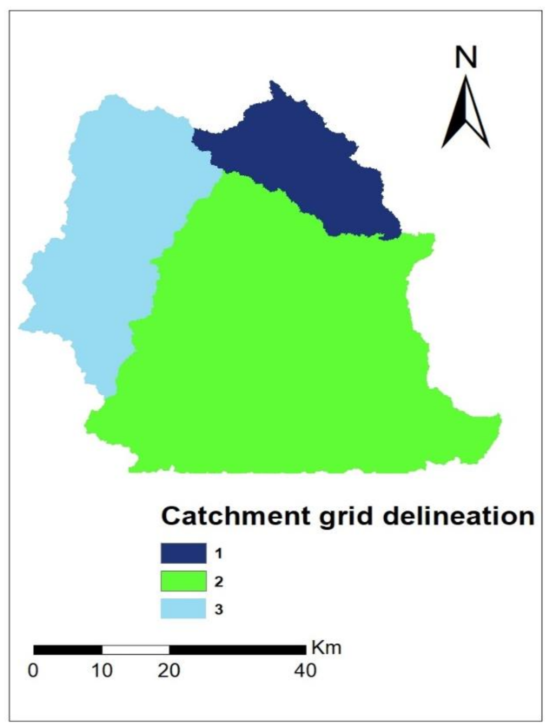

(d)

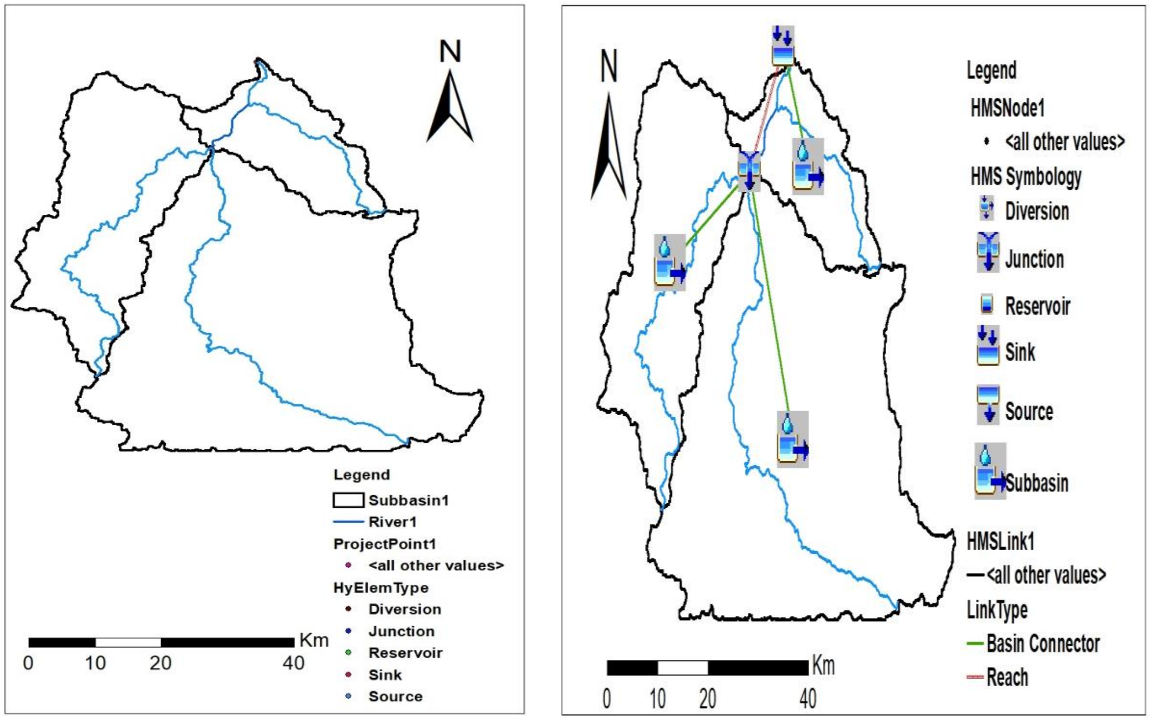

(e) (f)

Figure 4- 5 Terrain preprocessing for Gilglel catchment using Arc hydro and HEC-GeoHMS

(a) Raw DEM (b) Fill Sink (c) Flow Direction (d) Catchment Grid Delineation (e) Batch point watershed delineation at the outlet of Gilgel Abay River (f) HMS Legend and Schematic

The output from terrain processing in Arc-Hydro is not only delineation and schematic for the catchment but also extraction of basin characteristics from physical properties of the catchment. Among the basin characteristics soil and land use are the major ones.

Curve number grid was created using Hec-GeoHMS. The application uses merged land use soil type features and CN look up table to create the grid.

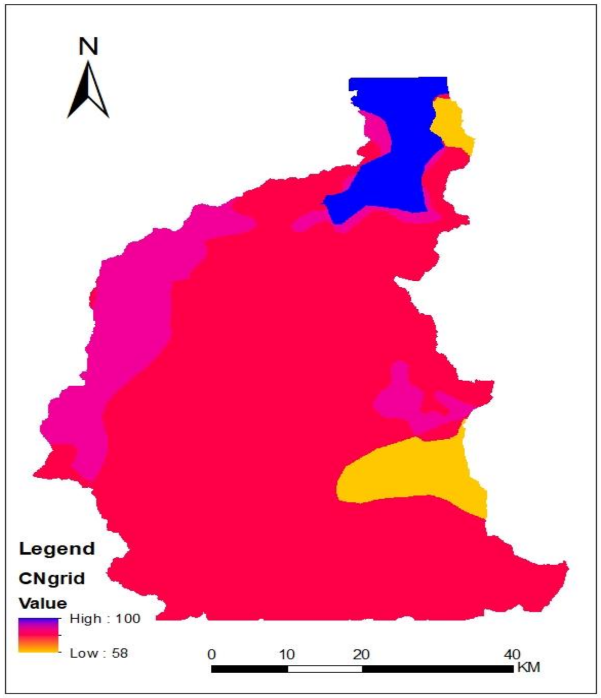

Figure 4- 6 Curve Number Grid for the Catchment

According to the output of the model, the following parameters were generated.

Table 4- 1Catchment Characteristics Parameters extracted from Arc-Hydro and Hec-GeoHMS

Components	**Parameters**	**Value**	**Unit**
Sub-Basin 1	CN	77.18	Dimensionless
	Ia	15	mm
	A	136.9	KM^2
	Basin Lag	19.28	min
Sub-Basin 2	CN	81.2	Dimensionless
	Ia	11.75	mm
	A	285.5	KM^2
	Basin Lag	14.7	m/m
	CN	75.6	Dimensionless
	Ia	16.35	mm

Sub-Basin 3	A	722.5	KM^2
	Basin Lag	24.5	min

4.5 HEC-HMS Calibration and Validation

Data's used for the model were areal precipitation, evapotranspiration, stream flow and base flow of the catchment area as well as the different watershed characteristics obtained from HEC-GeoHMS.

Table 4- 2 Optimized parameters of HEC-HMS for Gilgel catchment

Component	Parameter	Unit	Initial	Optimized
Subbasin-1	SCS Curve Number - Curve Number		77.18	58
Subbasin-1	SCS Curve Number - Initial Abstraction	mm	15	127
Subbasin-1	SCS Unit Hydrograph - Lag Time	min	19.28	19.28
Subbasin-2	SCS Curve Number - Curve Number		81.2	60.9
Subbasin-2	SCS Curve Number - Initial Abstraction	mm	11.75	131
Subbasin-2	SCS Unit Hydrograph - Lag Time	min	14.7	14.7
Subbasin-3	SCS Curve Number - Curve Number		75.6	56.7
Subbasin-3	SCS Curve Number - Initial Abstraction	mm	16.35	15.3
Subbasin-3	SCS Unit Hydrograph - Lag Time	min	24.5	24.5
Reach-1	Muskingum – K	hr	145	145.00
Reach-1	Muskingum – X		0.015	0.01500

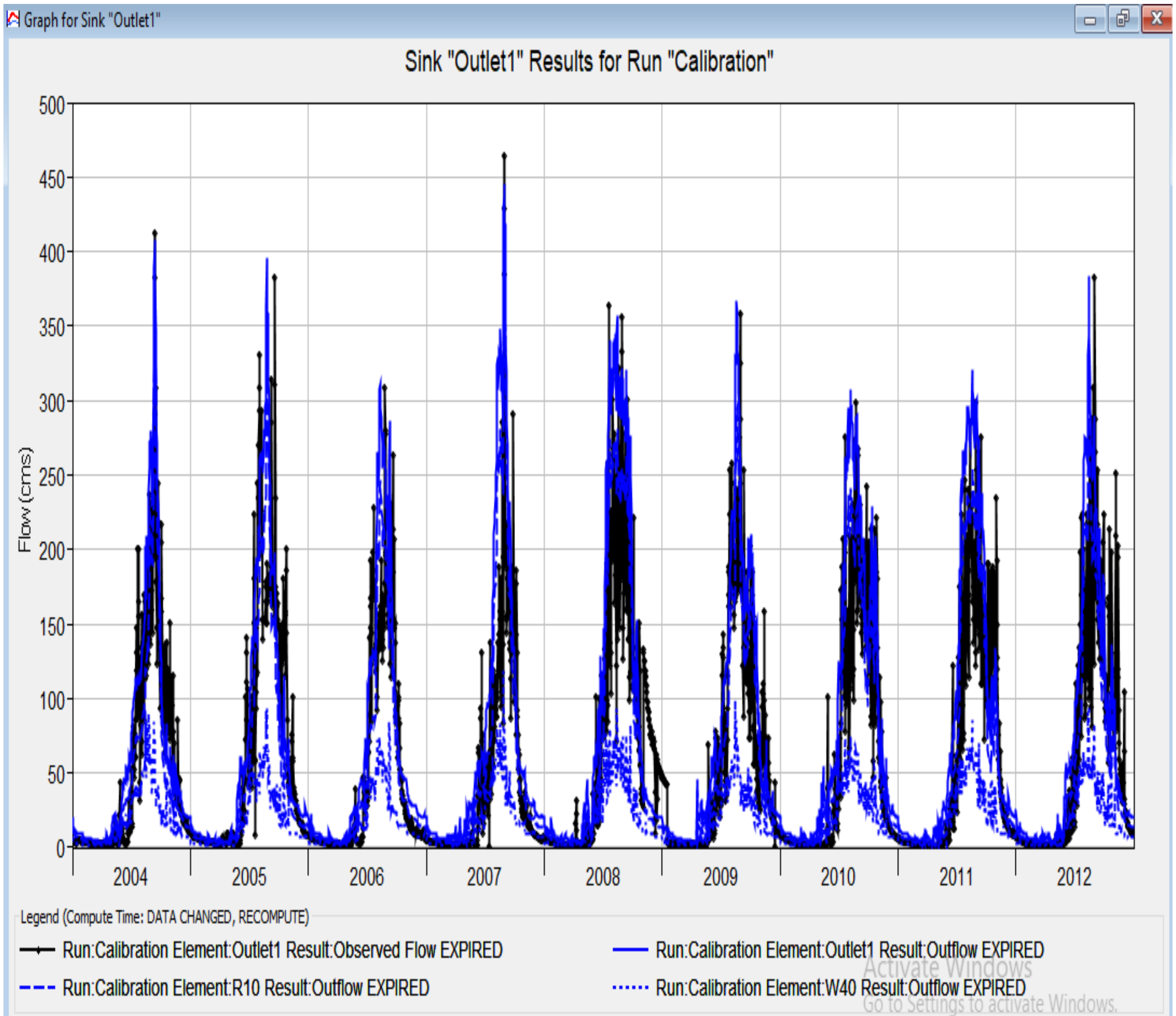

Figure 4- 7 Calibration of HEC-HMS Observation and Simulation Daily Flow Hydrographs

Table 4- 3 Calibration (2004-2012) Performance of HEC-HMS for Gilgel Abay Catchment

Performance	Value
Coefficient of Determination(R^2)	0.72
Nash-Sutcliffe (*Ens*)	0.513

Both the Calibration and Validation results showed good match between measured and Simulated stream flow and rainfall-data with acceptable range, coefficient of determination (R^2) which ranges from 1(best) to 0 and Nash-Sutcliffe (*Ens*), which ranges from 1(best) to negative infinity.

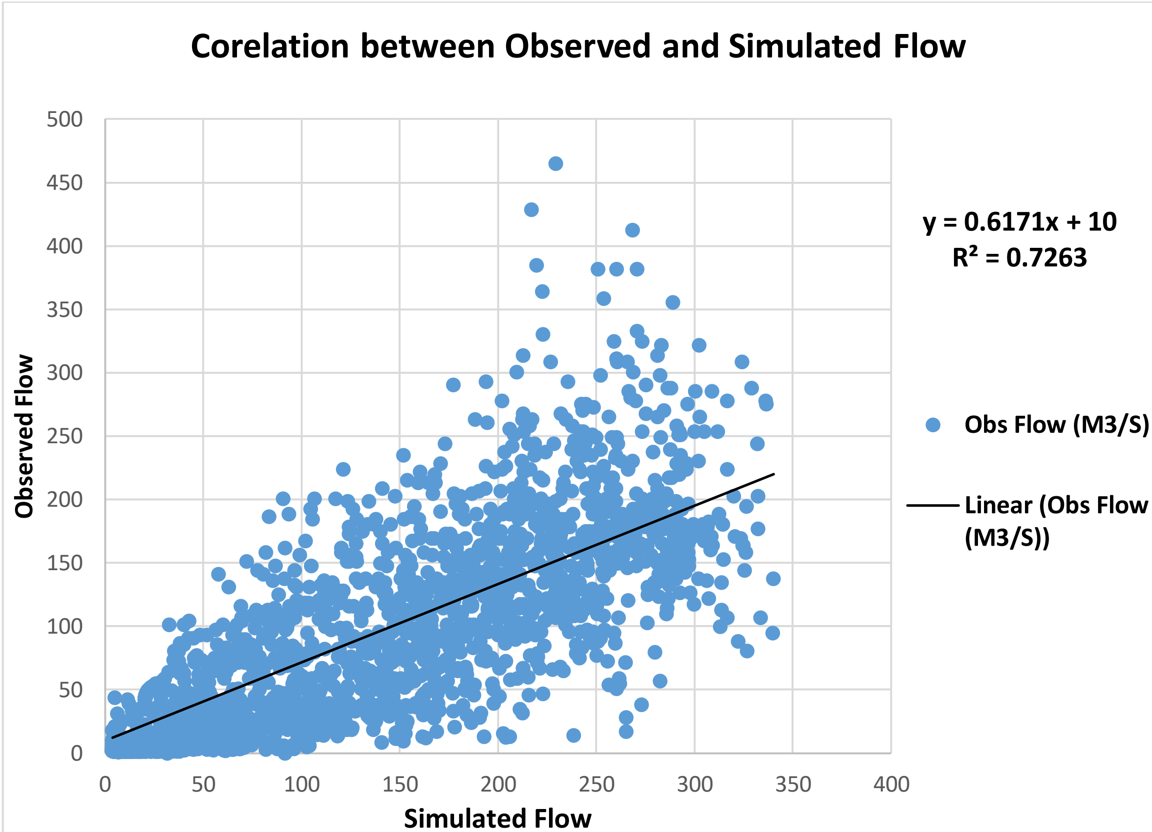

Figure 4- 8 Correlation between Observed and Simulated Flow

The scatter plot shows calculated value for each time step against the observed flow from the same step. The straight line on the plot represents equality of calculated and observed flows. If plotted points fall on the line, this shows that the model with specified parameters has predicted exactly the observed ordinate. If all of the plotted values fall above the equality line, the model is biased: it always over-predicts. Similarly if all points fall below the line, the model has consistently under-predicted.

The spread of points about the equality line also provides an indication of fit of the model. If the spread is great, the model does not match well with the observations. If the spread is small, the model parameter fit better. The scatter plot above shows only small number of points that spread greatly and also, the coefficient of determination value being 0.74 we can conclude that the model matches well with the observations.

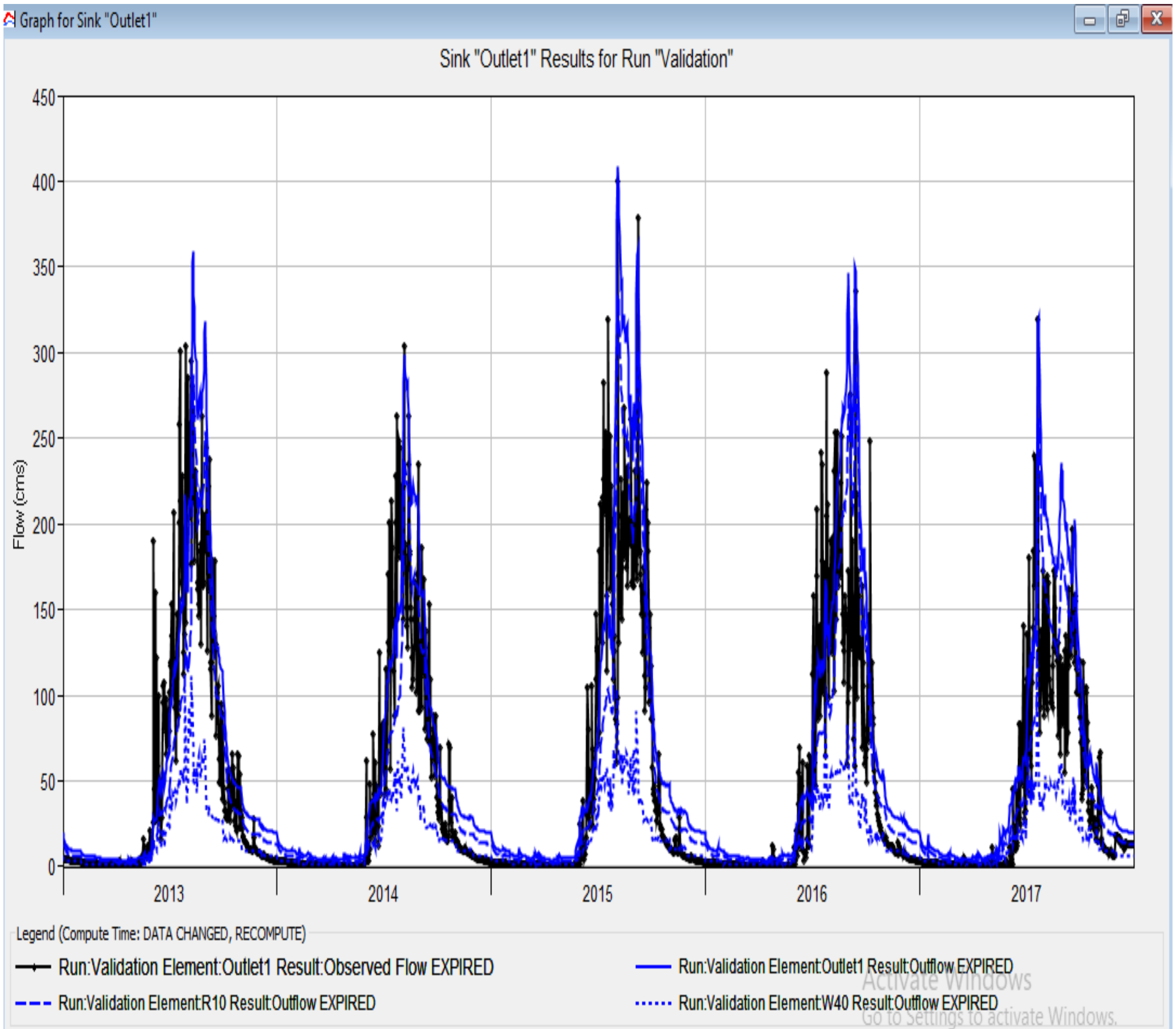

Figure 4- 9 Validation of HEC-HMS Observation and Simulation Daily Flow Hydrographs

Table 4- 4 Validation (2013-2017) Performance of HEC-HMS for Gilgel Abay Catchment

Performance	Value
Coefficient of Determination(R^2)	0.73
Nash-Sutcliffe (Ens)	0.542

The model simulation can be judged as satisfactory if NSE is greater than 50%, good if it is greater than 65% and very good if it is greater than 75% (Moriasi, D.N, 2007). Therefore both values obtained being greater than 50%, show that the simulation is satisfactory. Additionally, the coefficient of determination result show that there is a good agreement between the observed and simulated flow because both values are greater than 0.7 which indicates a strong linear relationship.

Overall, the results show that the efficiency evaluation criteria parameters resemble each other very well. Therefore, this values determined from calibration and validation of the HEC-HMS model are both acceptable.

4.5.1 Output of HEC-HMS by Frequency Storm

Values were generated for different flow conditions (return periods) on HEC-HMS. Minimum peak flow occurred for 2 years return period and maximum peak flow occurred for 100 year return period for 24 hours storm duration. The values obtained were 224 m^3/s and 502 m^3/s for the minimum and maximum frequency respectively.

Table 4- 5 Peak discharge for different return periods

No.	Return period	Peak flow (m^3/s)
1	2	224
2	10	367
3	25	438
4	50	440
5	100	502

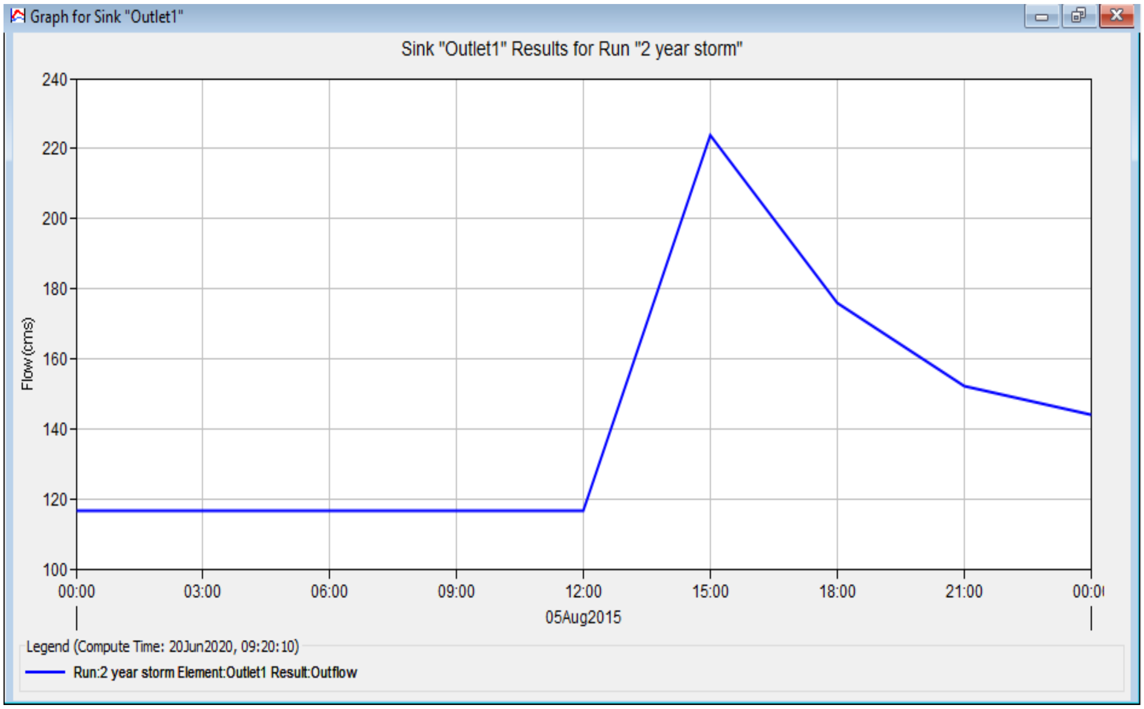

Figure 4- 10 Two years flow hydrograph

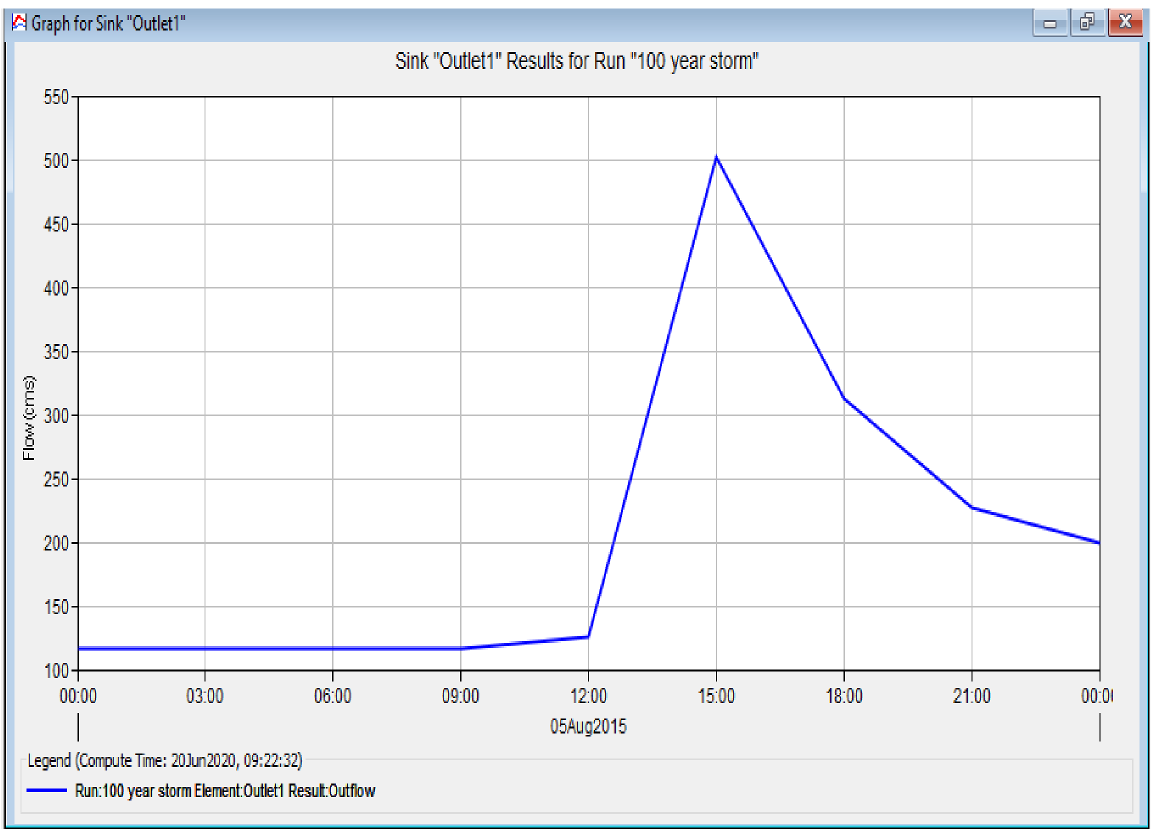

Figure 4- 11 Hundred years flow hydrograph

4.6 Flood Frequency Analysis Results

Finally, the results obtained from HEC-HMS values were then compared with frequency analysis results. The methods were selected according to their goodness of fit obtained from easy fit software. The software output showed that Gen. Extreme value was best goodness of fit. Then Log-Pearson 3, Lognormal and Gumbel follow respectively.

The outcome of HEC-HMS values were then compared with output value of different distribution methods which were estimated using their respective formula's to determine magnitude of hydrological event.

Table 4- 6 Comparison of flow values

Distribution Method	2	10	25	50	100
Gen. Extreme Value	354	417	440	455	468
Log Pearson 3	350	419	449	471	492
Log Normal	355	422	450	469	486
Gumbel	346	418	454	481	507
HEC-HMS	224	367	438	440	502

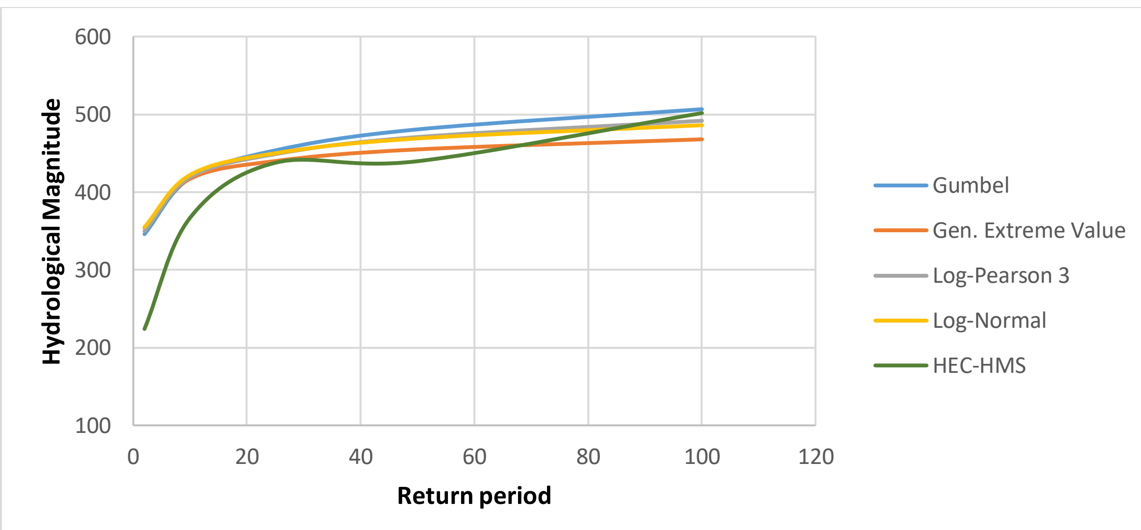

Figure 4- 12 Comparison of flow values for Gilgel Abay River

The figure above shows comparison of the calculated peak flood discharge values of HEC-HMS with the four frequency analysis results. The values indicate that there is no significant difference between the model results and frequency analysis results. Therefore, the model's peak flood discharge values can be used as an input data for flood modeling.

4.7 HEC-RAS Output

HEC-RAS needs cross section and flow data in order to provide the expected results. The flow data was determined in HEC-HMS by using hourly data frequency method and cross sectional data was created in ARC-GIS by HEC-GEORAS post processing.

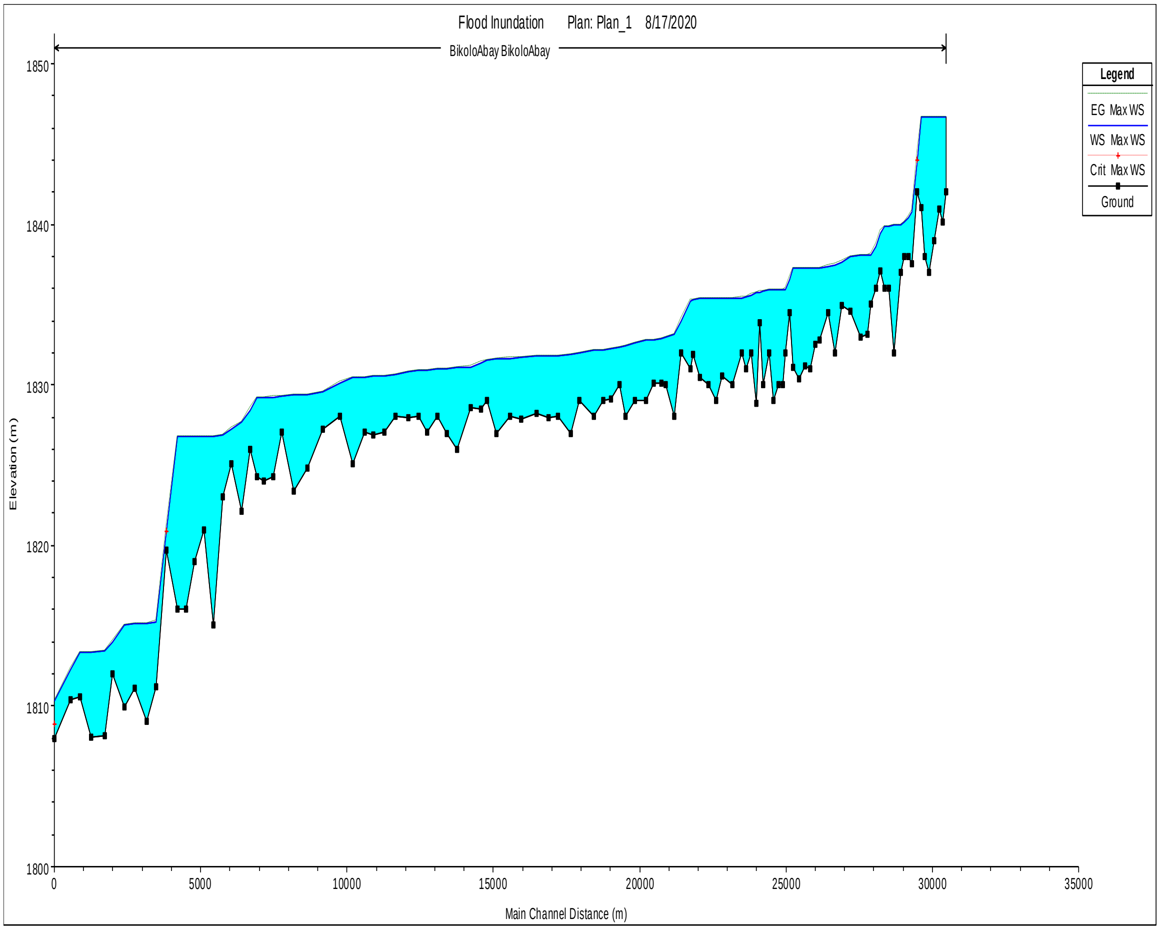

Figure 4- 13 Water Surface Profile for 2-Year Return Period 2D View

The model was run for five flow condition profiles to determine water surface profile of the reach. Simulation was successfully made for 2D unsteady flow condition and from the simulation the water surface profiles for all return periods showed that there was an over-breaching of river banks in some cross sections.

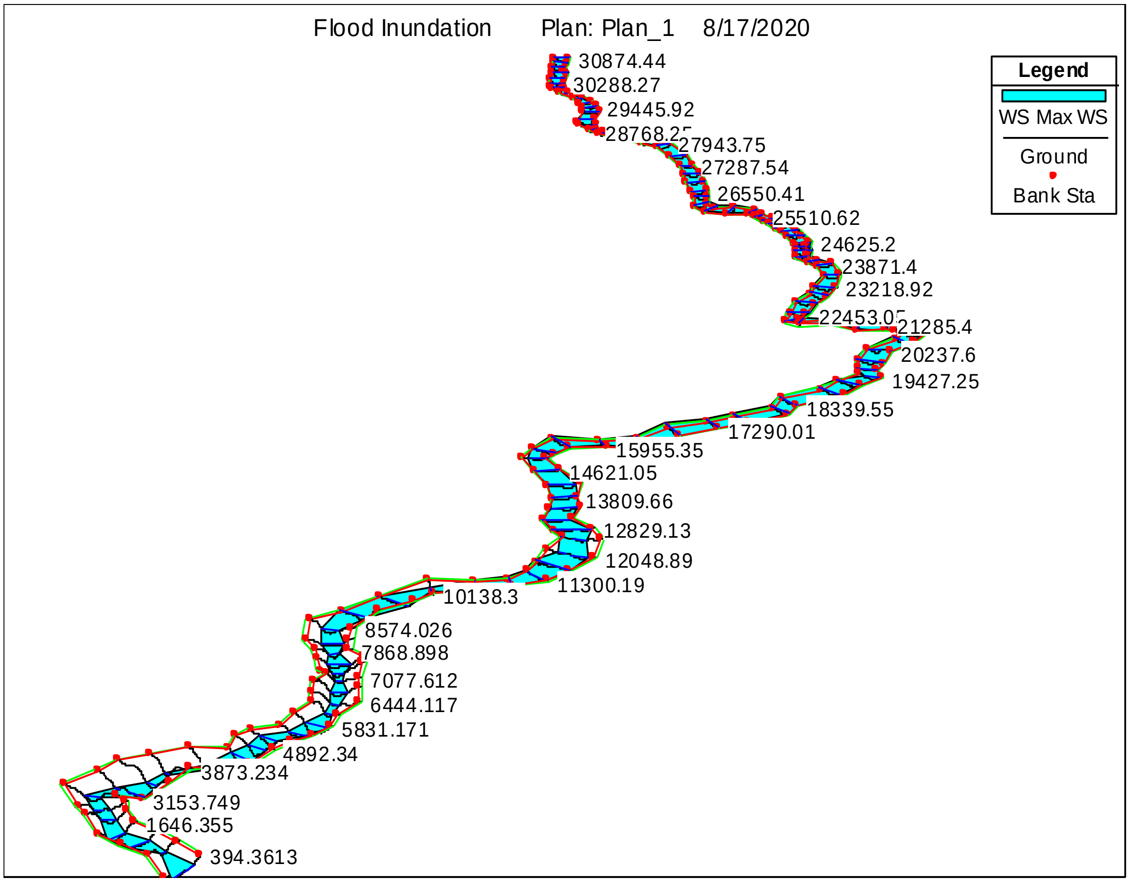

Figure 4- 14 Water Surface Profile for 100-Year Return Period 3D View

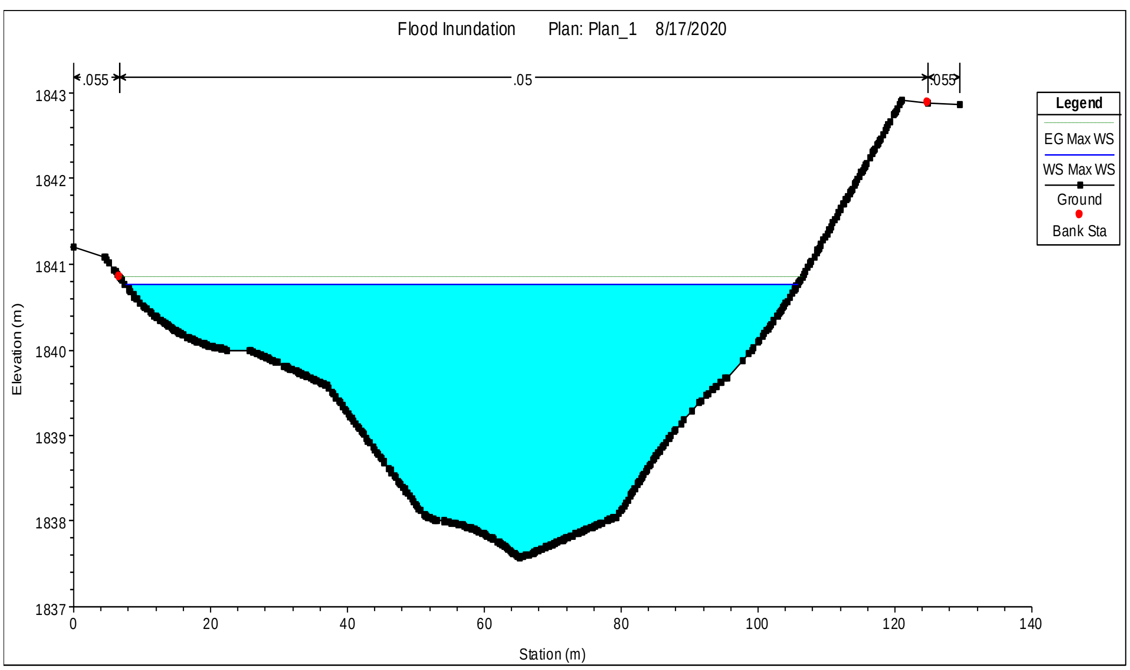

Figure 4- 15 Cross Section of River Station 29708.77 for 2 year period

4.8 Flood Mapping

After the simulation was complete, the results were displayed in RAS-Mapper. The maximum depth, velocity and water surface elevation of the model were obtained and were exported to ARC-GIS for mapping.

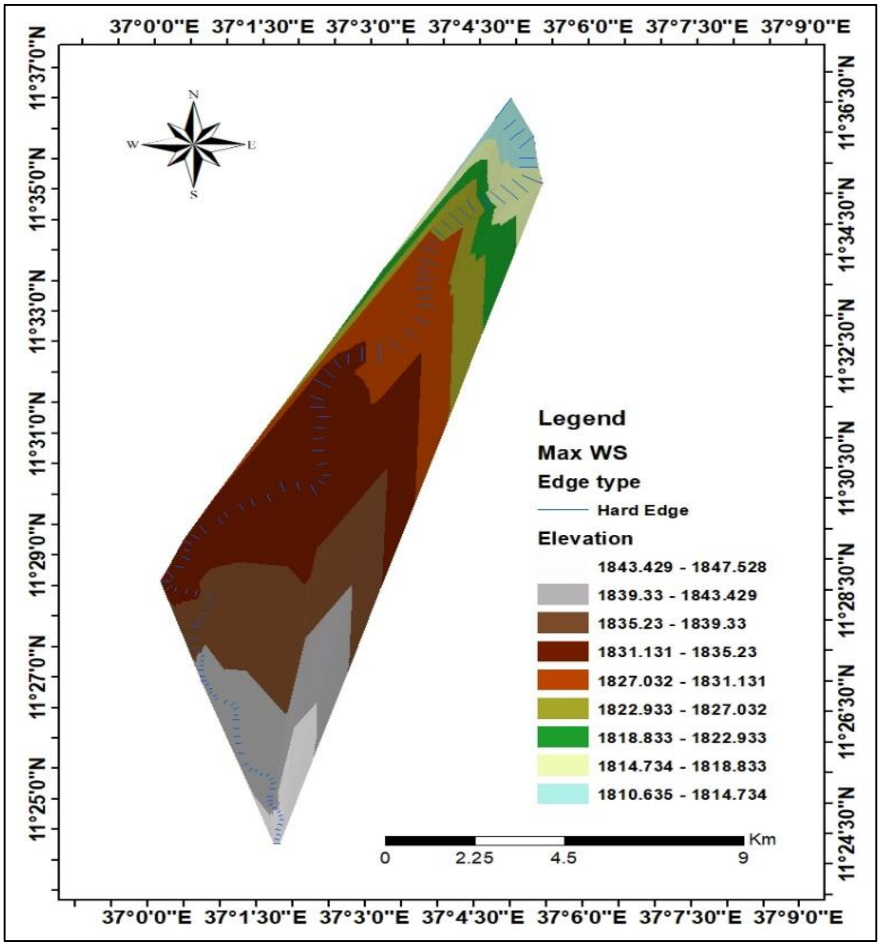

Figure 4- 16 Water Surface TIN Generated From Bounding Polygon

The modeling results of each return period was exported from HEC-RAS to ARC-GIS to generate flood maps. HEC-GEORAS was the tool used for post processing. Bounding polygon and water surface TIN was created from the given profiles and underlying TIN. Water surface TIN was first generated from cross sections and was intersected with the digital terrain model to create the flood plain polygons for flow scenario.

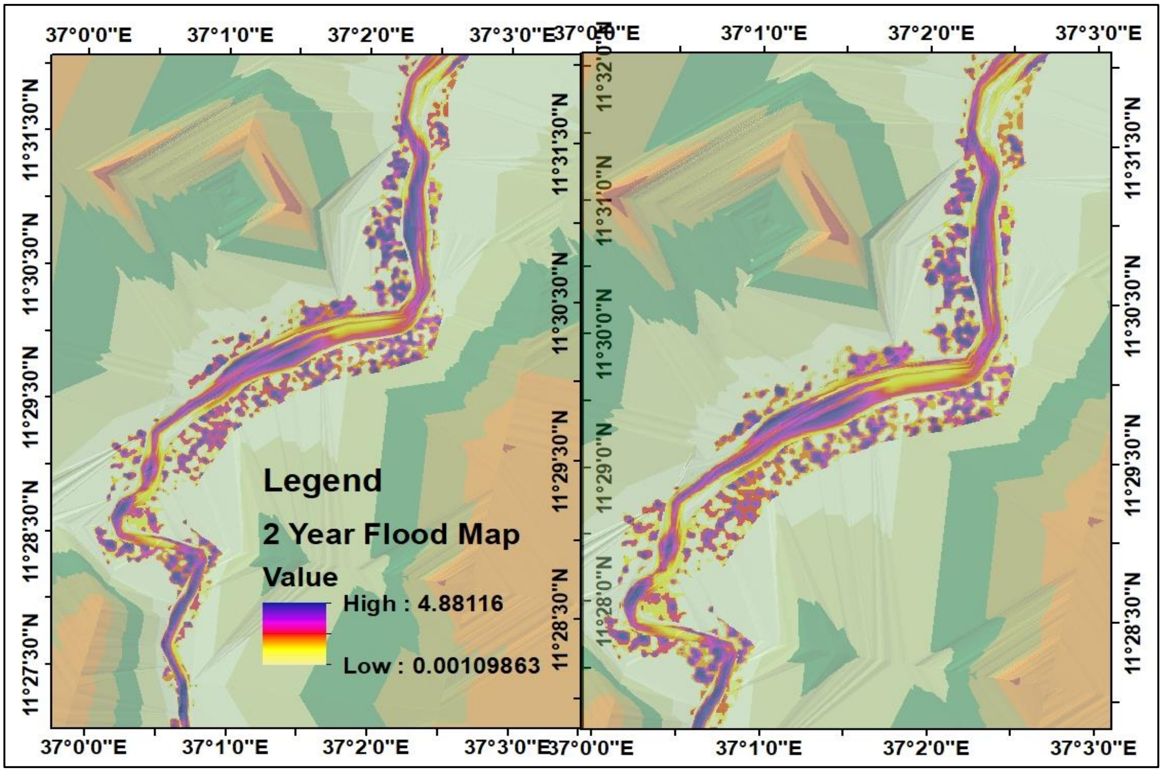

Figure 4- 17 Two Year Flood Map and Depth for the Study Area

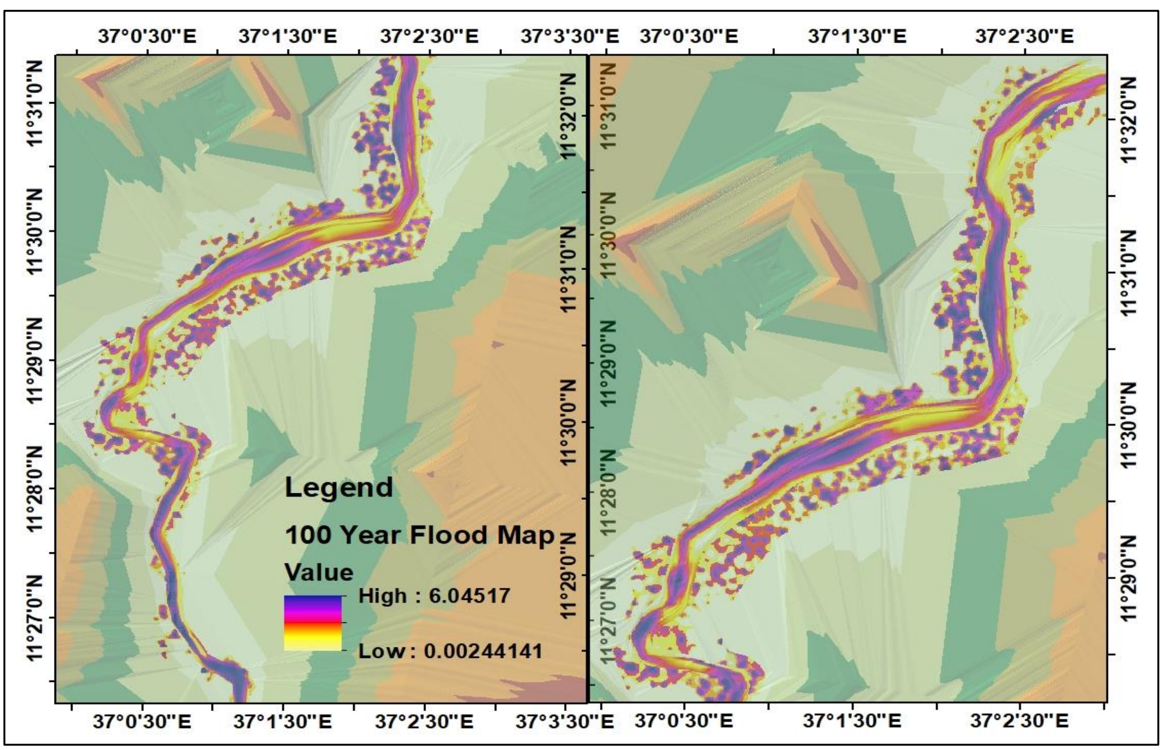

Figure 4- 18 Hundred Year Flood Map and Depth for the Study Area

The 2 year storm event's flood depth ranges from 0-4.8m with flooded area of 6.2 km^2. And the 100 year storm event's flood shown has depth value that ranges from 0-6 with flood area of 8.3 km^2.

4.9 Flood Damage

Damage caused by flood depends on several factors such as water depth, flood duration, velocity of flow, sediment concentration and pollution. This research only considered the damages due to flood water depth.

The method used to estimate direct flood damage on the agricultural land in Gilgel Abay catchment was the method of depth damage functions. Using this method the estimated damage to the agricultural land use with depth greater than 1m is 32.18 km^2.

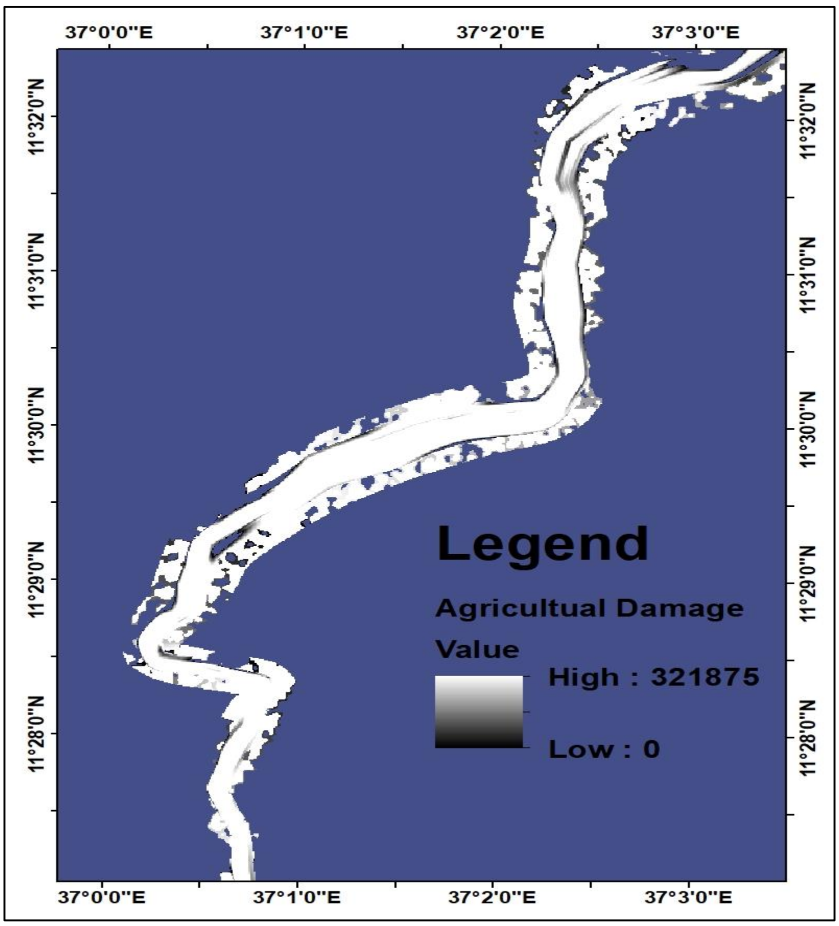

Figure 4- 19 Flood Damage of the Area

5. Conclusion and Recommendation

5.1 Conclusion

Flood inundation mapping and modeling for Gilgel-Abay River presents a systematic approach in the preparation of flood mapping and simulation with the application of 2D unsteady flow models and ARC-GIS. The programs used in the research include HEC-RAS, HEC-HMS and ARC-GIS, with its extensions HEC-GEOHMS, HEC-GEORAS and ARCHYDRO for interfacing purpose.

Catchment delineation and basin characterization were done using the appropriate extensions in ARC-GIS. Peak flood discharge for five return periods was estimated using HEC-HMS. The 2 and 100 year return peak flood discharge were found to be 223.9 and 501.6 m^3/s respectively by using ERA's IDF curve, region A2 for analysis of flood on the plain.

Flood affected areas were then delineated for 2 years and 100 years return peak flood discharge using HEC-RAS and ARC-GIS. Results showed that the total area affected by the flood was 8.3 km^2 and the area affected by 2 year flood inundation of 4.8 m was 6.2km^2.

5.2 Recommendation for Further Work

This research is important in providing policy makers with relevant data and also informing them about the performance of different measures that can be adopted to mitigate the scenario and their effects. Policy makers with their responsibility may then design a 'best strategy' for the area, taking into account financial constraints and political acceptability.

The first option considered in order to mitigate the flooding in Gilgel-Abay catchment is use of structural measures or engineering structures. Structural measures can be taken as prevention measures by reducing the amount of discharge running down the river for example by constructing reservoirs used for retention purposes or retention polders used for temporary storage of water. Retention polders are as an option recommended in this paper because most areas of the catchment are intensively cultivated and agricultural and also they have less ecological side effects than reservoirs.

Structural measures may also serve as flood protection by being constructed along the river for the purpose of flood defense. Embankments and flood walls are essential structures constructed along rivers to protect parts of the flood plain from flooding. The main drawbacks of these structures is that they may require maintenance and surveillance during flood events and are susceptible to failure. In this paper dikes and levees are recommended around the agricultural areas. Afforestation is also mandatory for planting trees increases the infiltration capacity of the land.

Other innovative options like bypass channels or 'green rivers' may be considered to provide more room for discharge or storage along rivers while allowing more natural ecological development in the floodplain.

The major constraint of this research was the availability of data. Therefore the following recommendations are made for further studies in the future.

- Topographic data with high resolution should be available enough in order to properly represent the topography of the floodplains and to model flows in overbanks.
- Hourly metrological data and longtime duration of flow data must also be available for an easy and more precise calibration and validation of hydrologic model.
- New technologies like LIDAR (Light Detection and Ranging) are better if used because of the quality of digital terrain representations, when generating TIN.

References

Ahmad H.F et al. (2016). One Dimensional Steady Flow Analysis Using HEC-RAS- A Case of River Jhelum, Jammu and Kashmir . *European Scientific Journal*.

Ajumuka, O. (2013). Probality distribution models for flood prediction in upper Benue river basin part 2. *Civil and Enviromental Research*.

Akerman. (2009). *HEC-GEORAS, GIS Tools for Support of HEC-RAS Using ARC-GIS.* Washington DC.: US Army of Corps Engineers, Institute for Water Resource (HEC).

Alem, M. (2018). *Best- fit probability distributions and return periods for maximum monthly rainfall in Bangladesh* . Climate,16.

Alem, M. (2018). Best- fit probability distributions and return periods for maximum monthly rainfall in Bangladesh . *Climate*, 16.

Alzahrani, A. (2017). *Application of Two-Dimensional Hydraulic Modeling in Riverine Systems using HEC-RAS.*

Amia, A. (2018). Integration of GIS and HEC-RAS in flood modeling of Martil river (Northern Morocco).

Aris. (2003). GIS Modeling of River and Tidal Flood Hazards in a Water front. *Case Study of Semarang City, Central Java, Indonesia*.

ASF. (2020). *Alaska Sattelite Facility*. Retrieved from https://asf.alaska.edu: https://asf.alaska.edu

Ashenafi, S. (2007). *Catchment modeling a preliminary application of isotopes for model validation in upper Blue nile basin, Lake Tana, Ethiopia.* UNESCO-IHE Deift, the Netherlands.

Awal R. et al. (2007). Flood plain analysis and risk assessment of Lakhandei river.

BCEOM. (1998). *Abay river bain integrated development master plan project Enviroment,* . Part 3 Limnology Addis Ababa, Ethiopia.

Bosamiya, B. (2018). Hydrological Modeling Using HEC-HMS. *International Journal for Research in Applied Science and Engineering Technology* .

Chase, Donald V. (2016). *Chapter 17, HEC-RAS Course Notes.*

Chow, V. T. (1988). *Applied Hydrology* . Singapore: McGraw Hill Book Company.

Cunderlik, M. (2003). *Hydrologic model selection for the CFCAS Project: Assessment of water resources risk and vulnerability to changing climatic conditions;*. Department of Civil and Enviromental Engineering: the University of Western Ontario, Canada 2003.

Darji, K. (2019). Rainfall-Runoff Modeling Using HEC-HMS Model: An Application of Regression Analysis. *Journal of Emerging Technologies and Innovative Research*.

Davis. (2009). *HEC-GEOHMS geospatial hydraulic modeling extension users manual* . Institute of Water resources.

Derdour, A. (2018). Modeling rainfall-runoff relations using HEC-HMS in a semi arid region: Case study in AIn Sefra watershed, Ksour Mountains (SW Algeria). *Journal of water and land development*.

Enku, T. (2014). Biohydrology of low flows in the humid Ethiopian highlands: The Gilgel Abay catchment. *Article in Biologia*.

Ethiopian Roads Authority, (. (2013). *Drainage design manual.* Addis Ababa, Ethiopia.

Feldman. (2000). *Hydrologic modeling system HEC-HMS technical reference manual.* Washington DC 20503: US Army of corps of Engineers HEC 609 Second St. Davis CA95616-4687.

Freeze R. A. (1975). A stochastic-conceptaual analysis of one-dimensional ground water flow in nonuniform homogenoums media. 725-741.

Gary. (2016). *HEC-RAS, River Analysis System Hydraulic Reference Manual Version 5.0.* Printed and Distributed by US Army of Corps of Engineers Hydrologic Engineering Center (HEC).

Gary W. Brunner, C.-H. (2016). *HEC-RAS River Analysis System, 2D Modeling User's Manual Version 5.0.* US Army Corps of Engineers.

Gary, W. (2014). *HEC-RAS river analysis system hydraulic reference manual version 4.1.* Rabat Report scientifique.

Guindoga, W. (2010). *Hydrologic impacts of landuse change in the upper Gilgel Abay River basin, Ethiopia: TOPMODEL Apllication.* MSc Thesis.

Halwatura D. et al. (2013). *Application of the HEC-HMS model for runoff simulation in a tropical catchment.* Environ. Model. 46, 155-162.

JGAHP. (2006). *Flash Appeal for the 2006 Flood disaster in Ethiopia.*

Jia Y. et al . (2009). *WebGIS-based system for rainfall runoff prediction and real time water resource assessment for Beijeing.* Comp. Geosci. 35, 1517-1528.

Josub M. et al. (2016). *The use of HEC-RAS modeling in flood risk analysis.*

Kebede, Y. (2016). Physico- Chemical water quality assessment of Gilgel Abay River in the Lake Tana basin, Ethiopia. *Civil and Enviromental Reasearch*.

Kute S. et al. (2014). Flood modeling of river Godavardi using HEC-RAS.

Lampros, V. (2009). Hydrological response to metrological drought indices in thessaly. *Greece, journal of hydrologic Engineering*.

M., A. (2003). GIS Modeling of River and Tidal Flood Hazards in a Water front City, Central Java,Indonesia.

Moriasi, D.N. (2007). Model Evaluation Guidelines for Systematic Qualification of Accuracy in Watershed Simulation.

MouKalled, . (2016). The Finite Volume Method in Computational Fluid Dynamics An Advanced Introduction with Open Foam and Matlab. *Cham: Springer*.

Nasa, e. o. (2006). Retrieved from Floods across Africa's Sahel: https://earthobservatory.nasa. gov

NDRM. (2020). *Joint Government Humanitarian Partners National Flood Contingency Plan 2020 Kiremt Season.* Addis Ababa: Government of Ethiopia- National Disaster Risk Managment Commision .

Ohimain, E. (2014). Selective impacts of the 2012 wwater floods on the vegetation and wildlife of wilber force island, Nigeria.

Olofintoye. (2009). Best-fit probability distribution model for prak daily rainfall of selected cities in Nigeria . *New York science Journal*, 12.

Pandya, U. (2017). River Cross Section Delineation from the Google Earth for Development of 1D HEC-RAS Model-A Case of Sabarmati River, Gujarat, India.

Partners, G. a. (2006). *Flash Appeal for the 2006 Flood Disaster in Ethiopia.*

Patel S.B et al. (2018). One dimensional Hydrodynamic Flood Modeling for Ambica River, South Goujarat. *Journal of Emerging Technologies and Innovative Researcn*.

Ratner, B. (2009). The Correlation Coefficient: Its Values range between +1/-1, or Do They? . *J Target Meas Anal Mark*, 17, 139-142.

Research, C. (2013). Probability distribution models for flood prediction in upper Benue:River basin. Benin.

Reshma, T. (2013). Simulation of event based runoff using HEC_HMS model for an experimental watershed. *International Journal of Hydraulic Engineering* .

SCHAFFENBERG, w. F. (2016). Hydrologic modeling system HEC-HMS v.4.2 users manual. *Davies, CA USACE Hydrologic Engineering Center*, 614.

Shahiriparsa et al. (2016). Floodplain Zoning Simulation by Using HEC-RAS and CCHE2D Models in the Sungai Maka River. *Air, Soil and Water Research*.

SMEC, I. (2007). *Hydrological study of the Tana Beles sub-basins.* Part 1. Sub-basin ground water investigation report.

Sok, K. a. (2016). Application of HEC-HMS model to assess stream flow and water resource avalability in stung sangker catchment of Mekong Tonie Sap lake basin in Cambodia.

Tessema, S. (2006). *Assessment of temporal hydrological variation due to landuse change using Remote sensing/ GIS: A case study of Lake Tana Basin.* MSc Thesis, TRITA-LWR.

Ukessays.com. (2018, November). The importance of flood inundation modeling environmental science essay.

Ven Te Chow, M. (1998). *L.W Applied Hydrology*. New York.

Vladyman. (2011). *Automating Hydraulic Analysis v 1.0, Basic Tutorial and Introduction.*

Vozinaki et al. (2017). Comparing 1D and Combined 1D/2D Hydraulic Simulations Using High Resolution Topographic Data: A Case Study of the Koiliaris Basin, Greece. *Hydrological Sciences Journal*.

Wale A. et al. (2009). Ungauged catchment contributions to Lake Tana's water balance. *Hydrological processes*, 23: 3682-3693.

Wang, M. (2016). Hydrological Modeling in a Semi-Arid Region Using HEC-HMS. *Journal of Water Resource and Hydraulic Engineering*.

WMO. (2008). *Guide to hydrological practice volume 1: Hydrology from measurment to hydrological information* . Geneva: World meteorological organization .

Annexes

Appendix A: Double Mass Curve of Stations

Table A- 1 Annual Precipitation of Stations

Year	ADET	DANGLA	MESHENTI	MERAWI
1992	1434.9	1353.2	1258.5	1477.3
1993	1193.7	1715.6	1304.9	1123.3
1994	1271.9	1317.9	1290.7	1497.7
1995	1347.6	1184.6	1059.3	1401.5
1996	1675.1	1654.7	1540.3	1291.7
1997	1381.2	1667.2	1228.6	1124.0
1998	1347.6	1569.4	1368.1	1341.9
1999	1156.6	1959.4	1576.3	1233.6
2000	1115.1	1895.7	1617.8	1464.2
2001	1358.8	1411.1	1404.7	1184.1
2002	955.7	1349.8	1190.6	896.9
2003	1118.2	1369.4	1461.0	1306.1
2004	1132.3	1627.9	1186.9	1143.2
2005	1123.5	1405.4	1181.5	1809.7
2006	1609.3	1869.0	2043.1	2112.9
2007	1104.2	1478.7	1451.2	1583.3
2008	1399.3	1858.1	1241.4	1648.1
2009	1031.5	1454.6	929.8	1513.3
2010	1174.5	1387.9	1295.2	1441.0
2011	1140.3	1599.2	1519.2	1597.5
2012	1048.8	1640.4	1571.4	1622.4
2013	1175.5	1920.4	1402.5	1464.3
2014	1215.2	2008.2	1458.7	1557.7
2015	1031.6	1731.0	1222.4	1147.2
2016	1084.5	1595.5	608.0	1203.0
2017	1255.2	1903.2	1168.8	969.2
2018	1431.8	1478.1	1529.5	3327.7

Table A- 2 Annual Cumulative of the Stations against ADET

Year	All Stations Average	Cumulative of ADET	Cumulative of All Stations
1992	1142.0	1434.9	1142.0
1993	1119.4	2628.6	2261.4
1994	1128.1	3900.5	3389.5
1995	1047.8	5248.1	4437.3
1996	1262.3	6923.2	5699.6
1997	1105.7	8304.4	6805.4
1998	1283.5	9652	8088.8

1999	1232.1	10808.6	9321.0
2000	1271.8	11923.7	10592.7
2001	1104.4	13282.5	11697.2
2002	897.1	14238.2	12594.3
2003	1098.9	15356.4	13693.3
2004	1051.4	16488.7	14744.6
2005	1147.4	17612.24	15892.0
2006	1564.2	19221.54	17456.2
2007	1186.4	20325.74	18642.6
2008	1264.4	21725.04	19907.0
2009	1024.8	22756.54	20931.8
2010	1103.5	23931.04	22035.3
2011	1187.3	25071.34	23222.6
2012	1212.4	26120.18	24435.0
2013	1233.0	27295.68	25668.0
2014	1292.7	28510.88	26960.7
2015	1042.4	29542.48	28003.1
2016	925.2	30626.98	28928.4
2017	1080.2	31882.18	30008.5
2018	1582.3	33313.98	31590.8

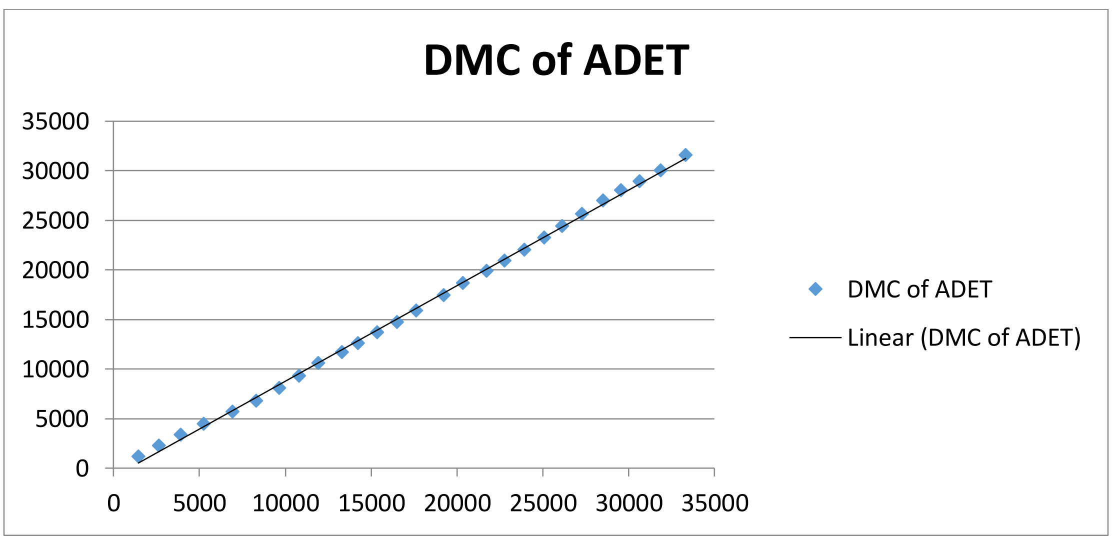

Figure A- 1 DMC of ADET

Table A- 3 Annual Cumulative of Stations near DANGLA

Year	All Stations Average	Cumulative of DANGLA	Cumulative of all Stations
1992	1142.0	1353.22	1142.0
1993	1119.4	3068.82	2261.4
1994	1128.1	4386.72	3389.5

1995	1047.8	5571.32	4437.3
1996	1262.3	7226.02	5699.6
1997	1105.7	8893.22	6805.4
1998	1283.5	10462.61	8088.8
1999	1232.1	12422.01	9321.0
2000	1271.8	14317.71	10592.7
2001	1104.4	15728.81	11697.2
2002	897.1	17078.61	12594.3
2003	1098.9	18448.01	13693.3
2004	1051.4	20075.91	14744.6
2005	1147.4	21481.31	15892.0
2006	1564.2	23350.31	17456.2
2007	1186.4	24829.01	18642.6
2008	1264.4	26687.11	19907.0
2009	1024.8	28141.71	20931.8
2010	1103.5	29529.61	22035.3
2011	1187.3	31128.81	23222.6
2012	1212.4	32769.21	24435.0
2013	1233.0	34689.61	25668.0
2014	1292.7	36697.81	26960.7
2015	1042.4	38428.81	28003.1
2016	925.2	40024.31	28928.4
2017	1080.2	41927.51	30008.5
2018	1582.3	43405.61	31590.8

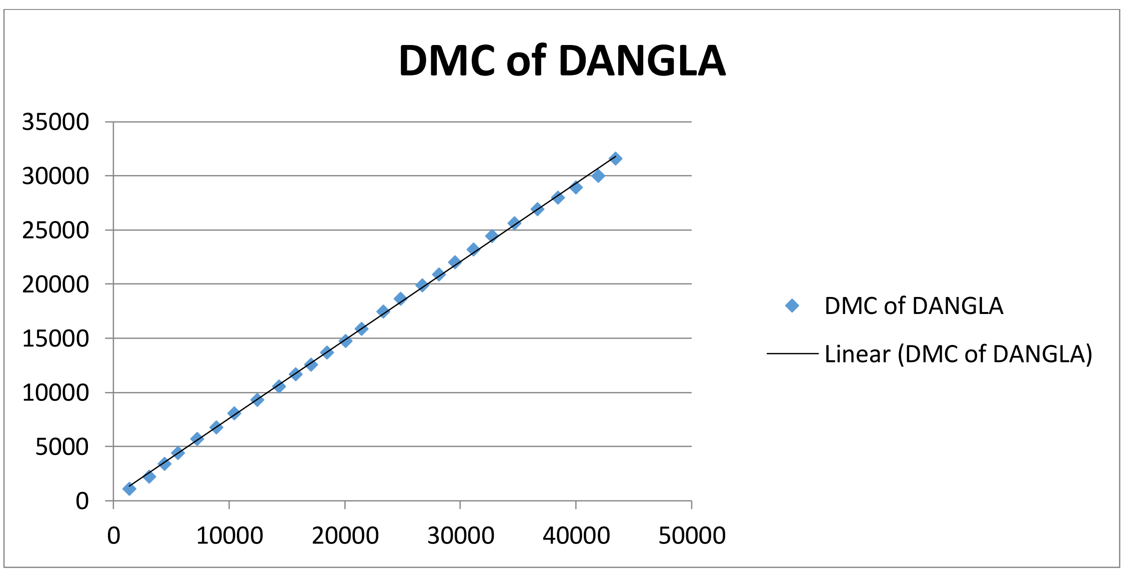

Figure A- 2 DMC of DANGLA

Table A- 4 Annual Cumulative of Stations against MESHENTI

Year	**All Stations Average**	**Cumulative of MESHENTI**	**Cumulative of all Stations**
1992	1142.0	1258.5	1142.0
1993	1119.4	2563.4	2261.4
1994	1128.1	3854.1	3389.5
1995	1047.8	4913.4	4437.3
1996	1262.3	6453.7	5699.6
1997	1105.7	7682.3	6805.4
1998	1283.5	9050.4	8088.8
1999	1232.1	10626.7	9321.0
2000	1271.8	12244.5	10592.7
2001	1104.4	13649.2	11697.2
2002	897.1	14839.8	12594.3
2003	1098.9	16300.8	13693.3
2004	1051.4	17487.7	14744.6
2005	1147.4	18669.2	15892.0
2006	1564.2	20712.3	17456.2
2007	1186.4	22163.5	18642.6
2008	1264.4	23404.9	19907.0
2009	1024.8	24334.7	20931.8
2010	1103.5	25629.9	22035.3
2011	1187.3	27149.1	23222.6
2012	1212.4	28720.5	24435.0
2013	1233.0	30123.0	25668.0
2014	1292.7	31581.7	26960.7
2015	1042.4	32804.1	28003.1
2016	925.2	33412.1	28928.4
2017	1080.2	34580.9	30008.5
2018	1582.3	36110.4	31590.8

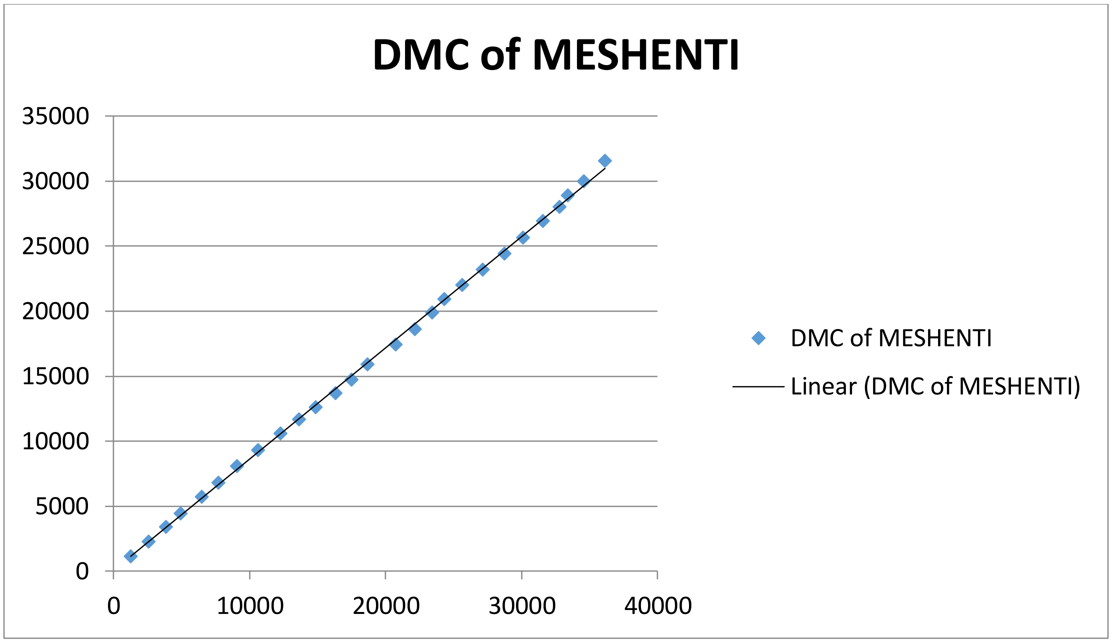

Figure A- 3 DMC of MESHENTI

Table A- 5 Annual Cumulative of Stations against MERAWI

Year	All Stations Average	Cumulative of MERAWI	Cumulative of all Stations
1992	1142.0	1477.3	1142.0
1993	1119.4	2600.6	2261.4
1994	1128.1	4098.3	3389.5
1995	1047.8	5499.8	4437.3
1996	1262.3	6791.5	5699.6
1997	1105.7	7915.5	6805.4
1998	1283.5	9257.3	8088.8
1999	1232.1	10490.9	9321.0
2000	1271.8	11955.1	10592.7
2001	1104.4	13139.2	11697.2
2002	897.1	14036.1	12594.3
2003	1098.9	15342.3	13693.3
2004	1051.4	16485.4	14744.6
2005	1147.4	18295.2	15892.0
2006	1564.2	20408.0	17456.2
2007	1186.4	21991.3	18642.6
2008	1264.4	23639.4	19907.0
2009	1024.8	25152.7	20931.8
2010	1103.5	26593.7	22035.3
2011	1187.3	28191.3	23222.6

2012	1212.4	29813.7	24435.0
2013	1233.0	31278.0	25668.0
2014	1292.7	32835.7	26960.7
2015	1042.4	33982.9	28003.1
2016	925.2	35185.9	28928.4
2017	1080.2	36155.0	30008.5
2018	1582.3	39482.7	31590.8

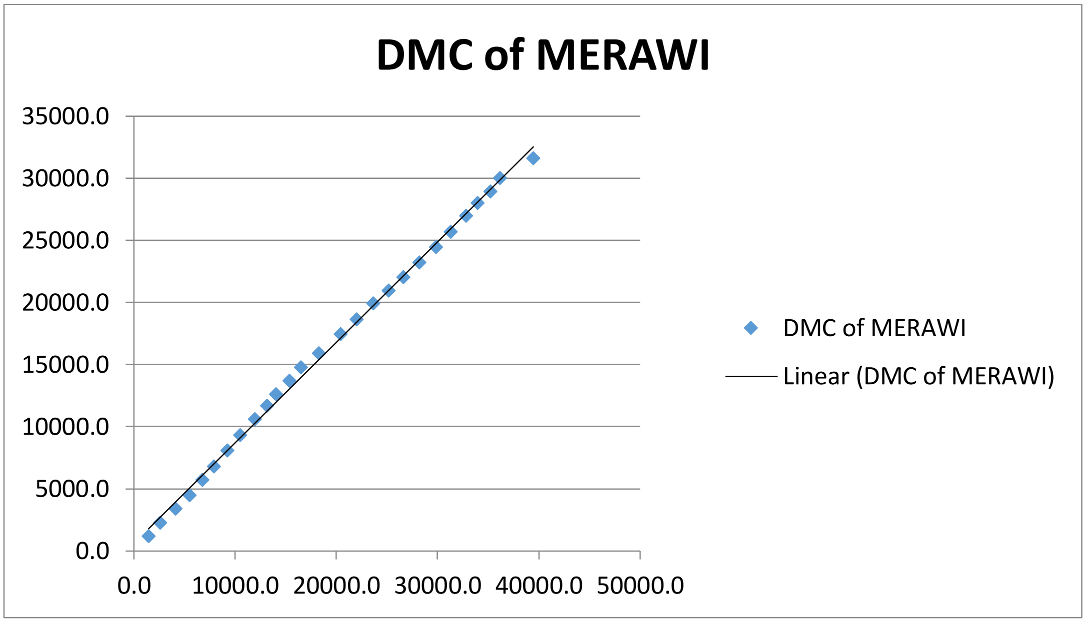

Figure A- 4 DMC of MERAWI

Appendix B: Homogeneity Test Analysis

Table A- 6 ADET Station Homogeneity Data

Year	**Jan**	**Feb**	**Mar**	**Apr**	**May**	**Jun**	**Jul**	**Aug**	**Sep**	**Oct**	**Nov**	**Dec**
1992	0	0	31	139	34	62	247	463	121	240	76	23
1993	0	36	43	57	187	70	301	140	183	129	39	9
1994	0	16	11	25	174	203	421	249	111	41	9	13
1995	0	0	35	36	135	154	392	329	143	28	19	77
1996	6	3	95	166	174	205	342	283	276	20	105	1
1997	3	0	49	20	247	159	255	195	238	171	44	0
1998	3	0	24	20	182	155	328	260	170	196	10	1
1999	26	0	2	24	96	131	333	243	116	143	27	16
2000	0	0	2	135	59	100	251	248	127	160	24	9
2001	0	4	3	34	137	194	341	369	146	95	25	11
2002	12	4	39	36	51	136	282	199	122	55	8	14
2003	0	8	10	6	16	163	341	292	205	52	22	3

2004	8	7	2	37	10	189	286	247	204	120	22	0
2005	2	0	28	40	30	105	332	214	193	153	27	0
2006	0	1	4	19	116	175	439	423	237	150	18	28
2007	4	1	14	20	94	272	314	161	138	60	27	0
2008	15	1	0	168	151	143	331	320	167	80	24	0
2009	0	11	35	33	46	101	298	282	125	80	7	15
2010	23	0	0	45	79	160	364	249	183	70	1	2
2011	21	0	24	71	162	84	339	214	155	70	1	2
2012	0	0	5	0	35	178	274	297	143	27	77	14
2013	0	0	11	6	113	158	374	267	113	110	25	0
2014	0	4	114	86	188	131	211	200	152	109	22	0
2015	0	2	22	1	139	142	181	189	124	156	50	26
2016	0	3	74	21	201	161	295	143	96	91	0	0
2017	0	41	18	122	111	80	402	181	143	104	53	0
2018	0	0	38	16	107	160	308	245	225	154	173	7
Sum	**122**	**140**	**731**	**1381**	**3073**	**3969**	**8579**	**6900**	**4354**	**2863**	**932**	**270**
Mean	5	5	27	51	114	147	318	256	161	106	35	10

Table A- 7 DANGLA Station Homogeneity Data

Year	**Jan**	**Feb**	**Mar**	**Apr**	**May**	**Jun**	**Jul**	**Aug**	**Sep**	**Oct**	**Nov**	**Dec**
1992	0	0	4	66	28	141	293	346	201	155	85	35
1993	0	2	46	61	166	239	369	345	324	148	16	0
1994	2	6	0	30	136	280	248	356	180	33	35	13
1995	1	0	61	42	130	209	221	263	178	56	3	21
1996	0	2	97	94	182	186	340	386	250	74	43	0
1997	0	0	36	53	210	206	351	380	175	164	91	3
1998	0	0	23	14	186	313	282	343	254	148	6	0
1999	2	0	0	36	244	281	389	371	330	264	36	8
2000	0	7	8	77	135	344	313	436	238	265	70	3
2001	0	0	15	14	157	318	390	259	150	98	3	7
2002	0	4	12	15	52	279	299	352	183	123	30	2
2003	0	5	8	2	23	331	339	279	302	27	55	0
2004	1	9	2	91	61	231	488	364	267	95	21	0
2005	4	1	29	7	48	271	319	345	321	54	7	0
2006	3	0	0	48	259	340	440	393	228	133	7	19
2007	0	1	12	51	132	268	314	384	198	60	58	0
2008	40	0	5	120	251	292	435	422	256	29	7	2
2009	0	7	19	12	24	317	334	433	121	161	27	0
2010	3	0	1	32	150	192	340	295	290	67	14	5
2011	4	2	31	21	229	272	339	433	217	48	4	0

2012	0	0	3	0	64	287	413	501	190	53	108	24
2013	0	0	1	0	169	207	570	376	392	189	13	2
2014	0	4	57	135	303	249	360	314	341	196	49	1
2015	0	0	41	1	272	269	259	355	290	86	138	19
2016	0	0	30	29	223	159	410	413	221	110	1	0
2017	0	45	0	198	302	241	332	357	322	107	0	0
2018	0	0	0	14	127	162	377	294	249	140	101	16
Sum	**59**	**93**	**539**	**1259**	**4263**	**6880**	**9564**	**9793**	**6666**	**3082**	**1028**	**180**
Mean	2	3	20	47	158	255	354	363	247	114	38	7

Table A- 8 MESHENTI Station Homogeneity Data

Year	Jan	Feb	Mar	Apr	May	Jun	Jul	Aug	Sep	Oct	Nov	Dec
1992	0	0	16	75	45	133	400	285	101	170	33	0
1993	0	0	7	20	103	214	455	229	163	109	5	0
1994	0	2	0	29	109	316	355	323	121	36	0	0
1995	0	1	8	16	136	138	313	260	127	18	11	32
1996	14	0	23	82	160	237	403	340	163	84	35	0
1997	0	0	65	6	208	113	375	170	124	154	12	0
1998	0	0	48	2	144	305	271	309	157	134	0	0
1999	4	0	0	14	82	349	432	329	194	169	3	1
2000	0	0	0	56	30	266	323	365	244	248	85	0
2001	0	1	7	8	96	293	282	437	184	82	0	16
2002	7	6	13	12	80	257	255	254	140	139	2	26
2003	0	4	8	1	2	321	488	265	278	71	5	18
2004	10	7	3	19	6	194	445	270	139	93	2	0
2005	1	0	23	17	44	161	384	223	228	89	12	0
2006	0	2	0	21	176	372	553	371	255	252	0	42
2007	25	3	19	32	109	382	269	295	124	165	29	0
2008	20	0	0	37	75	201	344	311	154	87	13	0
2009	0	0	13	10	27	67	331	300	76	105	0	0
2010	0	0	0	0	143	65	434	434	133	80	6	0
2011	0	0	0	0	169	343	307	437	220	30	14	0
2012	0	0	16	0	8	247	753	274	247	12	0	15
2013	0	0	41	9	120	137	560	329	131	51	25	0
2014	0	5	49	74	216	149	462	216	225	64	0	0
2015	0	1	16	256	363	372	72	31	52	50	10	0
2016	66	13	16	3	135	239	32	62	43	0	0	0
2017	53	29	52	167	144	280	162	211	71	0	0	0
2018	0	21	31	135	168	190	499	149	169	70	97	0

Sum	**198**	**95**	**474**	**1100**	**3099**	**6341**	**9958**	**7476**	**4263**	**2561**	**397**	**150**
Mean	7	4	18	41	115	235	369	277	158	95	15	6

Table A- 9 MERAWI Station Homogeneity Data

Year	**Jan**	**Feb**	**Mar**	**Apr**	**May**	**Jun**	**Jul**	**Aug**	**Sep**	**Oct**	**Nov**	**Dec**
1992	0	0	4	51	59	273	513	329	171	54	18	5
1993	14	28	20	70	119	116	308	188	154	90	13	2
1994	1	11	111	43	168	297	227	362	160	86	32	0
1995	0	2	16	37	187	292	345	279	159	49	6	30
1996	5	1	143	67	119	126	280	336	140	36	37	1
1997	85	0	51	15	159	105	207	194	134	144	28	1
1998	8	15	337	100	378	85	143	150	69	54	2	0
1999	28	0	50	23	81	217	273	254	123	165	14	6
2000	0	3	6	313	51	133	214	344	147	187	65	3
2001	0	1	70	12	126	161	323	289	134	56	5	7
2002	4	3	22	45	42	141	181	234	113	64	8	39
2003	0	5	9	63	8	164	292	450	171	30	16	97
2004	10	5	32	164	15	122	280	274	170	61	11	0
2005	8	3	55	20	107	215	446	285	297	110	264	0
2006	0	0	1	23	235	407	536	449	285	164	0	11
2007	0	1	27	27	111	455	274	271	280	87	52	0
2008	11	0	0	142	189	339	386	303	190	57	31	0
2009	0	6	31	16	57	199	469	469	116	108	20	22
2010	12	0	1	28	167	329	334	331	146	71	24	0
2011	21	0	29	10	164	402	258	338	264	84	28	0
2012	0	0	4	2	36	250	580	437	282	19	12	2
2013	0	0	0	16	154	221	511	240	160	136	28	0
2014	0	4	74	157	183	244	243	362	181	105	5	0
2015	0	0	8	0	226	244	282	208	125	0	53	0
2016	0	0	51	9	186	418	227	145	105	63	0	0
2017	0	51	1	48	199	182	153	175	129	31	0	0
2018	0	18	5	89	61	733	744	665	555	220	223	14
Sum	**207**	**156**	**1158**	**1590**	**3589**	**6870**	**9028**	**8359**	**4960**	**2331**	**995**	**240**
Mean	8	6	43	59	133	254	334	310	184	86	37	9

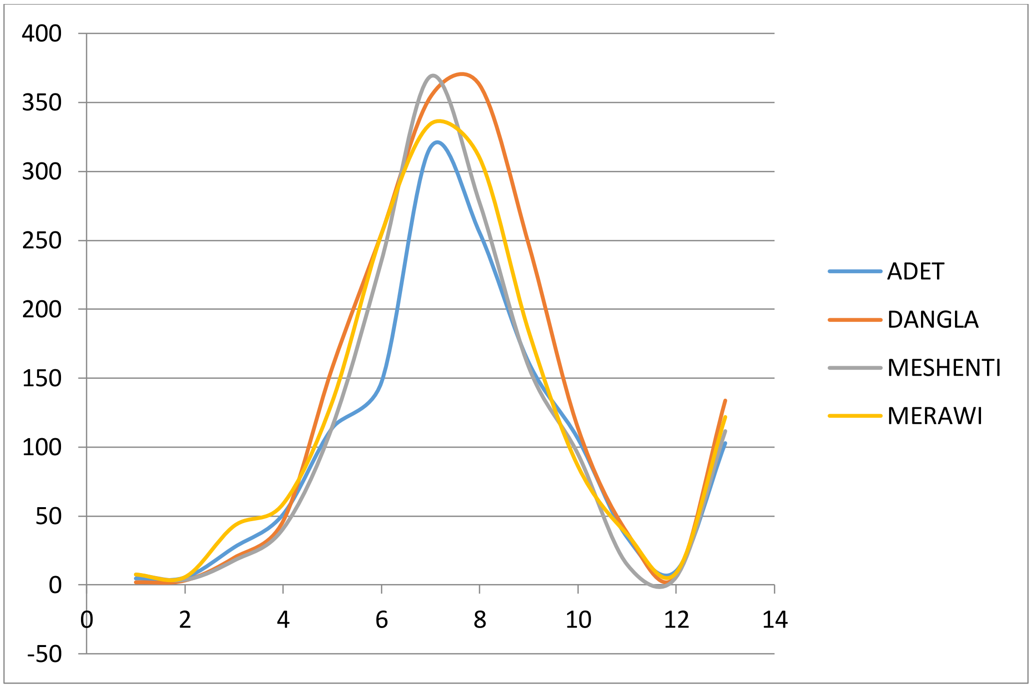

Figure A- 5 Homogeneity Test Graph

Appendix C: Estimated Monthly Flow Data

Table A- 10 Monthly Flow Data

Year	Jan	Feb	Mar	Apr	May	Jun	Jul	Aug	Sep	Oct	Nov	Dec
2002	157	100	81	59	91	418	3149	5464	4006	1273	293	168
2003	114	70	64	132	275	1660	5910	6736	4883	1306	331	196
2004	130	85	71	113	205	917	3764	6063	4354	2783	883	338
2005	171	106	98	151	278	2248	5826	5559	4645	2782	688	254
2006	149	95	76	63	222	1846	4576	5506	3559	725	314	197
2007	111	70	58	58	343	1319	2872	6168	3953	788	307	175
2008	111	66	127	117	612	2556	6292	6929	4251	2651	2042	1484
2009	91	54	54	50	570	1824	4987	6099	3752	1970	1024	327
2010	139	71	57	39	314	1929	4424	5721	4612	2980	550	203
2011	115	60	44	51	276	1732	5054	5793	3812	3798	590	236
2012	106	59	46	93	188	1471	4527	6300	4025	3936	1101	278
2013	119	65	56	54	186	2015	4678	6383	3861	1277	416	167
2014	96	50	44	31	31	1147	4492	5219	2991	897	304	130
2015	69	42	37	20	28	1305	5531	5711	5214	1014	306	125
2016	72	40	29	68	36	823	4259	5145	4130	1984	343	158
2017	81	41	51	31	53	1010	4059	3666	3607	1559	474	439

Appendix D: HEC-HMS Output

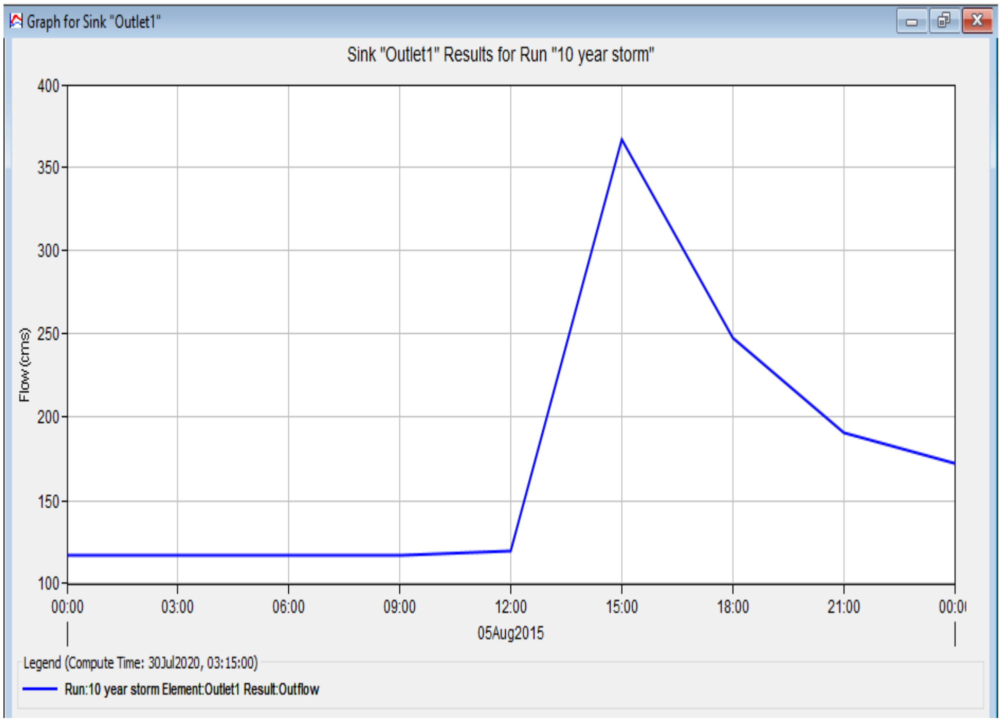

Figure A- 6 Ten Year Storm Hydrograph

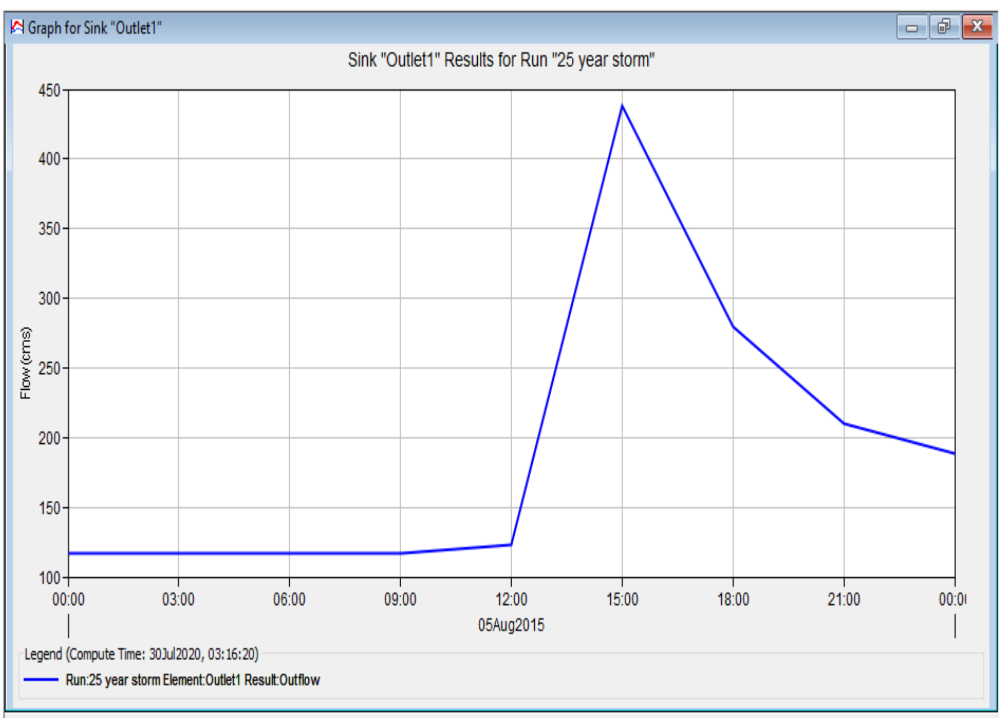

Figure A- 7 Twenty Five Year Storm Hydrograph

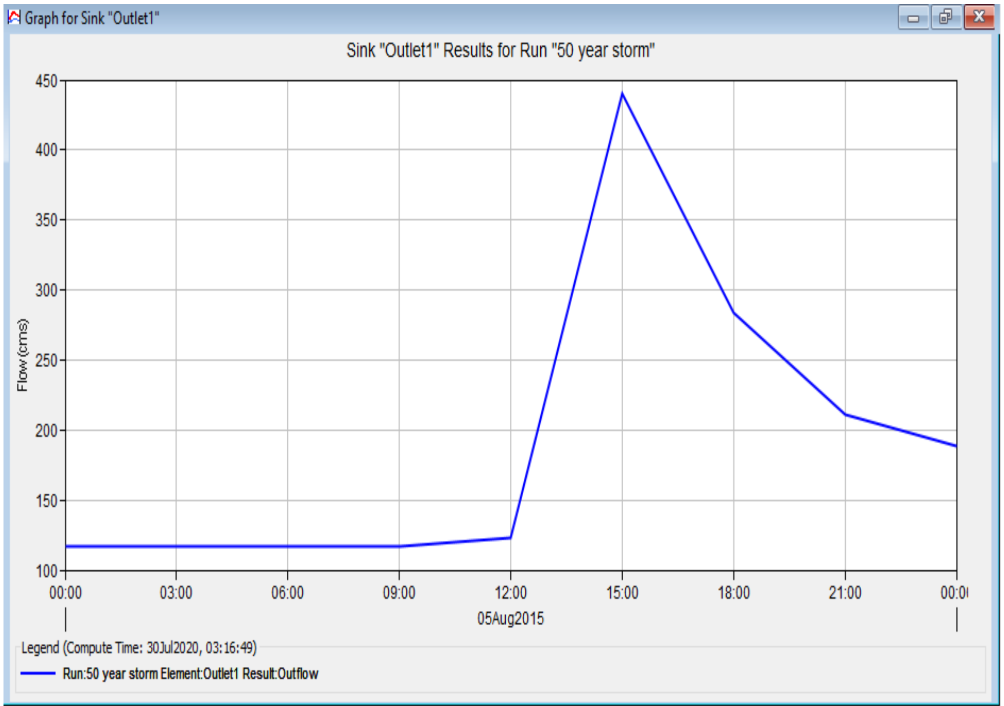

Figure A- 8 Fifty Year Storm Hydrograph

Appendix E: HEC-RAS Outputs

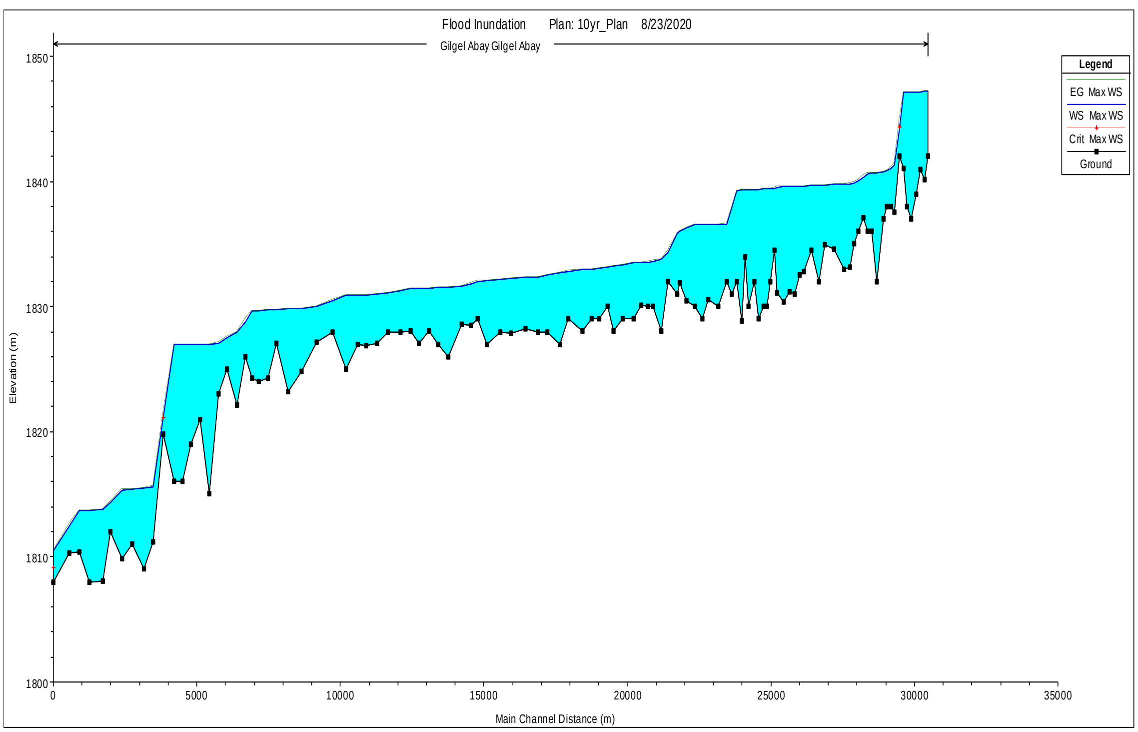

Figure A- 9 Water Surface Profile for 10 Year Storm

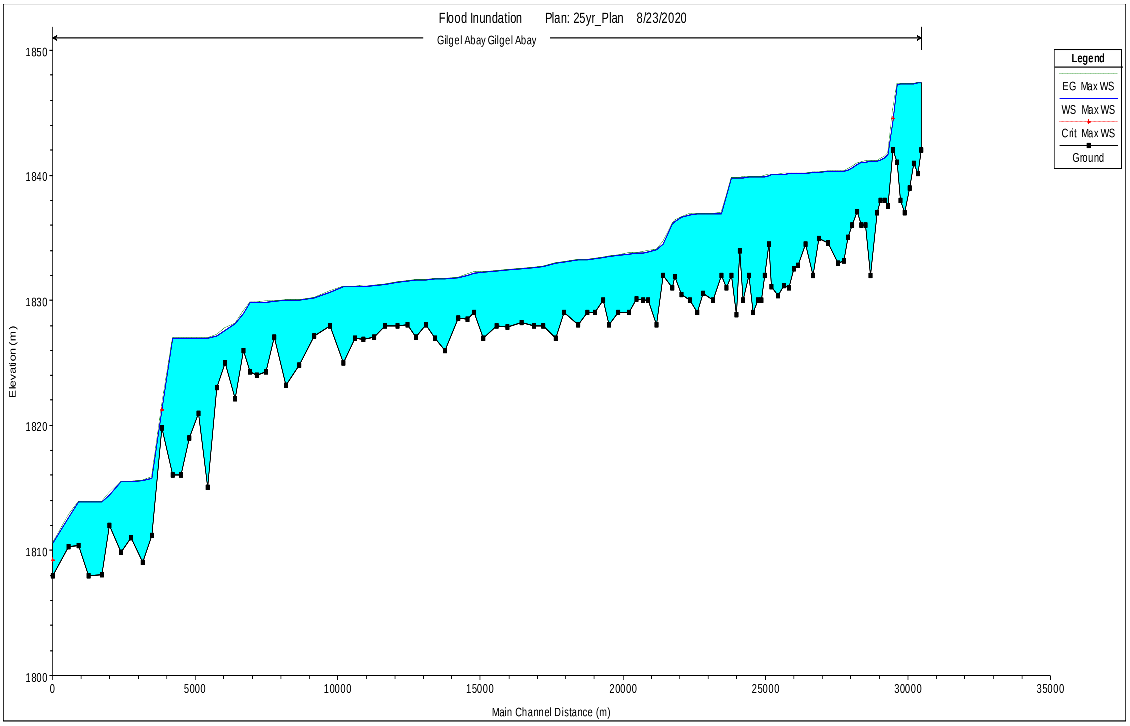

Figure A- 10 Water Surface Profile for 25 Year Storm

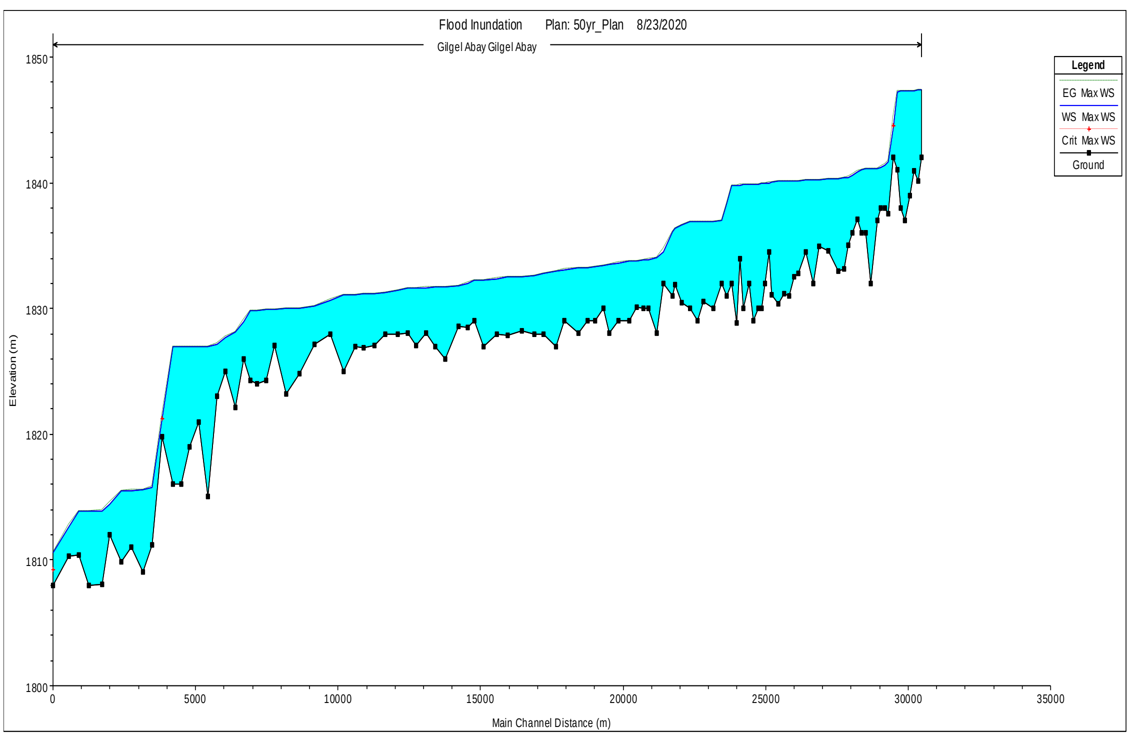

Figure A- 11 Water Surface Profile for 50 Year Storm

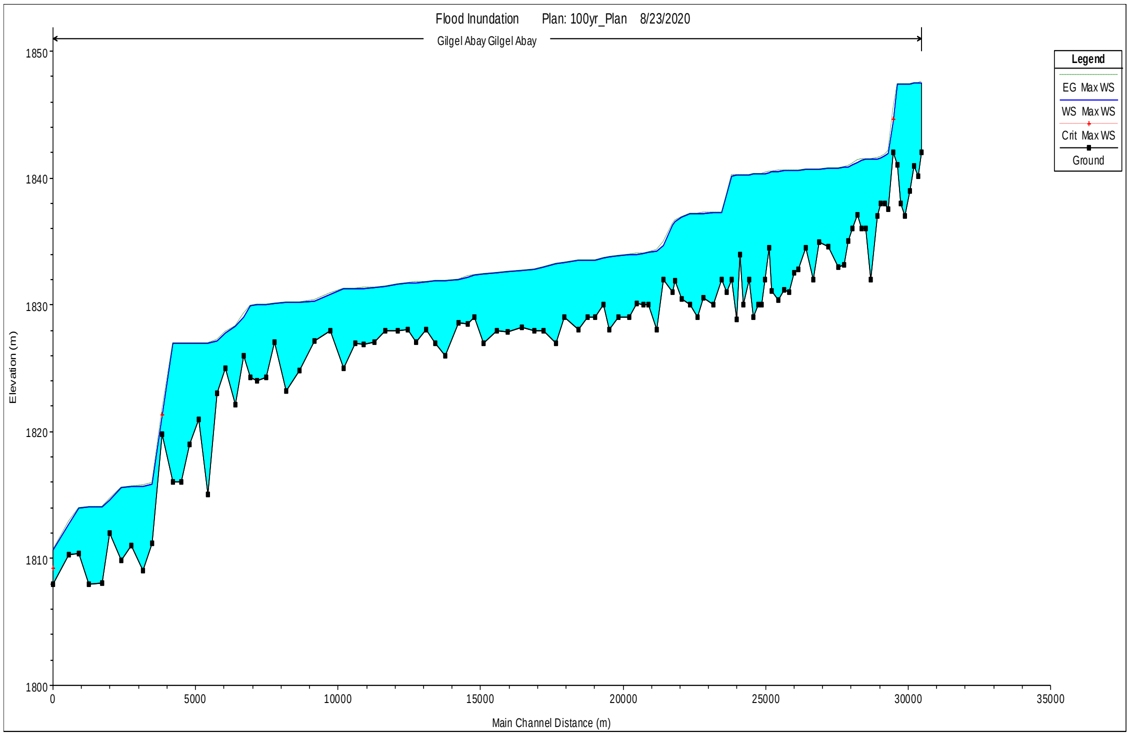

Figure A- 12 Water Surface Profile for 100 Year Storm

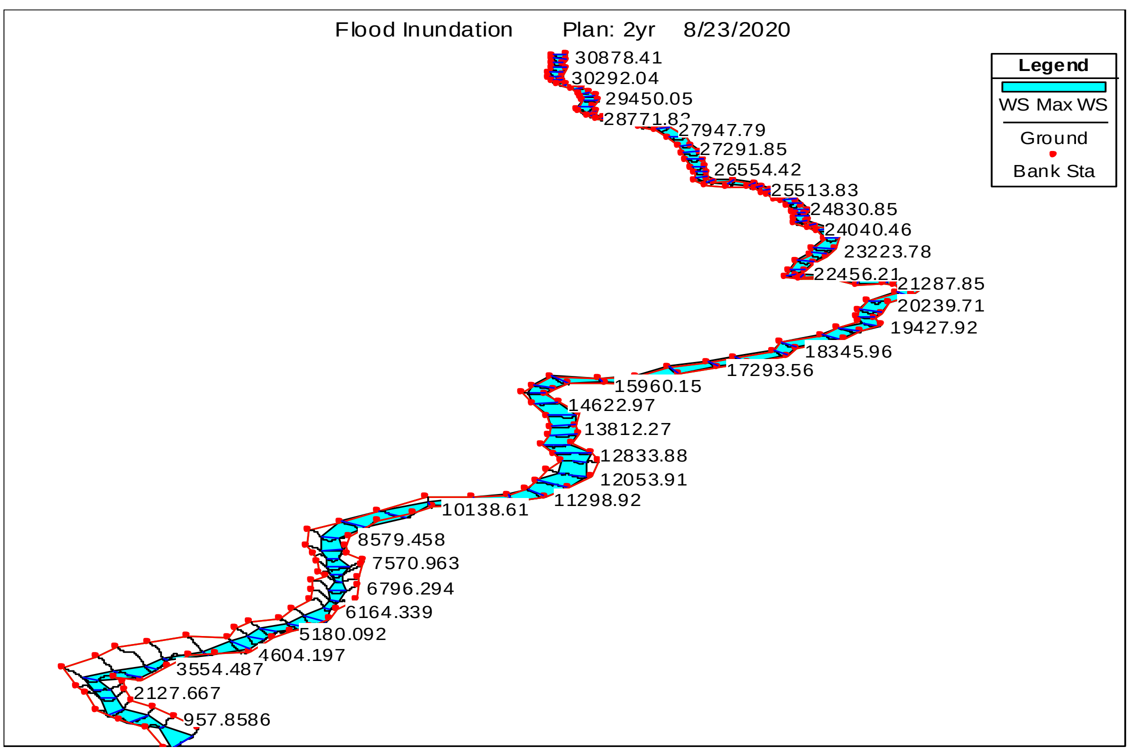

Figure A- 13 X-Y-Z Perspective of 3D View of 2 Year Flood

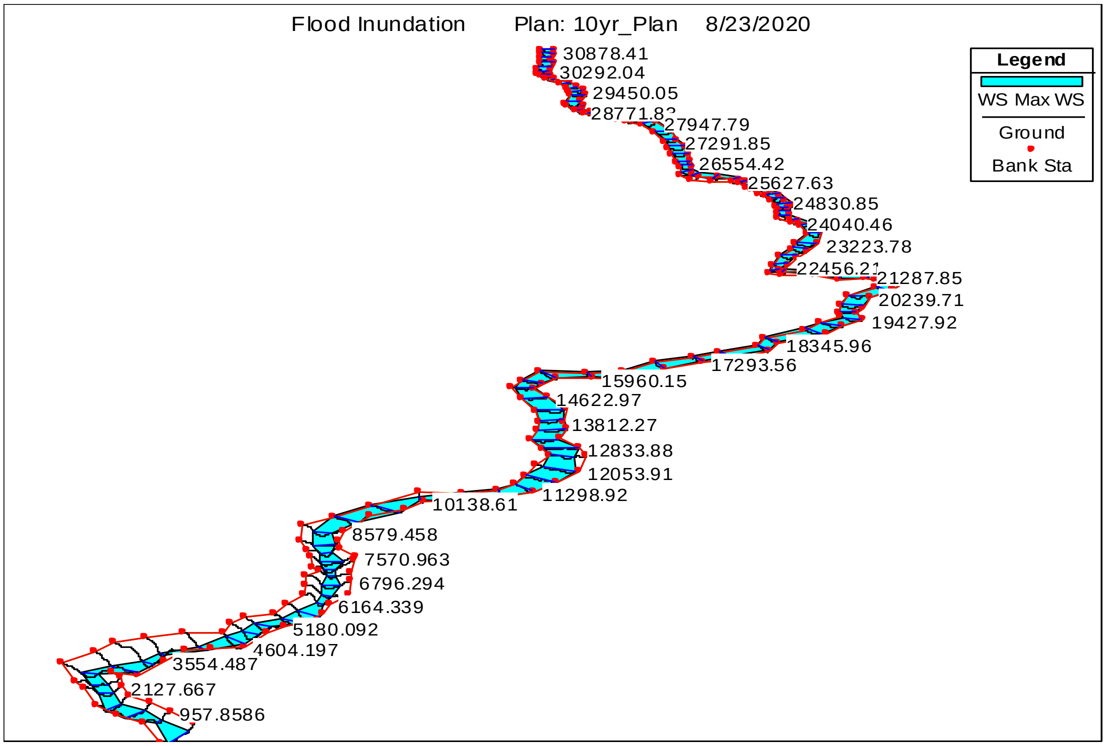

Figure A- 14 X-Y-Z Perspective of 3D View of 10 Year Flood

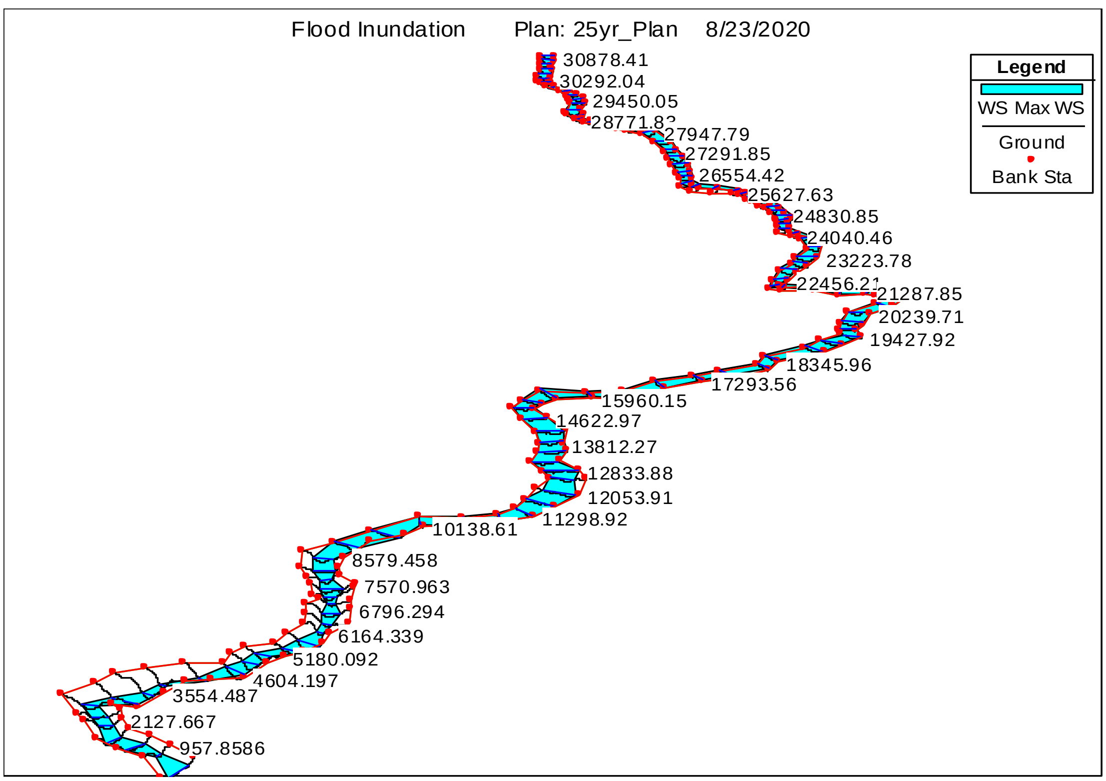

Figure A- 15 X-Y-Z Perspective of 3D View of 25 Year Flood

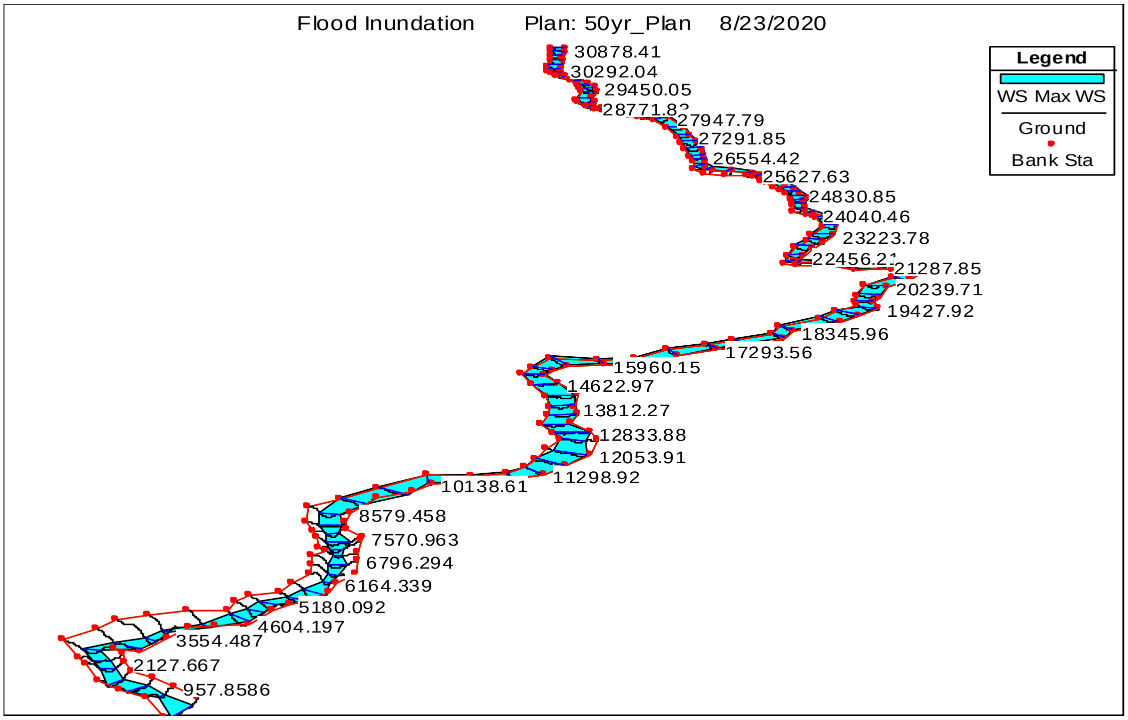

Figure A- 16 X-Y-Z Perspective of 3D View of 50 Year Flood

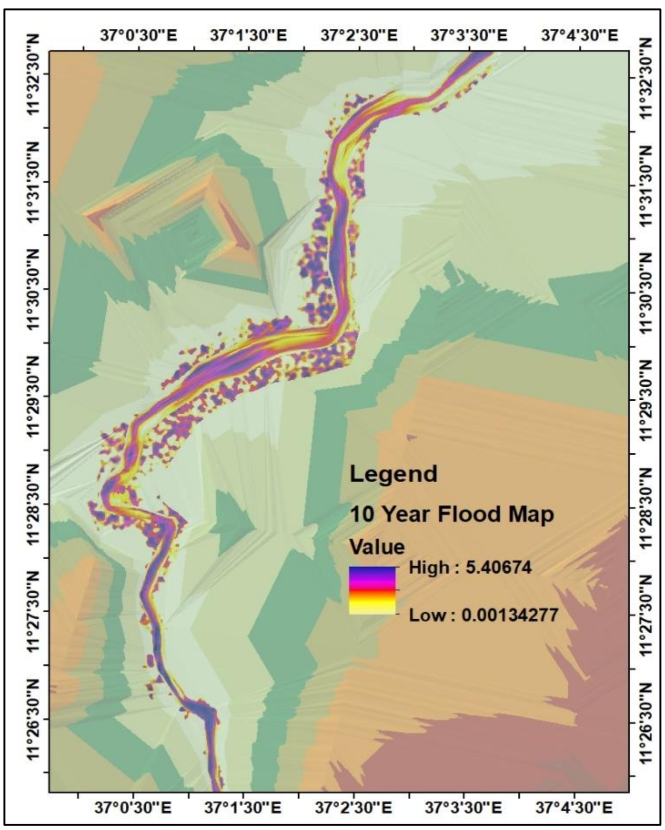

Figure A- 17 Ten Year Flood Map and Depth for the Area

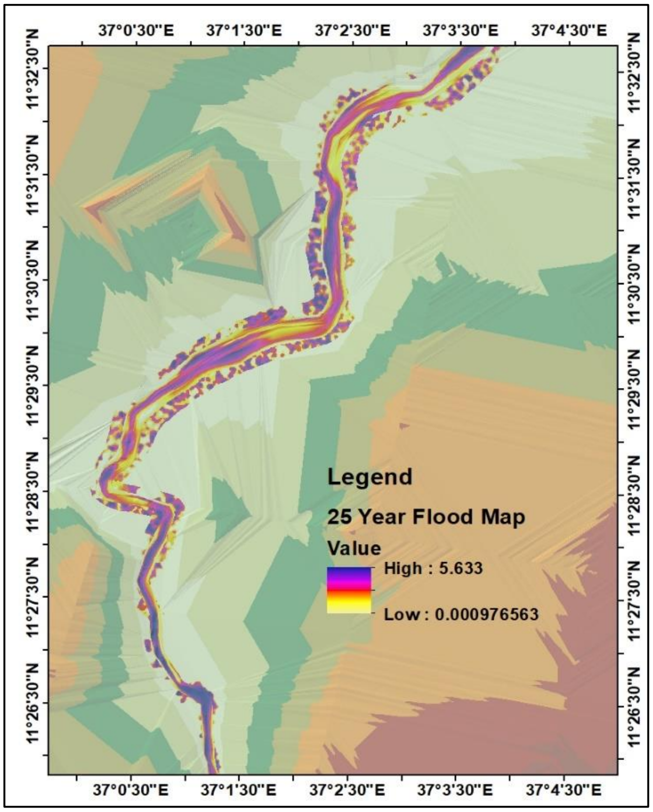

Figure A- 18 Twenty Five Year Flood Map and Depth for the Area

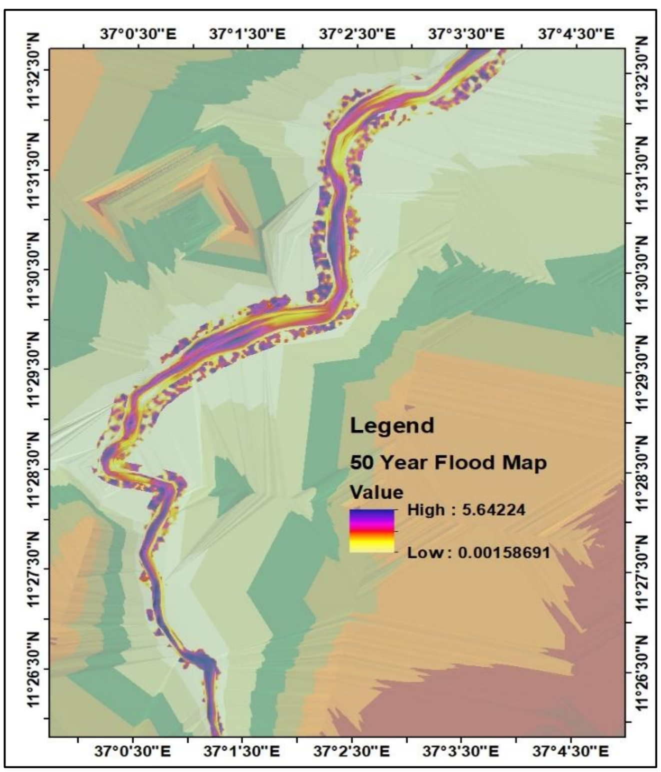

Figure A- 19 Fifty Year Flood Map and Depth for the Area

Maximum Water Surface Profile Output Tables, HEC-RAS

Table A- 11 Maximum Water Surface Profile for 2 Year Storm

Reach	River Sta	Profile	Q Total	Min Ch El	W.S. Elev	Crit W.S.	E.G. Elev	E.G. Slope	Vel Chnl	Flow Area	Top Width	Froude # Chl
			(m3/s)	(m)	(m)	(m)	(m)	(m/m)	(m/s)	(m2)	(m)	
Gilgel Abay	30878.41	Max WS	221.77	1842.02	1846.7		1846.71	0.000148	0.5	439.66	144.61	0.09
Gilgel Abay	30754.01	Max WS	221.5	1840.1	1846.69		1846.7	0.000038	0.34	647.11	136.87	0.05
Gilgel Abay	30623.44	Max WS	221.68	1840.99	1846.68		1846.69	0.000058	0.42	529.94	109.46	0.06
Gilgel Abay	30461.9	Max WS	221.61	1839	1846.67		1846.67	0.000016	0.27	835.16	133.42	0.03
Gilgel Abay	30292.04	Max WS	221.54	1837	1846.67		1846.67	0.000008	0.21	1054.38	136.24	0.02
Gilgel Abay	30137.44	Max WS	221.48	1838.02	1846.67		1846.67	0.000012	0.24	908.9	126.5	0.03
Gilgel Abay	30013.36	Max WS	221.5	1841	1846.65		1846.66	0.000063	0.42	529.92	119.33	0.06
Gilgel Abay	29881.01	Max WS	221.5	1842.01	1843.8	1843.98	1844.49	0.038547	3.66	60.56	67.24	1.23
Gilgel Abay	29712.37	Max WS	221.4	1837.57	1840.77		1840.86	0.00222	1.33	165.98	98.25	0.33
Gilgel Abay	29579.34	Max WS	221.1	1838	1840.45		1840.54	0.002574	1.33	166.54	110.38	0.35
Gilgel Abay	29450.05	Max WS	219.86	1837.99	1840.13		1840.2	0.002645	1.2	183.22	145.21	0.34
Gilgel Abay	29323.94	Max WS	219.66	1837	1839.99		1840.01	0.000399	0.66	330.39	153.08	0.14
Gilgel Abay	29085.98	Max WS	219.45	1832.01	1839.95		1839.95	0.000017	0.25	883.13	162.8	0.03
Gilgel Abay	28917.06	Max WS	219.31	1836	1839.93		1839.94	0.000149	0.49	443.5	153.69	0.09
Gilgel Abay	28771.83	Max WS	219.29	1836	1839.89		1839.91	0.000289	0.7	313.72	103.57	0.13
Gilgel Abay	28631.08	Max WS	217.9	1837.08	1839.49		1839.63	0.003964	1.66	131.38	86.25	0.43
Gilgel Abay	28461.73	Max WS	205.35	1836	1838.99		1839.08	0.002258	1.34	152.89	89.78	0.33
Gilgel Abay	28305.39	Max WS	200.36	1835	1838.76		1838.8	0.000558	0.89	226.09	84.58	0.17
Gilgel Abay	28168.07	Max WS	199.58	1833.19	1838.7		1838.71	0.000038	0.32	616.52	138.73	0.05

Gilgel Abay	27947.79	Max WS	199.33	1833	1838.69		1838.69	0.00003	0.29	678.5	151.62	0.04
Gilgel Abay	27593.15	Max WS	198.42	1834.61	1838.66		1838.67	0.000102	0.41	482.72	164.18	0.08
Gilgel Abay	27291.85	Max WS	197.81	1834.99	1838.58		1838.6	0.000318	0.64	309.41	126.5	0.13
Gilgel Abay	27065.43	Max WS	197.43	1832	1838.55		1838.55	0.000026	0.27	722.19	162.04	0.04
Gilgel Abay	26825.21	Max WS	197.08	1834.53	1838.52		1838.53	0.000099	0.4	493.53	170.57	0.07
Gilgel Abay	26554.42	Max WS	197.02	1832.77	1838.5		1838.51	0.000055	0.35	563.51	152.8	0.06
Gilgel Abay	26408.3	Max WS	196.75	1832.5	1838.49		1838.49	0.000033	0.32	607.31	119.4	0.05
Gilgel Abay	26216.51	Max WS	196.87	1831.01	1838.48		1838.48	0.000011	0.21	926.44	147.48	0.03
Gilgel Abay	26054.55	Max WS	196.83	1831.15	1838.47		1838.48	0.000013	0.23	854.2	138.7	0.03
Gilgel Abay	25852.31	Max WS	196.79	1830.35	1838.47		1838.47	0.000009	0.2	992.54	160.1	0.03
Gilgel Abay	25627.63	Max WS	196.69	1831.08	1838.46		1838.46	0.000033	0.35	561.04	98	0.05
Gilgel Abay	25513.83	Max WS	196.42	1834.54	1838.38		1838.41	0.000427	0.81	241.01	83.62	0.15
Gilgel Abay	25375.21	Max WS	196.47	1832	1838.34		1838.34	0.000039	0.35	556.76	111.46	0.05
Gilgel Abay	25276.05	Max WS	196.36	1830	1838.33		1838.34	0.000022	0.3	658.35	111.04	0.04
Gilgel Abay	25138.7	Max WS	196.45	1830.01	1838.32		1838.32	0.000023	0.29	671.94	118.68	0.04
Gilgel Abay	24980.18	Max WS	196.42	1829	1838.31		1838.31	0.00001	0.21	924.71	142.9	0.03
Gilgel Abay	24830.85	Max WS	196.39	1832	1838.3		1838.3	0.000022	0.27	721.65	139.92	0.04
Gilgel Abay	24628.31	Max WS	196.35	1830.01	1838.3		1838.3	0.000008	0.2	999.88	146.31	0.02
Gilgel Abay	24509.39	Max WS	196.36	1833.98	1838.27		1838.29	0.000136	0.54	363.68	97.57	0.09
Gilgel Abay	24384.22	Max WS	196.33	1828.83	1838.27		1838.27	0.000007	0.2	994.23	125.53	0.02
Gilgel Abay	24212.36	Max WS	196.32	1832	1838.25		1838.26	0.000042	0.35	555.6	115.35	0.05
Gilgel Abay	24040.46	Max WS	196.04	1831	1837.01		1837.02	0.000064	0.44	449	91.57	0.06
Gilgel Abay	23875.17	Max WS	195.4	1832	1835.82		1835.84	0.000123	0.45	432.93	145.16	0.08

Gilgel Abay	23572.69	Max WS	195.29	1830.01	1835.8		1835.81	0.000045	0.34	572.16	138.52	0.05
Gilgel Abay	23223.78	Max WS	195.25	1830.52	1835.79		1835.79	0.000033	0.26	750.93	219.77	0.04
Gilgel Abay	23021.91	Max WS	195.22	1829.01	1835.78		1835.79	0.000013	0.22	898.41	168.71	0.03
Gilgel Abay	22761.97	Max WS	195.28	1830	1835.77		1835.78	0.000026	0.26	744.09	179.49	0.04
Gilgel Abay	22456.21	Max WS	194.91	1830.43	1835.64		1835.65	0.00003	0.28	690.26	160.14	0.04
Gilgel Abay	22234.92	Max WS	194.52	1831.86	1835.47		1835.48	0.000135	0.47	410.29	135.21	0.09
Gilgel Abay	22136.4	Max WS	193.93	1831	1835.35		1835.36	0.000156	0.53	364.15	109.88	0.09
Gilgel Abay	21817.15	Max WS	195.48	1832	1833.91		1834.07	0.006618	1.75	111.93	100.42	0.53
Gilgel Abay	21567.81	Max WS	192.95	1828.02	1833.18		1833.18	0.000043	0.3	639.8	180.82	0.05
Gilgel Abay	21287.85	Max WS	191.8	1830.02	1833.05		1833.08	0.000728	0.75	255.1	152.59	0.19
Gilgel Abay	21128.65	Max WS	190.82	1830.03	1832.96		1832.98	0.00045	0.62	308.23	173.59	0.15
Gilgel Abay	20890.39	Max WS	190.38	1830.09	1832.9		1832.91	0.000175	0.42	456.23	228.69	0.09
Gilgel Abay	20606.21	Max WS	190.11	1829	1832.87		1832.88	0.000052	0.28	667.37	239.98	0.05
Gilgel Abay	20239.71	Max WS	188.05	1829.02	1832.73		1832.76	0.000635	0.73	258.91	148.68	0.18
Gilgel Abay	19929.67	Max WS	187.54	1828.01	1832.64		1832.65	0.000038	0.25	738.68	245.42	0.05
Gilgel Abay	19704.64	Max WS	186.69	1830.01	1832.55		1832.56	0.000319	0.55	341.95	177.69	0.13
Gilgel Abay	19427.92	Max WS	185.31	1829	1832.44		1832.45	0.00021	0.48	384.2	178.78	0.11
Gilgel Abay	19153.42	Max WS	185.11	1829	1832.41		1832.41	0.000079	0.31	605.48	265.54	0.06
Gilgel Abay	18847.24	Max WS	184.89	1828.01	1832.39		1832.39	0.000052	0.28	664.73	244.87	0.05
Gilgel Abay	18345.96	Max WS	183.72	1829.01	1832.24		1832.26	0.000454	0.55	334.28	225.77	0.14
Gilgel Abay	18057.74	Max WS	183.11	1827	1832.16		1832.17	0.000042	0.27	670.5	213.96	0.05
Gilgel Abay	17611.21	Max WS	181.51	1828	1831.99		1831.99	0.000067	0.3	597.85	232.86	0.06
Gilgel Abay	17293.56	Max WS	180.56	1828	1831.87		1831.87	0.000085	0.33	552.94	228.07	0.07

Gilgel Abay	16860.43	Max WS	179.92	1828.19	1831.82		1831.83	0.000066	0.28	645.71	283.18	0.06
Gilgel Abay	16358.08	Max WS	180.05	1827.84	1831.79		1831.8	0.000035	0.22	822.41	327.74	0.04
Gilgel Abay	15960.15	Max WS	179.49	1828	1831.7		1831.72	0.000357	0.62	289.44	136.54	0.14
Gilgel Abay	15493.99	Max WS	178.92	1827	1831.63		1831.63	0.00002	0.18	993.43	340.29	0.03
Gilgel Abay	15194.7	Max WS	178.71	1828.99	1831.59		1831.6	0.000133	0.37	487.41	240.59	0.08
Gilgel Abay	14963.08	Max WS	177.24	1828.51	1831.4		1831.43	0.001231	0.83	214.56	166.72	0.23
Gilgel Abay	14622.97	Max WS	174.98	1828.54	1831.15		1831.16	0.000381	0.49	355.67	251.07	0.13
Gilgel Abay	14170.82	Max WS	173.83	1826.01	1831.06		1831.07	0.000025	0.21	831.56	275.73	0.04
Gilgel Abay	13812.27	Max WS	173.85	1827.01	1831.04		1831.05	0.000076	0.3	576.4	249.33	0.06
Gilgel Abay	13490.45	Max WS	173.38	1828.01	1830.99		1831	0.000203	0.39	441.49	272.42	0.1
Gilgel Abay	13136.23	Max WS	172.85	1827.03	1830.94		1830.95	0.000102	0.32	544.27	274.49	0.07
Gilgel Abay	12833.88	Max WS	172.84	1828.03	1830.91		1830.92	0.0001	0.28	618.49	373.98	0.07
Gilgel Abay	12495.29	Max WS	172.32	1828	1830.81		1830.83	0.000405	0.6	289.35	160.38	0.14
Gilgel Abay	12053.91	Max WS	171.53	1828	1830.66		1830.67	0.000337	0.45	385.15	288.07	0.12
Gilgel Abay	11678.69	Max WS	171.39	1827.05	1830.58		1830.58	0.000093	0.26	649.27	400.27	0.07
Gilgel Abay	11298.92	Max WS	171.34	1826.84	1830.53		1830.53	0.000131	0.35	495.93	266.69	0.08
Gilgel Abay	11005.39	Max WS	171.27	1827.01	1830.5		1830.5	0.000082	0.3	569.75	263.47	0.07
Gilgel Abay	10589.51	Max WS	171.21	1825.02	1830.47		1830.47	0.000069	0.28	621.61	288.82	0.06
Gilgel Abay	10138.61	Max WS	171.06	1828	1830.12		1830.16	0.001535	0.93	183.54	141.36	0.26
Gilgel Abay	9572.952	Max WS	170.69	1827.12	1829.58		1829.6	0.000637	0.53	320.66	295.38	0.16
Gilgel Abay	9060.053	Max WS	169.99	1824.79	1829.42		1829.42	0.000052	0.24	702.51	321.63	0.05
Gilgel Abay	8579.458	Max WS	169.33	1823.23	1829.4		1829.4	0.00003	0.25	675.57	196.94	0.04
Gilgel Abay	8157.789	Max WS	168.82	1827.05	1829.34		1829.35	0.000223	0.44	388	220.07	0.1

Gilgel Abay	7876.896	Max WS	168.58	1824.24	1829.29		1829.3	0.000113	0.47	362.15	111.49	0.08
Gilgel Abay	7570.963	Max WS	168.3	1824.02	1829.28		1829.28	0.000026	0.22	767.81	241.08	0.04
Gilgel Abay	7312.366	Max WS	168.05	1824.29	1829.25		1829.26	0.000146	0.49	341.87	117.37	0.09
Gilgel Abay	7084.47	Max WS	167.93	1826.01	1828.43		1828.6	0.006217	1.83	91.72	73.13	0.52
Gilgel Abay	6796.294	Max WS	167.71	1822.09	1827.62		1827.62	0.000055	0.31	536.43	175.88	0.06
Gilgel Abay	6449.194	Max WS	167.38	1825.04	1827.26		1827.32	0.001816	1.1	151.79	102.93	0.29
Gilgel Abay	6164.339	Max WS	121.13	1823	1827		1827.02	0.000283	0.59	204.3	86.75	0.12
Gilgel Abay	5833.369	Max WS	121.06	1815.04	1826.96		1826.96	0.000001	0.06	2165.68	304.18	0.01
Gilgel Abay	5505.133	Max WS	121.08	1820.99	1826.95		1826.95	0.000014	0.16	773.95	249.36	0.03
Gilgel Abay	5180.092	Max WS	120.8	1818.97	1826.95		1826.95	0.000003	0.11	1143.38	228.4	0.02
Gilgel Abay	4892.707	Max WS	120.7	1816.02	1826.95		1826.95	0.000001	0.08	1446.82	225.05	0.01
Gilgel Abay	4604.197	Max WS	120.58	1816.01	1826.95		1826.95	0	0.05	2529.46	352.79	0.01
Gilgel Abay	4234.233	Max WS	169.04	1819.82	1820.92	1820.96	1821.26	0.033622	2.56	66.11	113.45	1.07
Gilgel Abay	3873.924	Max WS	168.38	1811.17	1815.28		1815.33	0.000689	0.92	182.21	77.52	0.19
Gilgel Abay	3554.487	Max WS	168.15	1809.04	1815.2		1815.2	0.000043	0.31	540.33	146.94	0.05
Gilgel Abay	3155.623	Max WS	168.07	1811	1815.15		1815.16	0.000183	0.39	434.08	249.53	0.09
Gilgel Abay	2781.871	Max WS	168	1809.86	1815.11		1815.11	0.000047	0.3	561.67	172.74	0.05
Gilgel Abay	2384.771	Max WS	168.33	1812	1813.98		1814.09	0.005353	1.46	115.02	114.79	0.47
Gilgel Abay	2127.667	Max WS	167.04	1808.02	1813.36		1813.37	0.000065	0.34	487.16	156.47	0.06
Gilgel Abay	1657.528	Max WS	166.85	1807.98	1813.34		1813.35	0.00002	0.19	860.16	265.71	0.03
Gilgel Abay	1292.115	Max WS	166.56	1810.38	1813.32		1813.32	0.00011	0.3	547.41	313.55	0.07
Gilgel Abay	957.8586	Max WS	166.36	1810.34	1812.19		1812.35	0.006505	1.72	96.6	87.34	0.52
Gilgel Abay	398.9698	Max WS	166.02	1808	1810.29	1808.86	1810.3	0.001017	0.52	320.02	436.15	0.19

Table A- 12 Maximum Water Surface Profile for 10 Year Storm

Reach	**River Sta**	**Profile**	**Q Total**	**Min Ch El**	**W.S. Elev**	**Crit W.S.**	**E.G. Elev**	**E.G. Slope**	**Vel Chnl**	**Flow Area**	**Top Width**	**Froude # Chl**
			(m3/s)	**(m)**	**(m)**	**(m)**	**(m)**	**(m/m)**	**(m/s)**	**(m2)**	**(m)**	
Gilgel Abay	30878.41	Max WS	364.84	1842.02	1847.19		1847.22	0.000244	0.71	510.9	144.61	0.12
Gilgel Abay	30754.01	Max WS	364.76	1840.1	1847.18		1847.19	0.000074	0.51	713.72	136.87	0.07
Gilgel Abay	30623.44	Max WS	364.69	1840.99	1847.15		1847.17	0.000117	0.63	581.35	109.46	0.09
Gilgel Abay	30461.9	Max WS	364.58	1839	1847.13		1847.14	0.000035	0.41	896.66	133.42	0.05
Gilgel Abay	30292.04	Max WS	364.45	1837	1847.13		1847.13	0.000018	0.33	1116.87	136.24	0.04
Gilgel Abay	30137.44	Max WS	364.34	1838.02	1847.12		1847.13	0.000026	0.38	966.43	126.5	0.04
Gilgel Abay	30013.36	Max WS	364.26	1841	1847.1		1847.12	0.000125	0.63	582.54	119.33	0.09
Gilgel Abay	29881.01	Max WS	364.78	1842.01	1844.18	1844.36	1845.02	0.038389	4.05	90.09	85.43	1.26
Gilgel Abay	29712.37	Max WS	362.51	1837.57	1841.35		1841.48	0.002353	1.61	225.68	105.28	0.35
Gilgel Abay	29579.34	Max WS	358.5	1838	1841.05		1841.17	0.002313	1.53	233.84	114.67	0.34
Gilgel Abay	29450.05	Max WS	353.95	1837.99	1840.82		1840.9	0.001637	1.23	287.42	152.12	0.29
Gilgel Abay	29323.94	Max WS	350.61	1837	1840.73		1840.76	0.000398	0.78	447.41	160.62	0.15
Gilgel Abay	29085.98	Max WS	349.3	1832.01	1840.7		1840.71	0.000029	0.35	1006.3	166.14	0.05
Gilgel Abay	28917.06	Max WS	348.04	1836	1840.67		1840.69	0.000183	0.62	560.09	160.13	0.11
Gilgel Abay	28771.83	Max WS	344.35	1836	1840.61		1840.65	0.000371	0.88	390.41	108.96	0.15
Gilgel Abay	28631.08	Max WS	323.26	1837.08	1840.34		1840.46	0.00215	1.54	209.97	96.62	0.33
Gilgel Abay	28461.73	Max WS	312.49	1836	1840.08		1840.16	0.001038	1.24	251.35	90.43	0.24
Gilgel Abay	28305.39	Max WS	305.5	1835	1839.89		1839.94	0.000415	0.95	321.63	84.58	0.16
Gilgel Abay	28168.07	Max WS	304.32	1833.19	1839.82		1839.83	0.000043	0.39	772.59	138.73	0.05
Gilgel Abay	27947.79	Max WS	303.19	1833	1839.81		1839.81	0.000034	0.36	848.44	151.62	0.05
Gilgel Abay	27593.15	Max WS	302.66	1834.61	1839.78		1839.79	0.000082	0.45	666.62	164.18	0.07
Gilgel Abay	27291.85	Max WS	301.27	1834.99	1839.7		1839.73	0.000214	0.67	451.83	126.5	0.11
Gilgel Abay	27065.43	Max WS	300.38	1832	1839.68		1839.68	0.000029	0.33	905.28	162.04	0.04
Gilgel Abay	26825.21	Max WS	299.99	1834.53	1839.65		1839.66	0.000078	0.44	685.96	170.57	0.07
Gilgel Abay	26554.42	Max WS	300.26	1832.77	1839.62		1839.63	0.000054	0.41	735.18	152.8	0.06
Gilgel Abay	26408.3	Max WS	299.65	1832.5	1839.61		1839.62	0.00004	0.4	740.77	119.4	0.05
Gilgel Abay	26216.51	Max WS	299.89	1831.01	1839.59		1839.6	0.000015	0.27	1090.53	147.48	0.03
Gilgel Abay	26054.55	Max WS	299.59	1831.15	1839.58		1839.59	0.000018	0.3	1007.97	138.7	0.04
Gilgel Abay	25852.31	Max WS	299.53	1830.35	1839.57		1839.58	0.000013	0.26	1169.48	160.1	0.03

Gilgel Abay	25627.63	Max WS	299.31	1831.08	1839.55		1839.56	0.000043	0.45	668.65	98	0.05
Gilgel Abay	25513.83	Max WS	298.96	1834.54	1839.46		1839.5	0.000353	0.9	331.6	83.62	0.14
Gilgel Abay	25375.21	Max WS	298.79	1832	1839.41		1839.42	0.000049	0.44	676.75	111.46	0.06
Gilgel Abay	25276.05	Max WS	298.93	1830	1839.41		1839.42	0.00003	0.38	777.68	111.04	0.05
Gilgel Abay	25138.7	Max WS	298.77	1830.01	1839.38		1839.39	0.000031	0.37	798.19	118.68	0.05
Gilgel Abay	24980.18	Max WS	298.74	1829	1839.36		1839.36	0.000014	0.28	1074.98	142.9	0.03
Gilgel Abay	24830.85	Max WS	298.65	1832	1839.35		1839.35	0.000028	0.34	868.27	139.92	0.04
Gilgel Abay	24628.31	Max WS	298.61	1830.01	1839.34		1839.34	0.000012	0.26	1152.85	146.31	0.03
Gilgel Abay	24509.39	Max WS	298.71	1833.98	1839.31		1839.33	0.000142	0.64	464.82	97.57	0.09
Gilgel Abay	24384.22	Max WS	298.58	1828.83	1839.31		1839.31	0.000011	0.27	1124.39	125.53	0.03
Gilgel Abay	24212.36	Max WS	298.6	1832	1839.28		1839.29	0.000052	0.44	674.14	115.35	0.06
Gilgel Abay	24040.46	Max WS	297.76	1831	1837.9		1837.91	0.000087	0.56	530.28	91.57	0.07
Gilgel Abay	23875.17	Max WS	295.88	1832	1836.59		1836.61	0.000133	0.54	544.08	145.16	0.09
Gilgel Abay	23572.69	Max WS	295.71	1830.01	1836.56		1836.57	0.000061	0.44	678.7	141.35	0.06
Gilgel Abay	23223.78	Max WS	295.59	1830.52	1836.54		1836.55	0.00004	0.32	917.43	220.89	0.05
Gilgel Abay	23021.91	Max WS	295.7	1829.01	1836.54		1836.54	0.00002	0.29	1025.11	168.71	0.04
Gilgel Abay	22761.97	Max WS	295.6	1830	1836.52		1836.52	0.000035	0.34	877.63	179.49	0.05
Gilgel Abay	22456.21	Max WS	295.51	1830.43	1836.32		1836.33	0.000043	0.37	799.06	160.14	0.05
Gilgel Abay	22234.92	Max WS	295.36	1831.86	1836.05		1836.06	0.000176	0.6	488.67	135.21	0.1
Gilgel Abay	22136.4	Max WS	294.84	1831	1835.84		1835.86	0.00023	0.71	417.77	109.88	0.12
Gilgel Abay	21817.15	Max WS	293.53	1832	1834.33		1834.52	0.005382	1.9	154.85	104.78	0.5
Gilgel Abay	21567.81	Max WS	287.47	1828.02	1833.77		1833.77	0.000058	0.39	746.13	180.82	0.06
Gilgel Abay	21287.85	Max WS	284.76	1830.02	1833.63		1833.67	0.000702	0.81	349.59	179.98	0.19
Gilgel Abay	21128.65	Max WS	283.21	1830.03	1833.55		1833.58	0.000402	0.68	413.58	183.6	0.15
Gilgel Abay	20890.39	Max WS	281.96	1830.09	1833.5		1833.51	0.000165	0.47	595.21	235.99	0.1
Gilgel Abay	20606.21	Max WS	281.71	1829	1833.47		1833.48	0.000062	0.35	812.72	245.37	0.06
Gilgel Abay	20239.71	Max WS	278.98	1829.02	1833.33		1833.37	0.000567	0.79	352.83	162.58	0.17
Gilgel Abay	19929.67	Max WS	277.29	1828.01	1833.25		1833.26	0.000045	0.31	888.51	245.42	0.05
Gilgel Abay	19704.64	Max WS	275.36	1830.01	1833.15		1833.17	0.000283	0.61	448.55	177.69	0.12
Gilgel Abay	19427.92	Max WS	273.44	1829	1833.03		1833.05	0.000245	0.55	495.57	211.73	0.12
Gilgel Abay	19153.42	Max WS	272.2	1829	1832.99		1833	0.000079	0.36	761.66	265.54	0.07
Gilgel Abay	18847.24	Max WS	272.73	1828.01	1832.97		1832.98	0.000061	0.34	810.46	254.54	0.06
Gilgel Abay	18345.96	Max WS	270.62	1829.01	1832.82		1832.84	0.000329	0.58	465.73	225.77	0.13
Gilgel Abay	18057.74	Max WS	268.62	1827	1832.74		1832.74	0.000052	0.34	792.9	213.96	0.06

Gilgel Abay	17611.21	Max WS	265.28	1828	1832.51		1832.52	0.000077	0.37	720.91	232.86	0.07
Gilgel Abay	17293.56	Max WS	262.36	1828	1832.37		1832.38	0.000096	0.39	668.38	228.07	0.07
Gilgel Abay	16860.43	Max WS	261.44	1828.19	1832.32		1832.32	0.000072	0.33	785.29	283.18	0.06
Gilgel Abay	16358.08	Max WS	260.93	1827.84	1832.28		1832.28	0.000042	0.27	980.64	327.74	0.05
Gilgel Abay	15960.15	Max WS	259.12	1828	1832.17		1832.19	0.0004	0.73	354.19	141.64	0.15
Gilgel Abay	15493.99	Max WS	258.32	1827	1832.08		1832.09	0.000025	0.22	1149.21	340.29	0.04
Gilgel Abay	15194.7	Max WS	257.82	1828.99	1832.03		1832.04	0.000144	0.43	593.98	240.59	0.09
Gilgel Abay	14963.08	Max WS	255.83	1828.51	1831.85		1831.88	0.001113	0.87	295.24	197.73	0.23
Gilgel Abay	14622.97	Max WS	252.1	1828.54	1831.63		1831.65	0.000303	0.53	479.64	257.06	0.12
Gilgel Abay	14170.82	Max WS	251.5	1826.01	1831.56		1831.57	0.000033	0.26	970.73	282.22	0.04
Gilgel Abay	13812.27	Max WS	250.67	1827.01	1831.53		1831.54	0.000084	0.36	699.07	249.33	0.07
Gilgel Abay	13490.45	Max WS	250.26	1828.01	1831.48		1831.49	0.000187	0.43	585.54	298.91	0.1
Gilgel Abay	13136.23	Max WS	249.57	1827.03	1831.44		1831.44	0.000103	0.37	681.49	280.68	0.08
Gilgel Abay	12833.88	Max WS	249.26	1828.03	1831.41		1831.41	0.000087	0.31	803.72	373.98	0.07
Gilgel Abay	12495.29	Max WS	248.11	1828	1831.28		1831.3	0.000569	0.63	391.51	254.86	0.16
Gilgel Abay	12053.91	Max WS	246.95	1828	1831.09		1831.1	0.000349	0.47	523.18	367.99	0.13
Gilgel Abay	11678.69	Max WS	246.45	1827.05	1831.01		1831.01	0.000088	0.3	820.95	400.27	0.07
Gilgel Abay	11298.92	Max WS	246.02	1826.84	1830.95		1830.96	0.000148	0.4	612.64	287.82	0.09
Gilgel Abay	11005.39	Max WS	245.89	1827.01	1830.91		1830.92	0.000096	0.36	680.35	268.7	0.07
Gilgel Abay	10589.51	Max WS	245.91	1825.02	1830.88		1830.88	0.000086	0.33	744.47	310.98	0.07
Gilgel Abay	10138.61	Max WS	245.06	1828	1830.5		1830.55	0.001456	1.02	239.12	153.45	0.26
Gilgel Abay	9572.952	Max WS	243.15	1827.12	1829.99		1830	0.000489	0.55	443.49	320.02	0.15
Gilgel Abay	9060.053	Max WS	242.59	1824.79	1829.86		1829.86	0.000058	0.29	844.16	325.58	0.06
Gilgel Abay	8579.458	Max WS	242.47	1823.23	1829.83		1829.84	0.000044	0.32	762.56	205.38	0.05
Gilgel Abay	8157.789	Max WS	242.41	1827.05	1829.77		1829.78	0.000232	0.5	483.64	228.51	0.11
Gilgel Abay	7876.896	Max WS	242.37	1824.24	1829.71		1829.72	0.000166	0.59	409.41	116.65	0.1
Gilgel Abay	7570.963	Max WS	242.3	1824.02	1829.69		1829.69	0.000037	0.28	868.03	248.71	0.05
Gilgel Abay	7312.366	Max WS	242.24	1824.29	1829.64		1829.66	0.000214	0.62	389.65	125.19	0.11
Gilgel Abay	7084.47	Max WS	242.24	1826.01	1828.78		1828.99	0.006197	2.04	118.75	80.28	0.54
Gilgel Abay	6796.294	Max WS	242.15	1822.09	1827.99		1828	0.000082	0.4	603.8	182.82	0.07
Gilgel Abay	6449.194	Max WS	242.05	1825.04	1827.52		1827.61	0.002326	1.35	179.58	108.5	0.33
Gilgel Abay	6164.339	Max WS	234.55	1823	1827.07		1827.13	0.000974	1.11	210.38	87.65	0.23
Gilgel Abay	5833.369	Max WS	121.06	1815.04	1826.96		1826.96	0.000001	0.06	2165.68	304.18	0.01
Gilgel Abay	5505.133	Max WS	121.08	1820.99	1826.95		1826.95	0.000014	0.16	773.95	249.36	0.03

Gilgel Abay	5180.092	Max WS	120.8	1818.97	1826.95		1826.95	0.000003	0.11	1143.38	228.4	0.02
Gilgel Abay	4892.707	Max WS	120.7	1816.02	1826.95		1826.95	0.000001	0.08	1446.82	225.05	0.01
Gilgel Abay	4604.197	Max WS	120.58	1816.01	1826.95		1826.95	0	0.05	2529.46	352.79	0.01
Gilgel Abay	4234.233	Max WS	241.75	1819.82	1821.12	1821.15	1821.48	0.032566	2.66	90.95	143.79	1.07
Gilgel Abay	3873.924	Max WS	241.69	1811.17	1815.61		1815.68	0.000985	1.16	208.01	82.05	0.23
Gilgel Abay	3554.487	Max WS	241.67	1809.04	1815.48		1815.49	0.000073	0.41	583.77	153.82	0.07
Gilgel Abay	3155.623	Max WS	241.51	1811	1815.42		1815.43	0.000245	0.48	502.93	259.93	0.11
Gilgel Abay	2781.871	Max WS	241.31	1809.86	1815.36		1815.37	0.000077	0.4	605.9	176.88	0.07
Gilgel Abay	2384.771	Max WS	242.33	1812	1814.31		1814.43	0.004837	1.55	155.85	131.59	0.46
Gilgel Abay	2127.667	Max WS	242.14	1808.02	1813.76		1813.77	0.000096	0.44	550.84	163.88	0.08
Gilgel Abay	1657.528	Max WS	241.39	1807.98	1813.73		1813.74	0.000029	0.25	965.01	271.5	0.04
Gilgel Abay	1292.115	Max WS	240.59	1810.38	1813.7		1813.71	0.000121	0.36	669.64	320	0.08
Gilgel Abay	957.8586	Max WS	240.09	1810.34	1812.48		1812.67	0.006716	1.97	122.16	92.79	0.55
Gilgel Abay	398.9698	Max WS	239.09	1808	1810.47	1809.11	1810.49	0.001021	0.59	402.03	447.67	0.2

Table A- 13 Maximum Water Surface Profile for 25 Year Storm

Reach	**River Sta**	**Profile**	**Q Total**	**Min Ch El**	**W.S. Elev**	**Crit W.S.**	**E.G. Elev**	**E.G. Slope**	**Vel Chnl**	**Flow Area**	**Top Width**	**Froude # Chl**
			(m3/s)	**(m)**	**(m)**	**(m)**	**(m)**	**(m/m)**	**(m/s)**	**(m2)**	**(m)**	
Gilgel Abay	30878.41	Max WS	435.75	1842.02	1847.38		1847.41	0.000295	0.81	537.87	144.61	0.13
Gilgel Abay	30754.01	Max WS	435.68	1840.1	1847.36		1847.38	0.000094	0.59	738.84	136.87	0.08
Gilgel Abay	30623.44	Max WS	435.6	1840.99	1847.32		1847.35	0.00015	0.73	600.23	109.46	0.1
Gilgel Abay	30461.9	Max WS	435.47	1839	1847.3		1847.31	0.000046	0.47	918.97	133.42	0.06
Gilgel Abay	30292.04	Max WS	435.32	1837	1847.29		1847.3	0.000024	0.38	1139.5	136.24	0.04
Gilgel Abay	30137.44	Max WS	435.15	1838.02	1847.28		1847.29	0.000035	0.44	987.14	126.5	0.05
Gilgel Abay	30013.36	Max WS	435.02	1841	1847.25		1847.28	0.000161	0.72	601.14	119.33	0.1
Gilgel Abay	29881.01	Max WS	436.06	1842.01	1844.32	1844.52	1845.26	0.037486	4.3	101.47	86.29	1.27
Gilgel Abay	29712.37	Max WS	428.6	1837.57	1841.65		1841.79	0.002188	1.67	257.31	107.34	0.34
Gilgel Abay	29579.34	Max WS	418.67	1838	1841.38		1841.5	0.001957	1.54	272.5	117.04	0.32
Gilgel Abay	29450.05	Max WS	402.3	1837.99	1841.2		1841.27	0.001159	1.17	344.92	152.12	0.25
Gilgel Abay	29323.94	Max WS	394.3	1837	1841.13		1841.16	0.000324	0.77	511.4	160.62	0.14
Gilgel Abay	29085.98	Max WS	390.85	1832.01	1841.1		1841.11	0.000029	0.36	1073.93	167.72	0.05
Gilgel Abay	28917.06	Max WS	390.03	1836	1841.08		1841.1	0.000165	0.62	625.9	163.94	0.1
Gilgel Abay	28771.83	Max WS	386.74	1836	1841.02		1841.06	0.000333	0.89	435.62	110.57	0.14

Gilgel Abay	28631.08	Max WS	373.48	1837.08	1840.82		1840.92	0.001553	1.46	256.54	100.13	0.29
Gilgel Abay	28461.73	Max WS	365.1	1836	1840.61		1840.68	0.000806	1.22	299.04	90.43	0.21
Gilgel Abay	28305.39	Max WS	358.34	1835	1840.42		1840.47	0.000375	0.98	366.41	84.58	0.15
Gilgel Abay	28168.07	Max WS	354.61	1833.19	1840.35		1840.36	0.000043	0.42	845.78	138.73	0.05
Gilgel Abay	27947.79	Max WS	353.92	1833	1840.33		1840.34	0.000034	0.38	928.1	151.62	0.05
Gilgel Abay	27593.15	Max WS	353.84	1834.61	1840.3		1840.32	0.000076	0.47	752.8	164.18	0.07
Gilgel Abay	27291.85	Max WS	352.02	1834.99	1840.23		1840.25	0.000187	0.68	518.35	126.5	0.11
Gilgel Abay	27065.43	Max WS	350.91	1832	1840.2		1840.21	0.00003	0.35	990.43	162.04	0.05
Gilgel Abay	26825.21	Max WS	351.4	1834.53	1840.18		1840.19	0.000072	0.45	775.44	170.57	0.07
Gilgel Abay	26554.42	Max WS	350.47	1832.77	1840.15		1840.16	0.000053	0.43	815.07	152.8	0.06
Gilgel Abay	26408.3	Max WS	350.44	1832.5	1840.13		1840.14	0.000042	0.44	802.85	119.4	0.05
Gilgel Abay	26216.51	Max WS	350.4	1831.01	1840.11		1840.12	0.000016	0.3	1166.89	147.48	0.03
Gilgel Abay	26054.55	Max WS	350.33	1831.15	1840.1		1840.1	0.000019	0.32	1079.45	138.7	0.04
Gilgel Abay	25852.31	Max WS	350.02	1830.35	1840.09		1840.09	0.000014	0.28	1251.8	160.1	0.03
Gilgel Abay	25627.63	Max WS	349.74	1831.08	1840.07		1840.08	0.000047	0.49	718.75	98	0.06
Gilgel Abay	25513.83	Max WS	349.71	1834.54	1839.97		1840.01	0.000329	0.94	373.8	83.62	0.14
Gilgel Abay	25375.21	Max WS	349.25	1832	1839.91		1839.93	0.000052	0.48	732.7	111.46	0.06
Gilgel Abay	25276.05	Max WS	349.44	1830	1839.91		1839.92	0.000033	0.42	833.33	111.04	0.05
Gilgel Abay	25138.7	Max WS	349.38	1830.01	1839.88		1839.89	0.000034	0.41	856.85	118.68	0.05
Gilgel Abay	24980.18	Max WS	349.02	1829	1839.85		1839.85	0.000016	0.3	1144.76	142.9	0.03
Gilgel Abay	24830.85	Max WS	349.14	1832	1839.84		1839.84	0.00003	0.37	936.43	139.92	0.05
Gilgel Abay	24628.31	Max WS	349.08	1830.01	1839.83		1839.83	0.000013	0.29	1223.88	146.31	0.03
Gilgel Abay	24509.39	Max WS	348.88	1833.98	1839.79		1839.82	0.000143	0.68	511.87	97.57	0.1
Gilgel Abay	24384.22	Max WS	348.96	1828.83	1839.79		1839.79	0.000013	0.29	1184.85	125.53	0.03
Gilgel Abay	24212.36	Max WS	348.96	1832	1839.76		1839.77	0.000055	0.48	729.25	115.35	0.06
Gilgel Abay	24040.46	Max WS	347.71	1831	1838.32		1838.33	0.000095	0.61	568.46	91.57	0.08
Gilgel Abay	23875.17	Max WS	345.13	1832	1836.96		1836.97	0.000134	0.58	597.03	145.16	0.09
Gilgel Abay	23572.69	Max WS	345.07	1830.01	1836.92		1836.93	0.000066	0.47	729.8	141.35	0.07
Gilgel Abay	23223.78	Max WS	345.07	1830.52	1836.9		1836.91	0.000041	0.35	997.02	220.89	0.05
Gilgel Abay	23021.91	Max WS	344.94	1829.01	1836.89		1836.9	0.000023	0.32	1085.7	168.71	0.04
Gilgel Abay	22761.97	Max WS	344.83	1830	1836.87		1836.88	0.000038	0.37	941.47	179.49	0.05
Gilgel Abay	22456.21	Max WS	344.77	1830.43	1836.65		1836.66	0.000048	0.4	851.61	160.14	0.06
Gilgel Abay	22234.92	Max WS	344.6	1831.86	1836.33		1836.35	0.000187	0.65	527.24	135.21	0.11
Gilgel Abay	22136.4	Max WS	344.15	1831	1836.08		1836.11	0.000257	0.77	444.17	109.88	0.12

Gilgel Abay	21817.15	Max WS	340.22	1832	1834.53		1834.72	0.004863	1.93	175.96	106.91	0.48
Gilgel Abay	21567.81	Max WS	333.75	1828.02	1834.03		1834.04	0.000064	0.42	794.41	180.82	0.06
Gilgel Abay	21287.85	Max WS	329.4	1830.02	1833.89		1833.93	0.000621	0.83	396.97	180.8	0.18
Gilgel Abay	21128.65	Max WS	326.65	1830.03	1833.82		1833.84	0.000381	0.71	462.58	187.73	0.14
Gilgel Abay	20890.39	Max WS	326.34	1830.09	1833.76		1833.78	0.000161	0.5	657.9	237.88	0.1
Gilgel Abay	20606.21	Max WS	325.33	1829	1833.74		1833.74	0.000065	0.37	877.73	247.36	0.06
Gilgel Abay	20239.71	Max WS	322.61	1829.02	1833.6		1833.64	0.000539	0.81	397.17	168.74	0.17
Gilgel Abay	19929.67	Max WS	320.25	1828.01	1833.52		1833.53	0.000048	0.34	954.95	245.42	0.05
Gilgel Abay	19704.64	Max WS	318.6	1830.01	1833.41		1833.43	0.000273	0.64	495.59	177.69	0.12
Gilgel Abay	19427.92	Max WS	315.48	1829	1833.29		1833.31	0.000241	0.57	552.93	221.84	0.12
Gilgel Abay	19153.42	Max WS	314.89	1829	1833.26		1833.27	0.00008	0.38	831.85	265.54	0.07
Gilgel Abay	18847.24	Max WS	314.34	1828.01	1833.23		1833.24	0.00007	0.36	882.69	280.27	0.06
Gilgel Abay	18345.96	Max WS	312.14	1829.01	1833.08		1833.1	0.000296	0.6	523.86	225.77	0.12
Gilgel Abay	18057.74	Max WS	310.94	1827	1832.99		1832.99	0.000056	0.37	846.56	213.96	0.06
Gilgel Abay	17611.21	Max WS	307.56	1828	1832.74		1832.75	0.000082	0.4	773.94	232.86	0.07
Gilgel Abay	17293.56	Max WS	304.37	1828	1832.59		1832.6	0.000102	0.42	717.19	228.07	0.08
Gilgel Abay	16860.43	Max WS	303.49	1828.19	1832.52		1832.53	0.000077	0.36	843.54	283.18	0.07
Gilgel Abay	16358.08	Max WS	302.37	1827.84	1832.48		1832.48	0.000045	0.29	1046.3	327.74	0.05
Gilgel Abay	15960.15	Max WS	301.35	1828	1832.36		1832.39	0.000432	0.79	381.28	143.59	0.15
Gilgel Abay	15493.99	Max WS	300.01	1827	1832.27		1832.27	0.000029	0.25	1212.16	340.29	0.04
Gilgel Abay	15194.7	Max WS	298.63	1828.99	1832.21		1832.22	0.000154	0.47	636.26	240.59	0.09
Gilgel Abay	14963.08	Max WS	296.21	1828.51	1832.02		1832.06	0.001046	0.9	329.95	199.9	0.22
Gilgel Abay	14622.97	Max WS	292.15	1828.54	1831.82		1831.83	0.000298	0.55	526.73	257.06	0.12
Gilgel Abay	14170.82	Max WS	290.72	1826.01	1831.74		1831.75	0.000037	0.28	1022.22	284.47	0.05
Gilgel Abay	13812.27	Max WS	289.49	1827.01	1831.71		1831.72	0.000092	0.39	743.19	249.33	0.07
Gilgel Abay	13490.45	Max WS	288.78	1828.01	1831.66		1831.67	0.000191	0.45	637.68	302.69	0.1
Gilgel Abay	13136.23	Max WS	287.91	1827.03	1831.61		1831.62	0.000111	0.39	729.74	282.78	0.08
Gilgel Abay	12833.88	Max WS	287.18	1828.03	1831.58		1831.58	0.00009	0.33	867.06	373.98	0.07
Gilgel Abay	12495.29	Max WS	285.69	1828	1831.45		1831.48	0.000535	0.66	435.68	257.22	0.16
Gilgel Abay	12053.91	Max WS	283.34	1828	1831.28		1831.29	0.00031	0.48	593.4	375.18	0.12
Gilgel Abay	11678.69	Max WS	282.14	1827.05	1831.2		1831.21	0.000085	0.31	898.16	400.27	0.07
Gilgel Abay	11298.92	Max WS	281.93	1826.84	1831.14		1831.15	0.000167	0.42	671.91	324.2	0.09
Gilgel Abay	11005.39	Max WS	281.8	1827.01	1831.1		1831.11	0.000101	0.39	730.43	271.02	0.08
Gilgel Abay	10589.51	Max WS	281.64	1825.02	1831.06		1831.07	0.000096	0.35	803.28	333.09	0.07

Gilgel Abay	10138.61	Max WS	280.6	1828	1830.67		1830.73	0.001426	1.05	267.18	162.79	0.26
Gilgel Abay	9572.952	Max WS	278.49	1827.12	1830.17		1830.18	0.000515	0.55	510.26	385.81	0.15
Gilgel Abay	9060.053	Max WS	278.01	1824.79	1830.04		1830.05	0.000062	0.31	904.71	330.38	0.06
Gilgel Abay	8579.458	Max WS	277.93	1823.23	1830.01		1830.02	0.000051	0.35	800.28	209.19	0.06
Gilgel Abay	8157.789	Max WS	277.79	1827.05	1829.95		1829.96	0.000236	0.53	524.91	232.13	0.11
Gilgel Abay	7876.896	Max WS	277.73	1824.24	1829.88		1829.9	0.00019	0.65	429.79	118.84	0.11
Gilgel Abay	7570.963	Max WS	277.76	1824.02	1829.86		1829.86	0.000042	0.3	910.83	251.95	0.05
Gilgel Abay	7312.366	Max WS	277.75	1824.29	1829.81		1829.83	0.000245	0.68	410.4	128.42	0.12
Gilgel Abay	7084.47	Max WS	277.72	1826.01	1828.93		1829.16	0.006194	2.12	130.84	83.31	0.54
Gilgel Abay	6796.294	Max WS	277.66	1822.09	1828.15		1828.16	0.000094	0.44	633.41	185.8	0.08
Gilgel Abay	6449.194	Max WS	277.59	1825.04	1827.64		1827.74	0.002491	1.44	192.8	111.05	0.35
Gilgel Abay	6164.339	Max WS	277.56	1823	1827.13		1827.21	0.001272	1.29	215.56	88.38	0.26
Gilgel Abay	5833.369	Max WS	121.06	1815.04	1826.96		1826.96	0.000001	0.06	2165.68	304.18	0.01
Gilgel Abay	5505.133	Max WS	121.08	1820.99	1826.95		1826.95	0.000014	0.16	773.95	249.36	0.03
Gilgel Abay	5180.092	Max WS	120.8	1818.97	1826.95		1826.95	0.000003	0.11	1143.38	228.4	0.02
Gilgel Abay	4892.707	Max WS	120.7	1816.02	1826.95		1826.95	0.000001	0.08	1446.82	225.05	0.01
Gilgel Abay	4604.197	Max WS	120.58	1816.01	1826.95		1826.95	0	0.05	2529.46	352.79	0.01
Gilgel Abay	4234.233	Max WS	277.46	1819.82	1821.19	1821.22	1821.57	0.031028	2.71	102.32	151.39	1.05
Gilgel Abay	3873.924	Max WS	277.2	1811.17	1815.74		1815.82	0.001121	1.26	219.13	83.82	0.25
Gilgel Abay	3554.487	Max WS	277.07	1809.04	1815.6		1815.61	0.000088	0.46	602.25	156.22	0.07
Gilgel Abay	3155.623	Max WS	276.89	1811	1815.53		1815.54	0.000273	0.52	531.82	264.01	0.12
Gilgel Abay	2781.871	Max WS	276.72	1809.86	1815.46		1815.47	0.000093	0.44	624.14	178.5	0.08
Gilgel Abay	2384.771	Max WS	276.16	1812	1814.44		1814.57	0.004628	1.59	173.59	137	0.45
Gilgel Abay	2127.667	Max WS	276.06	1808.02	1813.92		1813.93	0.000109	0.48	578.07	166.94	0.08
Gilgel Abay	1657.528	Max WS	276.02	1807.98	1813.9		1813.9	0.000033	0.27	1009.09	273.97	0.05
Gilgel Abay	1292.115	Max WS	275.85	1810.38	1813.86		1813.87	0.000125	0.38	721.08	322.52	0.08
Gilgel Abay	957.8586	Max WS	275.74	1810.34	1812.6		1812.82	0.006788	2.07	133.44	94.74	0.56
Gilgel Abay	398.9698	Max WS	275.62	1808	1810.56	1809.2	1810.58	0.001005	0.62	442.41	454.02	0.2

Table A- 14 Maximum Water Surface Profile for 50 Year Storm

Reach	**River Sta**	**Profile**	**Q Total**	**Min Ch El**	**W.S. Elev**	**Crit W.S.**	**E.G. Elev**	**E.G. Slope**	**Vel Chnl**	**Flow Area**	**Top Width**	**Froude # Chl**
			(m3/s)	**(m)**	**(m)**	**(m)**	**(m)**	**(m/m)**	**(m/s)**	**(m2)**	**(m)**	
Gilgel Abay	30878.41	Max WS	437.88	1842.02	1847.38		1847.42	0.000296	0.81	538.62	144.61	0.13

Gilgel Abay	30754.01	Max WS	437.82	1840.1	1847.37		1847.39	0.000095	0.6	739.55	136.87	0.08
Gilgel Abay	30623.44	Max WS	437.73	1840.99	1847.32		1847.35	0.000151	0.73	600.77	109.46	0.1
Gilgel Abay	30461.9	Max WS	437.61	1839	1847.3		1847.31	0.000046	0.48	919.59	133.42	0.06
Gilgel Abay	30292.04	Max WS	437.45	1837	1847.3		1847.31	0.000024	0.38	1140.13	136.24	0.04
Gilgel Abay	30137.44	Max WS	437.27	1838.02	1847.29		1847.3	0.000035	0.44	987.67	126.5	0.05
Gilgel Abay	30013.36	Max WS	437.15	1841	1847.25		1847.28	0.000162	0.73	601.6	119.33	0.1
Gilgel Abay	29881.01	Max WS	438.21	1842.01	1844.32	1844.52	1845.26	0.037444	4.3	101.81	86.31	1.27
Gilgel Abay	29712.37	Max WS	430.95	1837.57	1841.66		1841.8	0.002184	1.67	258.4	107.42	0.34
Gilgel Abay	29579.34	Max WS	420.17	1838	1841.39		1841.51	0.001937	1.53	273.93	117.04	0.32
Gilgel Abay	29450.05	Max WS	400.49	1837.99	1841.22		1841.28	0.001124	1.15	347.19	152.12	0.24
Gilgel Abay	29323.94	Max WS	395.24	1837	1841.14		1841.17	0.00032	0.77	514.01	160.62	0.14
Gilgel Abay	29085.98	Max WS	393.47	1832.01	1841.12		1841.13	0.000029	0.37	1076.67	167.72	0.05
Gilgel Abay	28917.06	Max WS	389.37	1836	1841.09		1841.11	0.000162	0.62	628.71	164.12	0.1
Gilgel Abay	28771.83	Max WS	386.97	1836	1841.04		1841.08	0.000329	0.88	437.51	110.57	0.14
Gilgel Abay	28631.08	Max WS	375.41	1837.08	1840.84		1840.94	0.001534	1.45	258.52	100.32	0.29
Gilgel Abay	28461.73	Max WS	366.41	1836	1840.63		1840.71	0.000794	1.22	301.06	90.43	0.21
Gilgel Abay	28305.39	Max WS	359.01	1835	1840.44		1840.49	0.000371	0.97	368.32	84.58	0.15
Gilgel Abay	28168.07	Max WS	357.52	1833.19	1840.37		1840.38	0.000043	0.42	848.84	138.73	0.05
Gilgel Abay	27947.79	Max WS	357.44	1833	1840.36		1840.36	0.000035	0.38	931.44	151.62	0.05
Gilgel Abay	27593.15	Max WS	355.43	1834.61	1840.33		1840.34	0.000075	0.47	756.44	164.18	0.07
Gilgel Abay	27291.85	Max WS	354.79	1834.99	1840.25		1840.28	0.000186	0.68	521.12	126.5	0.11
Gilgel Abay	27065.43	Max WS	354.21	1832	1840.23		1840.23	0.00003	0.36	993.98	162.04	0.05
Gilgel Abay	26825.21	Max WS	353.12	1834.53	1840.2		1840.21	0.000071	0.45	779.17	170.57	0.07
Gilgel Abay	26554.42	Max WS	352.66	1832.77	1840.17		1840.18	0.000052	0.43	818.41	152.8	0.06
Gilgel Abay	26408.3	Max WS	352.64	1832.5	1840.15		1840.16	0.000042	0.44	805.43	119.4	0.05
Gilgel Abay	26216.51	Max WS	351.9	1831.01	1840.13		1840.14	0.000016	0.3	1170.14	147.48	0.03
Gilgel Abay	26054.55	Max WS	352.51	1831.15	1840.12		1840.12	0.000019	0.33	1082.49	138.7	0.04
Gilgel Abay	25852.31	Max WS	351.66	1830.35	1840.11		1840.11	0.000014	0.28	1255.33	160.1	0.03
Gilgel Abay	25627.63	Max WS	351.88	1831.08	1840.09		1840.1	0.000047	0.49	720.83	98	0.06
Gilgel Abay	25513.83	Max WS	351.66	1834.54	1839.99		1840.03	0.000327	0.94	375.59	83.62	0.14
Gilgel Abay	25375.21	Max WS	351.44	1832	1839.94		1839.95	0.000052	0.48	735.04	111.46	0.06
Gilgel Abay	25276.05	Max WS	351.41	1830	1839.93		1839.94	0.000033	0.42	835.7	111.04	0.05
Gilgel Abay	25138.7	Max WS	351.39	1830.01	1839.9		1839.91	0.000034	0.41	859.36	118.68	0.05
Gilgel Abay	24980.18	Max WS	351.23	1829	1839.87		1839.87	0.000016	0.31	1147.72	142.9	0.03

Gilgel Abay	24830.85	Max WS	351.21	1832	1839.86		1839.86	0.000031	0.37	939.28	139.92	0.05
Gilgel Abay	24628.31	Max WS	351.15	1830.01	1839.85		1839.85	0.000013	0.29	1226.89	146.31	0.03
Gilgel Abay	24509.39	Max WS	351.09	1833.98	1839.81		1839.84	0.000143	0.68	513.83	97.57	0.1
Gilgel Abay	24384.22	Max WS	351.07	1828.83	1839.81		1839.81	0.000013	0.3	1187.41	125.53	0.03
Gilgel Abay	24212.36	Max WS	351.01	1832	1839.78		1839.79	0.000055	0.48	731.57	115.35	0.06
Gilgel Abay	24040.46	Max WS	350.01	1831	1838.33		1838.35	0.000095	0.61	570.11	91.57	0.08
Gilgel Abay	23875.17	Max WS	347.55	1832	1836.97		1836.99	0.000134	0.58	599.35	145.16	0.09
Gilgel Abay	23572.69	Max WS	347.33	1830.01	1836.94		1836.95	0.000066	0.47	731.99	141.35	0.07
Gilgel Abay	23223.78	Max WS	347.22	1830.52	1836.92		1836.93	0.000041	0.35	1000.53	220.89	0.05
Gilgel Abay	23021.91	Max WS	347.08	1829.01	1836.91		1836.92	0.000023	0.32	1088.31	168.71	0.04
Gilgel Abay	22761.97	Max WS	347.02	1830	1836.89		1836.9	0.000038	0.37	944.33	179.49	0.05
Gilgel Abay	22456.21	Max WS	346.91	1830.43	1836.67		1836.67	0.000048	0.41	853.92	160.14	0.06
Gilgel Abay	22234.92	Max WS	346.8	1831.86	1836.34		1836.36	0.000187	0.66	528.93	135.21	0.11
Gilgel Abay	22136.4	Max WS	346.47	1831	1836.09		1836.12	0.000258	0.78	445.34	109.88	0.12
Gilgel Abay	21817.15	Max WS	342.24	1832	1834.54		1834.73	0.004832	1.93	176.99	107	0.48
Gilgel Abay	21567.81	Max WS	336.1	1828.02	1834.05		1834.05	0.000064	0.42	796.83	180.82	0.06
Gilgel Abay	21287.85	Max WS	331.45	1830.02	1833.91		1833.94	0.000616	0.83	399.45	180.8	0.18
Gilgel Abay	21128.65	Max WS	330.45	1830.03	1833.83		1833.86	0.000383	0.71	465.1	187.73	0.14
Gilgel Abay	20890.39	Max WS	328.09	1830.09	1833.78		1833.79	0.00016	0.5	661.26	237.88	0.1
Gilgel Abay	20606.21	Max WS	327.44	1829	1833.75		1833.76	0.000065	0.37	881.12	247.47	0.06
Gilgel Abay	20239.71	Max WS	324.72	1829.02	1833.62		1833.65	0.000537	0.81	399.58	169.12	0.17
Gilgel Abay	19929.67	Max WS	322.08	1828.01	1833.54		1833.54	0.000048	0.34	958.53	245.42	0.05
Gilgel Abay	19704.64	Max WS	320.42	1830.01	1833.43		1833.45	0.000271	0.64	498.21	177.69	0.12
Gilgel Abay	19427.92	Max WS	317.88	1829	1833.31		1833.33	0.000242	0.57	556.1	222.61	0.12
Gilgel Abay	19153.42	Max WS	317.09	1829	1833.27		1833.28	0.000079	0.38	835.72	265.54	0.07
Gilgel Abay	18847.24	Max WS	316.51	1828.01	1833.25		1833.26	0.00007	0.36	886.82	280.49	0.06
Gilgel Abay	18345.96	Max WS	314.53	1829.01	1833.1		1833.11	0.000295	0.6	527.12	225.77	0.12
Gilgel Abay	18057.74	Max WS	313.19	1827	1833		1833.01	0.000056	0.37	849.59	213.96	0.06
Gilgel Abay	17611.21	Max WS	309.57	1828	1832.75		1832.76	0.000082	0.4	776.85	232.86	0.07
Gilgel Abay	17293.56	Max WS	307.02	1828	1832.6		1832.61	0.000102	0.43	719.91	228.07	0.08
Gilgel Abay	16860.43	Max WS	305.7	1828.19	1832.53		1832.54	0.000077	0.36	846.91	283.18	0.07
Gilgel Abay	16358.08	Max WS	304.96	1827.84	1832.49		1832.49	0.000045	0.29	1050	327.74	0.05
Gilgel Abay	15960.15	Max WS	303.6	1828	1832.37		1832.4	0.000433	0.79	382.86	143.7	0.16
Gilgel Abay	15493.99	Max WS	302.39	1827	1832.28		1832.28	0.000029	0.25	1215.81	340.29	0.04

Gilgel Abay	15194.7	Max WS	301.33	1828.99	1832.22		1832.23	0.000155	0.47	638.7	240.59	0.09
Gilgel Abay	14963.08	Max WS	298.42	1828.51	1832.03		1832.07	0.001041	0.9	332.04	200.02	0.22
Gilgel Abay	14622.97	Max WS	294.7	1828.54	1831.83		1831.84	0.000298	0.56	529.53	257.06	0.12
Gilgel Abay	14170.82	Max WS	293.06	1826.01	1831.76		1831.76	0.000038	0.29	1025.31	284.61	0.05
Gilgel Abay	13812.27	Max WS	291.95	1827.01	1831.72		1831.73	0.000092	0.39	745.79	249.33	0.07
Gilgel Abay	13490.45	Max WS	291.04	1828.01	1831.67		1831.68	0.000191	0.45	640.83	303.23	0.1
Gilgel Abay	13136.23	Max WS	289.72	1827.03	1831.62		1831.63	0.000111	0.4	732.69	282.92	0.08
Gilgel Abay	12833.88	Max WS	289.39	1828.03	1831.59		1831.59	0.00009	0.33	870.96	373.98	0.07
Gilgel Abay	12495.29	Max WS	287.5	1828	1831.47		1831.49	0.000531	0.66	438.52	257.35	0.16
Gilgel Abay	12053.91	Max WS	285.87	1828	1831.29		1831.3	0.000308	0.48	597.81	375.66	0.12
Gilgel Abay	11678.69	Max WS	284.73	1827.05	1831.21		1831.22	0.000085	0.32	903.04	400.27	0.07
Gilgel Abay	11298.92	Max WS	284.41	1826.84	1831.15		1831.16	0.000167	0.42	675.77	324.31	0.09
Gilgel Abay	11005.39	Max WS	283.9	1827.01	1831.11		1831.12	0.000101	0.39	733.58	271.14	0.08
Gilgel Abay	10589.51	Max WS	283.98	1825.02	1831.07		1831.08	0.000096	0.35	807.25	334.02	0.07
Gilgel Abay	10138.61	Max WS	282.66	1828	1830.69		1830.74	0.001432	1.05	269.03	164.25	0.26
Gilgel Abay	9572.952	Max WS	280.78	1827.12	1830.18		1830.2	0.000512	0.55	514.35	387.09	0.15
Gilgel Abay	9060.053	Max WS	280.23	1824.79	1830.05		1830.06	0.000063	0.31	908.2	330.85	0.06
Gilgel Abay	8579.458	Max WS	280.1	1823.23	1830.02		1830.03	0.000051	0.35	802.52	209.47	0.06
Gilgel Abay	8157.789	Max WS	279.99	1827.05	1829.96		1829.97	0.000237	0.53	527.26	232.33	0.11
Gilgel Abay	7876.896	Max WS	279.95	1824.24	1829.89		1829.91	0.000191	0.65	430.94	118.96	0.11
Gilgel Abay	7570.963	Max WS	279.98	1824.02	1829.87		1829.87	0.000042	0.31	913.27	252.16	0.05
Gilgel Abay	7312.366	Max WS	279.95	1824.29	1829.81		1829.84	0.000247	0.68	411.63	128.62	0.12
Gilgel Abay	7084.47	Max WS	279.93	1826.01	1828.94		1829.17	0.006203	2.13	131.52	83.49	0.54
Gilgel Abay	6796.294	Max WS	279.89	1822.09	1828.16		1828.17	0.000095	0.44	635.12	185.98	0.08
Gilgel Abay	6449.194	Max WS	279.82	1825.04	1827.65		1827.75	0.002504	1.45	193.51	111.17	0.35
Gilgel Abay	6164.339	Max WS	279.77	1823	1827.13		1827.21	0.001289	1.3	215.75	88.4	0.27
Gilgel Abay	5833.369	Max WS	121.06	1815.04	1826.96		1826.96	0.000001	0.06	2165.68	304.18	0.01
Gilgel Abay	5505.133	Max WS	121.08	1820.99	1826.95		1826.95	0.000014	0.16	773.95	249.36	0.03
Gilgel Abay	5180.092	Max WS	120.8	1818.97	1826.95		1826.95	0.000003	0.11	1143.38	228.4	0.02
Gilgel Abay	4892.707	Max WS	120.7	1816.02	1826.95		1826.95	0.000001	0.08	1446.82	225.05	0.01
Gilgel Abay	4604.197	Max WS	120.58	1816.01	1826.95		1826.95	0	0.05	2529.46	352.79	0.01
Gilgel Abay	4234.233	Max WS	279.48	1819.82	1821.2	1821.22	1821.57	0.031043	2.72	102.8	151.55	1.05
Gilgel Abay	3873.924	Max WS	279.05	1811.17	1815.75		1815.83	0.001125	1.27	219.86	83.93	0.25
Gilgel Abay	3554.487	Max WS	278.96	1809.04	1815.61		1815.62	0.000089	0.46	603.44	156.36	0.08

Gilgel Abay	3155.623	Max WS	278.76	1811	1815.54		1815.55	0.000274	0.52	533.83	264.29	0.12
Gilgel Abay	2781.871	Max WS	278.55	1809.86	1815.47		1815.48	0.000094	0.45	625.44	178.62	0.08
Gilgel Abay	2384.771	Max WS	278.22	1812	1814.45		1814.58	0.004619	1.59	174.61	137.28	0.45
Gilgel Abay	2127.667	Max WS	278.11	1808.02	1813.93		1813.94	0.00011	0.48	579.38	167.09	0.08
Gilgel Abay	1657.528	Max WS	278.03	1807.98	1813.9		1813.91	0.000033	0.27	1011.25	274.09	0.05
Gilgel Abay	1292.115	Max WS	277.83	1810.38	1813.87		1813.88	0.000126	0.38	723.53	322.65	0.08
Gilgel Abay	957.8586	Max WS	277.73	1810.34	1812.6		1812.82	0.0068	2.07	133.99	94.82	0.56
Gilgel Abay	398.9698	Max WS	277.54	1808	1810.57	1809.2	1810.59	0.001006	0.62	444.23	454.34	0.2

Table A- 15 Maximum Water Surface Profile for 100 Year Storm

Reach	River Sta	Profile	Q Total	Min Ch El	W.S. Elev	Crit W.S.	E.G. Elev	E.G. Slope	Vel Chnl	Flow Area	Top Width	Froude # Chl
			(m3/s)	(m)	(m)	(m)	(m)	(m/m)	(m/s)	(m2)	(m)	
Gilgel Abay	30878.41	Max WS	499.51	1842.02	1847.53		1847.57	0.00034	0.89	559.82	144.61	0.14
Gilgel Abay	30754.01	Max WS	499.4	1840.1	1847.51		1847.53	0.000114	0.66	759.19	136.87	0.09
Gilgel Abay	30623.44	Max WS	499.24	1840.99	1847.46		1847.49	0.000182	0.81	615.38	109.46	0.11
Gilgel Abay	30461.9	Max WS	498.92	1839	1847.43		1847.45	0.000057	0.53	936.75	133.42	0.06
Gilgel Abay	30292.04	Max WS	498.46	1837	1847.43		1847.43	0.00003	0.43	1157.44	136.24	0.05
Gilgel Abay	30137.44	Max WS	498.6	1838.02	1847.41		1847.43	0.000044	0.5	1003.49	126.5	0.06
Gilgel Abay	30013.36	Max WS	497.66	1841	1847.37		1847.41	0.000195	0.81	615.61	119.33	0.11
Gilgel Abay	29881.01	Max WS	499.32	1842.01	1844.44	1844.65	1845.45	0.036139	4.47	111.78	87.15	1.26
Gilgel Abay	29712.37	Max WS	480.23	1837.57	1841.94		1842.08	0.001915	1.66	289.23	109.41	0.33
Gilgel Abay	29579.34	Max WS	452.01	1838	1841.73		1841.83	0.00145	1.44	312.86	117.04	0.28
Gilgel Abay	29450.05	Max WS	439.32	1837.99	1841.59		1841.65	0.000822	1.09	403.9	152.12	0.21
Gilgel Abay	29323.94	Max WS	434.14	1837	1841.53		1841.56	0.000266	0.75	575.82	160.62	0.13
Gilgel Abay	29085.98	Max WS	434.08	1832.01	1841.51		1841.52	0.00003	0.38	1141.87	167.72	0.05
Gilgel Abay	28917.06	Max WS	433.06	1836	1841.48		1841.5	0.00015	0.62	693.49	168.21	0.1
Gilgel Abay	28771.83	Max WS	428.35	1836	1841.43		1841.47	0.000297	0.89	480.82	110.57	0.14
Gilgel Abay	28631.08	Max WS	420.99	1837.08	1841.26		1841.36	0.001212	1.39	302.04	104.14	0.26
Gilgel Abay	28461.73	Max WS	412.86	1836	1841.08		1841.16	0.000668	1.21	341.96	90.43	0.2
Gilgel Abay	28305.39	Max WS	404.85	1835	1840.9		1840.95	0.000344	1	406.53	84.58	0.15
Gilgel Abay	28168.07	Max WS	401.36	1833.19	1840.82		1840.83	0.000044	0.44	911.26	138.73	0.05
Gilgel Abay	27947.79	Max WS	401.31	1833	1840.8		1840.81	0.000035	0.4	999.4	151.62	0.05
Gilgel Abay	27593.15	Max WS	399.79	1834.61	1840.77		1840.79	0.00007	0.48	829.96	164.18	0.07

Gilgel Abay	27291.85	Max WS	399.05	1834.99	1840.7		1840.72	0.000169	0.69	577.77	126.5	0.1
Gilgel Abay	27065.43	Max WS	398.36	1832	1840.67		1840.68	0.00003	0.37	1066.54	162.04	0.05
Gilgel Abay	26825.21	Max WS	398.24	1834.53	1840.65		1840.66	0.000067	0.47	855.38	170.57	0.07
Gilgel Abay	26554.42	Max WS	396.66	1832.77	1840.61		1840.62	0.000051	0.45	886.41	152.8	0.06
Gilgel Abay	26408.3	Max WS	397.13	1832.5	1840.59		1840.6	0.000044	0.46	858.31	119.4	0.06
Gilgel Abay	26216.51	Max WS	397.06	1831.01	1840.57		1840.58	0.000017	0.32	1235.13	147.48	0.04
Gilgel Abay	26054.55	Max WS	396.98	1831.15	1840.56		1840.56	0.000021	0.35	1143.42	138.7	0.04
Gilgel Abay	25852.31	Max WS	396.58	1830.35	1840.55		1840.55	0.000015	0.3	1325.41	160.1	0.03
Gilgel Abay	25627.63	Max WS	396.25	1831.08	1840.52		1840.54	0.00005	0.52	763.52	98	0.06
Gilgel Abay	25513.83	Max WS	396.22	1834.54	1840.42		1840.46	0.00031	0.96	411.57	83.62	0.14
Gilgel Abay	25375.21	Max WS	395.66	1832	1840.36		1840.38	0.000054	0.51	782.71	111.46	0.06
Gilgel Abay	25276.05	Max WS	395.64	1830	1840.36		1840.37	0.000035	0.45	883.12	111.04	0.05
Gilgel Abay	25138.7	Max WS	395.83	1830.01	1840.32		1840.33	0.000036	0.44	909.34	118.68	0.05
Gilgel Abay	24980.18	Max WS	395.57	1829	1840.28		1840.29	0.000017	0.33	1207.03	142.9	0.04
Gilgel Abay	24830.85	Max WS	395.38	1832	1840.27		1840.28	0.000032	0.4	997.23	139.92	0.05
Gilgel Abay	24628.31	Max WS	395.18	1830.01	1840.26		1840.27	0.000014	0.31	1287.35	146.31	0.03
Gilgel Abay	24509.39	Max WS	395.29	1833.98	1840.22		1840.25	0.000142	0.71	553.86	97.57	0.1
Gilgel Abay	24384.22	Max WS	395.26	1828.83	1840.22		1840.22	0.000014	0.32	1238.87	125.53	0.03
Gilgel Abay	24212.36	Max WS	395.18	1832	1840.19		1840.2	0.000057	0.51	778.47	115.35	0.06
Gilgel Abay	24040.46	Max WS	393.81	1831	1838.69		1838.71	0.000101	0.65	602.79	91.57	0.08
Gilgel Abay	23875.17	Max WS	390.26	1832	1837.29		1837.3	0.000133	0.61	645.04	145.16	0.09
Gilgel Abay	23572.69	Max WS	390.44	1830.01	1837.25		1837.26	0.000069	0.5	776.14	141.35	0.07
Gilgel Abay	23223.78	Max WS	390.21	1830.52	1837.23		1837.24	0.000042	0.36	1069.34	220.89	0.05
Gilgel Abay	23021.91	Max WS	390.27	1829.01	1837.22		1837.23	0.000025	0.34	1140.66	168.71	0.04
Gilgel Abay	22761.97	Max WS	390.13	1830	1837.2		1837.2	0.00004	0.39	999.47	179.49	0.05
Gilgel Abay	22456.21	Max WS	390.11	1830.43	1836.95		1836.96	0.000051	0.43	899.66	160.14	0.06
Gilgel Abay	22234.92	Max WS	390.05	1831.86	1836.59		1836.62	0.000193	0.69	562.92	135.21	0.11
Gilgel Abay	22136.4	Max WS	389.7	1831	1836.3		1836.34	0.000277	0.83	468.68	109.88	0.13
Gilgel Abay	21817.15	Max WS	383.35	1832	1834.72		1834.91	0.004443	1.96	195.82	108.96	0.47
Gilgel Abay	21567.81	Max WS	375.31	1828.02	1834.27		1834.28	0.000068	0.45	838.22	180.82	0.07
Gilgel Abay	21287.85	Max WS	371.23	1830.02	1834.13		1834.17	0.000561	0.84	440.03	180.8	0.17
Gilgel Abay	21128.65	Max WS	369.19	1830.03	1834.05		1834.08	0.000359	0.73	507.2	187.73	0.14
Gilgel Abay	20890.39	Max WS	367.52	1830.09	1834		1834.01	0.000155	0.51	714.68	237.88	0.09
Gilgel Abay	20606.21	Max WS	366.66	1829	1833.97		1833.98	0.000067	0.39	936.91	249.02	0.06

Gilgel Abay	20239.71	Max WS	363.39	1829.02	1833.84		1833.88	0.000514	0.83	438.62	174.29	0.17
Gilgel Abay	19929.67	Max WS	361.63	1828.01	1833.77		1833.77	0.00005	0.36	1014.85	245.42	0.06
Gilgel Abay	19704.64	Max WS	359.31	1830.01	1833.65		1833.67	0.000265	0.67	537.96	177.69	0.12
Gilgel Abay	19427.92	Max WS	355.99	1829	1833.53		1833.55	0.000232	0.59	606	225.84	0.11
Gilgel Abay	19153.42	Max WS	355.29	1829	1833.5		1833.5	0.00008	0.4	894.96	265.54	0.07
Gilgel Abay	18847.24	Max WS	354.71	1828.01	1833.47		1833.48	0.000071	0.37	949.73	285.02	0.07
Gilgel Abay	18345.96	Max WS	352.42	1829.01	1833.31		1833.33	0.000275	0.61	576.31	225.77	0.12
Gilgel Abay	18057.74	Max WS	351.2	1827	1833.21		1833.22	0.00006	0.39	894.64	213.96	0.06
Gilgel Abay	17611.21	Max WS	347.16	1828	1832.94		1832.95	0.000086	0.42	820.9	232.86	0.07
Gilgel Abay	17293.56	Max WS	344.38	1828	1832.78		1832.79	0.000108	0.45	760.44	228.07	0.08
Gilgel Abay	16860.43	Max WS	342.82	1828.19	1832.71		1832.71	0.000081	0.38	895.25	283.18	0.07
Gilgel Abay	16358.08	Max WS	341.86	1827.84	1832.65		1832.66	0.000048	0.31	1104.34	327.74	0.05
Gilgel Abay	15960.15	Max WS	339.4	1828	1832.52		1832.56	0.000454	0.84	405.54	145.3	0.16
Gilgel Abay	15493.99	Max WS	337.7	1827	1832.43		1832.44	0.000031	0.27	1267.97	340.29	0.04
Gilgel Abay	15194.7	Max WS	337.05	1828.99	1832.36		1832.38	0.000163	0.5	673.75	240.59	0.1
Gilgel Abay	14963.08	Max WS	332.67	1828.51	1832.18		1832.22	0.000987	0.92	361.43	201.84	0.22
Gilgel Abay	14622.97	Max WS	327.19	1828.54	1831.98		1832	0.000289	0.57	569.58	257.06	0.12
Gilgel Abay	14170.82	Max WS	325.64	1826.01	1831.91		1831.92	0.000041	0.3	1069.56	286.56	0.05
Gilgel Abay	13812.27	Max WS	324.31	1827.01	1831.87		1831.88	0.000096	0.41	783.57	249.33	0.07
Gilgel Abay	13490.45	Max WS	323.4	1828.01	1831.82		1831.83	0.000188	0.47	685.92	303.23	0.1
Gilgel Abay	13136.23	Max WS	321.86	1827.03	1831.77		1831.77	0.000115	0.42	774.56	284.82	0.08
Gilgel Abay	12833.88	Max WS	321.41	1828.03	1831.73		1831.74	0.000091	0.35	925.78	373.98	0.07
Gilgel Abay	12495.29	Max WS	319.52	1828	1831.62		1831.64	0.0005	0.67	477.31	259.35	0.16
Gilgel Abay	12053.91	Max WS	317.42	1828	1831.46		1831.47	0.000279	0.48	659.91	381.83	0.12
Gilgel Abay	11678.69	Max WS	316.88	1827.05	1831.38		1831.39	0.000083	0.33	970	400.27	0.07
Gilgel Abay	11298.92	Max WS	316	1826.84	1831.31		1831.32	0.000161	0.43	728.77	324.31	0.09
Gilgel Abay	11005.39	Max WS	315.88	1827.01	1831.27		1831.28	0.000104	0.41	777.44	273.17	0.08
Gilgel Abay	10589.51	Max WS	315.71	1825.02	1831.23		1831.24	0.0001	0.37	861.2	344.09	0.07
Gilgel Abay	10138.61	Max WS	314.39	1828	1830.83		1830.89	0.00149	1.07	294.56	181.05	0.27
Gilgel Abay	9572.952	Max WS	311.98	1827.12	1830.33		1830.34	0.00045	0.55	571.04	389.47	0.14
Gilgel Abay	9060.053	Max WS	311.38	1824.79	1830.2		1830.21	0.000066	0.32	958.46	334.85	0.06
Gilgel Abay	8579.458	Max WS	311.44	1823.23	1830.17		1830.18	0.000058	0.37	834.17	216.8	0.06
Gilgel Abay	8157.789	Max WS	311.31	1827.05	1830.1		1830.12	0.000242	0.55	561.25	235.2	0.11
Gilgel Abay	7876.896	Max WS	311.2	1824.24	1830.03		1830.05	0.000212	0.7	447.74	120.68	0.12

Gilgel Abay	7570.963	Max WS	311.15	1824.02	1830.01		1830.01	0.000047	0.33	948.36	254.84	0.05
Gilgel Abay	7312.366	Max WS	311.13	1824.29	1829.95		1829.97	0.000273	0.73	428.75	131.19	0.13
Gilgel Abay	7084.47	Max WS	311.12	1826.01	1829.05		1829.3	0.0062	2.2	141.54	85.56	0.55
Gilgel Abay	6796.294	Max WS	311.1	1822.09	1828.29		1828.3	0.000105	0.47	659.08	188.37	0.08
Gilgel Abay	6449.194	Max WS	310.92	1825.04	1827.73		1827.85	0.002678	1.53	203.42	113.09	0.36
Gilgel Abay	6164.339	Max WS	310.39	1823	1827.15		1827.25	0.001546	1.43	217.69	88.67	0.29
Gilgel Abay	5833.369	Max WS	174.16	1815.04	1826.96		1826.96	0.000001	0.08	2167.8	304.28	0.01
Gilgel Abay	5505.133	Max WS	174.03	1820.99	1826.96		1826.96	0.000028	0.22	774.88	249.6	0.04
Gilgel Abay	5180.092	Max WS	171.72	1818.97	1826.95		1826.95	0.000007	0.15	1143.59	228.43	0.02
Gilgel Abay	4892.707	Max WS	120.7	1816.02	1826.95		1826.95	0.000001	0.08	1446.82	225.05	0.01
Gilgel Abay	4604.197	Max WS	120.58	1816.01	1826.95		1826.95	0	0.05	2529.46	352.79	0.01
Gilgel Abay	4234.233	Max WS	313.08	1819.82	1821.25	1821.29	1821.66	0.031281	2.83	110.68	154.65	1.07
Gilgel Abay	3873.924	Max WS	312.78	1811.17	1815.87		1815.97	0.001242	1.36	230.34	85.56	0.26
Gilgel Abay	3554.487	Max WS	312.64	1809.04	1815.72		1815.74	0.000103	0.5	620.96	158.47	0.08
Gilgel Abay	3155.623	Max WS	312.55	1811	1815.64		1815.66	0.000296	0.56	561.51	268.05	0.12
Gilgel Abay	2781.871	Max WS	312.44	1809.86	1815.57		1815.58	0.000109	0.49	642.72	180.27	0.08
Gilgel Abay	2384.771	Max WS	312.39	1812	1814.57		1814.7	0.004485	1.63	191.52	142.19	0.45
Gilgel Abay	2127.667	Max WS	312.26	1808.02	1814.07		1814.08	0.000124	0.52	602.32	169.28	0.09
Gilgel Abay	1657.528	Max WS	311.78	1807.98	1814.04		1814.04	0.000037	0.3	1047.89	276.04	0.05
Gilgel Abay	1292.115	Max WS	311.31	1810.38	1814		1814.01	0.000132	0.41	765.92	324.61	0.08
Gilgel Abay	957.8586	Max WS	311.04	1810.34	1812.7		1812.94	0.007007	2.18	142.93	96.15	0.57
Gilgel Abay	398.9698	Max WS	310.5	1808	1810.64	1809.27	1810.66	0.001027	0.65	474.57	459.82	0.21